GALLIUM NITRIDE CHEMICAL MECHANICAL PLANARIZATION DEVELOPMENT THROUGH TOOL SET-UP, PROCESS AND POST CMP CLEANING OPTIMIZATION

A Thesis

by

Şebnem Özbek

Submitted to the
Graduate School of Sciences and Engineering
In Partial Fulfillment of the Requirements for
the Degree of

Master of Science

in the
Department of Mechanical Engineering

Özyeğin University
July 2018

GALLIUM NITRIDE CHEMICAL MECHANICAL PLANARIZATION DEVELOPMENT THROUGH TOOL SET-UP, PROCESS AND POST CMP CLEANING OPTIMIZATION

Approved by:

_____

Associated Professor G. Bahar Başım,
Advisor
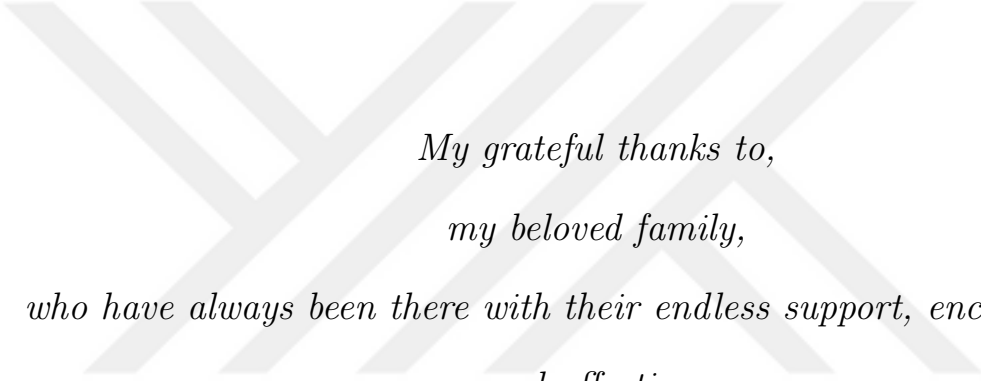Department of Mechanical Engineering
Özyeğin University

_____

Assistant Professor Özkan Bebek
Department of Mechanical Engineering
Özyeğin University

_____

Assistant Professor Sedat Nizamoğlu
Department of Electrical and Electronics
Engineering
Koç University

Date Approved: 10 July 2018

My grateful thanks to,

my beloved family,

who have always been there with their endless support, encouragement

and affection.

my dearest aunt İrem Gören,

who always inspired me with her brilliant stand to all the toughs in

life in the most artful manner.

ABSTRACT

In this thesis, a new Chemical Mechanical Planarization (CMP) process and a complementary tool set-up are introduced to enhance Gallium Nitride (GaN) material removal rates while controlling the post planarization surface quality. The key process variables are studied to set them at an optimal level, while a new slurry feeding methodology is introduced in addition to a new tool set up to enable high material removal rates and acceptable surface quality through close control of the process chemistry. Post-CMP cleaning procedures are also studied with glass slides (as a model) to determine the particle and contaminant detachment efficiency by using regular and viscoelastic fluids. A new particle removal procedure is introduced for post CMP cleaning, which can help preserve the surface quality of the wafer.

CMP of GaN is a new study area, which is getting attention due to the recently developed wide range of applications of GaN as a material in high power, high frequency and high temperature microelectronic device manufacturing. Due to its wide bandgap energy and high electron mobility GaN is the material of choice for heterojunction field effects transistors (HFETs) and its derivatives as a barrier layer, high electron mobility transistors (HEMTs) for power switching with AlGaN/GaN stacking as a buffer layer as well as for the applications for heterojunction bipolar transistors (HBTs) and bipolar junction transistors (BJTs). However, its challenging mechanical properties such as hardness and being prone to fracturing in addition to the chemical correspondence to slurry additives based on crystallographic orientation result in complicated processes and ineffective use of consumables in order to planarize the surface of GaN. Therefore, this study focuses on the optimization of the planarization process of GaN bulk wafers to reduce the CMP processing time through

increasing material removal rates and maintaining surface quality so that the process becomes more efficient and sustainable.

In addition to the CMP process optimization for removal rates and the surface quality during the polishing action, this study also focuses on the post CMP cleaning procedures improvements. Post CMP cleaning procedures require effective removal of slurry particles from the polished wafer surfaces without damaging the surface quality. The decrease in size of microelectronic devices make the processors more vulnerable to any abrasive particles remaining on the wafer surface post CMP to prevent shorts and defective devices. However, the existing methods of post CMP cleaning are insufficient for removing particles at nano-level, therefore a new methodology of using viscoelastic fluids in cleaning solutions is studied. This method is efficient for removing particles within micron size ranges, which tend to form through agglomeration of primary particles and known to result in the defectivity almost 100% as they strongly adsorb onto the wafer surface.

Chapter 1 summarizes the literature review on the chemical mechanical planarization process, the application areas of CMP and the main components of the polisher; such as the polishing pad, conditioner and the slurry. This chapter also gives a brief explanation about the driving force for introducing new compound semiconductors in microelectronic device manufacturing other than silicon, such as GaN. Application of GaN in electronic devices as well as the growth of GaN and the chemical mechanical planarization of Gallium Nitride are also given in detail. Furthermore, the chapter explains the different methods implemented for post CMP cleaning with their relative advantages and disadvantages. Finally, brief information is given about the modeling approaches of the CMP optimization procedure.

Chapter 2 focuses on the preliminary surface characterization of gallium (Ga) rich and nitrogen (N) rich faces of GaN bulk coupons. These characterization methods involve wettability, surface topography and roughness, surface chemical composition,

surface charge and absorbance measurements. These measurements outline the differences of the Ga and N rich faces which is critical in terms of understanding the chemical reactions taking place during the CMP process as well as the post CMP performance of the wafers.

Chapter 3 outlines the design of an effective CMP process for GaN, by both experimentally and mathematically. The experimental method evaluates the effects of the slurry pH, slurry solids loading, slurry flow rate, applied pressure, chemical composition and temperature of the slurry. Post CMP evaluations are evaluated in terms of material removal rate and surface roughness for each experiment. This chapter also includes an optimized CMP tool set-up which utilizes a slurry pool by chemical control of the dissolution reaction through continuous neutralization. Finally, the chapter gives the preliminary study for the mathematical optimization based on the experimental measurements.

Chapter 4 focuses on the improvement of post CMP cleaning procedures through detailed surface analyses including surface energy and work of adhesion. The chapter starts with the glass slide experiments, where the aim is to obtain varying surface roughness values by using different size of slurry abrasive particles. The surfaces of the glass slides are evaluated in terms of wettability as well, where wettability of the surface highly effects the post CMP cleaning efficiency. Finally, a new method is introduced for post CMP cleaning which utilizes viscoelastic fluids to remove particles.

Finally, chapter 5 gives a general conclusion of the thesis and outlines recommendations for the future work.

ÖZETÇE

Bu tez çalışmasında, yeni bir Kimyasal Mekanik Düzlemleme (CMP) prosesi ve tamamlayıcı bir takım kurulumu, düzlemleme sonrası yüzey pürüzlülüğünü kontrol ederken Galyum Nitrat (GaN) malzeme aşınım oranını arttırmak için tanıtılmıştır. Yeni bir süspansiyon akış metodu ve buna ek olarak yeni bir deney düzeneği, proses kimyasının yakın kontrolü ile yüksek malzeme aşınım oranı ve kabul edilebilir yüzey pürüzlülüğünü sağlayacak şekilde kurulmuştur. CMP sonrası temizleme prosedürleri, parçacık ve kontaminasyon gidermenin etkinliğini belirlemek için cam lamlarla da çalışılmıştır. CMP sonrası temizliği için yarı iletken kuponun yüzey kalitesini korumaya yardımcı olabilecek yeni bir parçacık giderme işlemi denenmiştir.

GaN CMP, yeni geliştirilen bir çalışma alanıdır ve yeni geliştirilen geniş uygulama yelpazesi sayesinde yüksek güç, yüksek frekans ve yüksek sıcaklıktaki mikroelektronik cihaz imalatında dikkat çekmektedir. Geniş bant genişliği enerjisi ve yüksek elektron hareketliliğinden dolayı, GaN, birok uygulamada tercih edilir. Bunların arasında, engel katmanı olarak kullanıldığı heterojunction alan etkileri transistörleri (HFET) ve benzerleri, AlGaN/GaN güç geçişi sağlayan yüksek elektron hareketlilik transistörleri (HEMT) tampon olarak kullanılır. Fakat, mekanik özellikleri, GaN yüzeyini düzlemek için karmaşık süreçlere ve sarf malzemelerinin etkisiz kullanımına neden olur. Bu nedenle, bu çalışma, prosesin sürdürülebilir hale gelmesi iin malzeme aşınım oranlarının arttırılması yoluyla CMP işlem süresinin azaltılması için GaN yarı iletken kuponlarının düzlemleme sürecinin optimizasyonuna odaklanmalıdır.

Düzlemleme işlemi sırasında malzeme aşınım oranları ve yüzey kalitesi için CMP proses optimizasyonuna ek olarak, bu çalışma aynı zamanda CMP sonrası temizleme prosedürleri iyileştirmelerine odaklanmaktadır. CMP sonrası temizleme prosedürleri,

yüzey kalitesine zarar vermeden düzlemlenmiş yarı iletken kuponlarının yüzeylerinden süspansiyon parçacıklarının etkili bir şekilde çıkarılmasını gerektirir. Mikroelektronik cihazların boyutundaki azalma, işlemcileri, şort ve kusurlu cihazları önlemek için CMP'de yarı iletken yüzeylerinin üzerinde kalan tüm aşındırıcı parçacıklara karşı daha hassas hale getirir. Fakat, mevcut CMP temizleme yöntemleri, nano seviyesinde partiküllerin yüzeyden gidermek için yetersizdir, bu nedenle, temizleme çözeltilerinde viskoelastik akışkanların kullanılmasına yönelik yeni bir metodoloji incelenmiştir. Bu yöntem, parçacıkların bir araya gelmesi ile oluşan, ve yarı iletken yüzeye tutunarak neredeyse %100 oranda hasara sebep olan, mikron büyüklüündeki parçacıkların giderilmesi için etkilidir.

Bölüm 1, kimyasal mekanik düzlemleme süreci, CMP'nin uygulama alanları ve düzlemleme ana bileşenleri ile ilgili literatür taramasını özetlemektedir. Düzlemleme ana bileşenleri, cilalama pedi, ped aşındırıcısı ve süspansiyondan oluşmaktadır. Bu bölüm ayrıca, mikroelektronik cihaz imalatında GaN gibi silikon dışındaki yeni bileşik yarı iletkenlerin arayışındaki itici güç hakkında kısa bir açıklama sunmaktadır. GaN'ın, elektronik cihazlarda uygulanması, GaN'ın büyümesi ve GaN kimyasal mekanik düzlemleme süresi de detaylı olarak sunulmuştur. Ayrca, bölüm CMP sonrası temizleme için göreceli avantajları ve dezavantajları ile uygulanan farklı yöntemleri açıklamıştır. Son olarak, CMP optimizasyon prosedürünün modelleme yaklaşımları hakkında kısa bir bilgi verilmiştir.

Bölüm 2, kupon yüzlerinin her iki tarafının da, galyum (Ga) zengin ve azotlu (N) zengin, karakterizasyonuna odaklanmaktadır. Bu karakterizasyon yöntemleri yüzey ıslanılabilırlığı, yüzey topografisi ve pürüzlülük, yüzey kimyasal bileşimi, yüzey yükü ve absorbans ölçümlerini içerir. Bu ölçümler, CMP prosesi sırasında meydana gelen kimyasal reaksiyonları ve ayrıca kuponların CMP performansının anlaşılması açısından kritik olan Ga ve N açısından zengin yüzlerin farklılıklarını ortaya koymaktadır.

Bölüm 3, hem deneysel hem de matematiksel olarak, GaN için etkili bir CMP sürecinin tasarımını özetlemektedir. Deney metodu, süspansiyon pH'ı, süspansiyondaki paracık oranı, süspansiyon akış hızı, uygulanan basınç, kimyasal bileşim ve süspansiyonun sıcaklığının etkilerini değerlendirir. CMP sonrası değerlendirmeleri, her bir deney için malzeme aşınım oranı ve yüzey pürüzlülüğü açısından değerlendirilir. Bu bölüm ayrca sürekli nötralizasyon yoluyla özünme reaksiyonunun kimyasal kontrolü ile bir süspansiyon havuzunu kullanan optimize edilmiş bir CMP aletini içerir. Son olarak, bölüm deneysel ölçümlere dayanan matematiksel optimizasyon için ön çalşma verir.

Bölüm 4, yüzey enerji ve yapışma çalışmalar da dahil olmak üzere detaylı yüzey analizleri ile CMP sonrası temizleme prosedürlerinin iyileştirilmesine odaklanmaktadır. Bu bölüm, farklı boyutlarda süspansiyon aşındırıcı parçacıklar kullanılarak farklı yüzey pürüzlülük değerleri elde etmek olan cam deneyleri ile başlar. Cam yüzeyleri, ıslatılabilirlik aısından değerlendirilmekte olup, yüzeyin ıslanabilirliği, CMP temizleme sonrası verimliliğini büyük ölüde etkilemektedir. Son olarak, partikülleri çıkarmak için viskoelastik sıvılar kullanan CMP sonrası temizlemesi için yeni bir yöntem eklenmiştir.

Son olarak, bölüm 5, tezin genel bir sonucunu verir ve gelecekteki çalışmalar için tavsiyeleri özetlemektedir.

ACKNOWLEDGEMENTS

TABLE OF CONTENTS

LIST OF TABLES

LIST OF FIGURES

CHAPTER I

INTRODUCTION

The improvements on microelectronics manufacturing following the Moores law require the transistor sizes to be reduced continuously and the devices to operate at higher voltages resulting in increased operational temperatures. As the crystallographic nature of silicon cannot meet these demands sufficiently anymore, new semiconductor materials are being investigated for advanced devices [Aid14]. Gallium Nitride (GaN) has become one of the promising semiconductors in manufacturing for the newly developed high voltage microelectronic devices due to its wide bandgap, high electron mobility in addition to the high temperature and voltage resistance [Lid14]. In particular, GaN is extensively used in light emitting diode (LED) applications are used extensively because of its direct band gap. However, in order to use GaN in such applications, the surface of the wafer must be planarized. For this process, chemical mechanical planarization (CMP), which is used for planarization of Silicon [Hon17] and many other semiconductors, is seen as one of the best choices in the literature [Shu04].

Based on the fact that the GaN as a material is chemically inert and a mechanically very hard, CMP applications take a very long time and become an expensive process due to the multiplicity of consumables used and the prolonged production process. Also, due to the fact that CMP process has numerous unknowns and the research about CMP of GaN is not as much established as CMP of silicon, the process is acknowledged to be much more difficult. The complexity of CMP is that, each material requires a unique slurry formulation, selection of a proper polishing pad, adjustment of slurry flow rate and pad and polishing head rotational velocity and

down force [Ban08]. On the other hand, even if the CMP process is properly implemented, post CMP cleaning performance still plays a critical role on the efficiency of the manufactured devices [Ste04]. It must be assured that the particles, particularly the ones with larger sizes ($\sim$ 1 micron) that tend to form due to agglomeration of primary slurry particles originating from the CMP slurry are effectively removed from the wafer surface post planarization.

1.1 Literature Review

1.1.1 Chemical Mechanical Planarization

The continuous efforts in the semiconductor industry to achieve better electronic devices at higher performance at lower unit costs drives the chemical mechanical planarization (CMP) process to provide planarization of larger wafer sizes (300 mm in x and y-axis) with nanoscale material removal removal in the z-axis. CMP is a process to flatten the wafer surface at the atomic scale to achieve multi-layer-metalization and it is supported by the chemical reactions and the mechanical actions. The CMP process was first used for planarization of the inter layer dielectrics (ILD), which were silicon dioxide layers. The integrated photolithography, metal deposition and metal etch, surface planarization [Oli04] processes of the metal and dielectric layers can limit yield of the electronic devices during the process of a microelectronics circuit (IC). Among the repeated processes, such as evaporation, sputtering, deposition, coating and etching, CMP process is the key to ensure global planarization [Ste04].

1.1.1.1 Brief History of CMP Process

CMP was first introduced in 1950 for minimizing the surface defects on the silicon wafers which are utilized to manufacture the IC devices [Bon77]. In 1980, CMP was implemented to planarize ILD layers by IBM and the first technical paper was published by B. Davari [Dav89]. Since then, application of CMP became a unit process and the steps and materials it is used for have gotten many more with current

utilization within the $20 - 30$ steps of modern IC manufacturing [Bab16].

1.1.1.2   Applications of CMP

CMP was preliminary developed for Shallow Trench Isolation (STI) and Inter Layer Dielectric (ILD planarization). As the new integration schemes and new materials are introduced to device design to meet the microelectronics industry demands, the application of CMP is continuously expanded. CMP is currently being implemented for materials such as, Al, Cu, Ti, W, TiN, polymers like SILK, porous SiO_2 to enable interconnection, passivation, stop layers for step height control as well as flat panel and packaging applications [Ste04].

1.1.2   CMP Process

In CMP process, there are many variable components including polishing head that transfers the load onto the wafer, wafer to be polished, the polymeric pad, polishing slurry and the pad conditioner. The wafer is held underneath the polishing head and then the wafer is pressured against the pad under an adjustable force to maintain a constant pressure on the wafer. In the meanwhile, the slurry containing formulation chemicals and nanoscale abrasive particles is fed to the system on to the polishing pad at a selected flow rate and the homogeneous distribution of the slurry is ensured by the pad and the conditioner that is designed to maintain the pad fibers active which are carrying the slurry underneath the wafer surface.

1.1.2.1   Pad

During the CMP process, the polishing pad plays crucial roles including the delivery of the slurry to the wafer surface and making sure that the mechanical load applied by the polishing head is transferred onto the wafer surface distributing the normal and the shear forces. There are four main types of polishing pads used for CMP. Felts and polymer-impregnated felts, porometrics, filled polymer sheets and unfilled

textures polymer sheets [Oli04]. Their micro structures differ and therefore they are applicable for different materials. In this thesis, polyurethane based top pad stacked by a more porous Suba IV was used, which is commercially named as IC 1000/Suba IV stacked pad. Multilayer or stacked pads are used in order to ensure better and uniform polishing through softer sub-pad yet by enabling planarization through the harder and denser top pad that is grooved to enable slurry transfer. Polyurethane pads typically have porous micro structures, which plays a crucial role in determining the density of the pad. The density of a pad is important, since the hardness and Youngs modulus of these pad are linearly correlated with the density of the pad.

The pad grooves help ensure the homogeneous slurry transfer throughout the wafer surface under the applied pressure. There are different groove types, circular grooves, XY grooves, logarithmic grooves are the main types among other types possible. The aim of these grooves is to decrease the hydrodynamic pressure formed by the slurry that may occur at the transfer to the pad-wafer interface [Doy04]. Commercial pads are usually made up of circular grooves and XY grooves. Groove depth, width and concentration directly affect the removal rate at high velocity to pressure ratios. In low velocity to pressure ratios, the groove design does not affect the removal rate as much as the high velocity to pressure ratios [Nag07]. It is also proven that with the non-grooved pad designs both the used and the fresh slurry tend to stay between the wafer and the pad interface, where with the grooved pads, the transportation of the new slurry is more effectively provided. On the other hand, the excess slurry causes decrease in the frictional forces, therefore decreasing the removal rate and hence an efficient slurry transfer is critical to CMP performance [Ili17].

1.1.2.2   Conditioner

The roughness of the CMP pad is related with the pad asperities and it is maintained by in-situ or ex-situ conditioning. The conditioner is used synergistic for keeping the

CMP pad fibers active against glazing and hence providing a homogeneous slurry flow. The conditioner itself is a metallic and round plate with diamond abrasives embedded it to through various patterns. When a conditioner is not utilized during the CMP process, the pad roughness decreases due to active glazing through the asperities wearing off and pad surface flattening. This would cause a decrease in the material removal rates [Her99].

The surface asperities of the pad increases the CMP removal rates yet the hard asperities also increase the possibility of scratches and defects on the wafer since slurry particles may get stuck on the asperities of the pad and may cause two body friction and gouge on the wafer surface [Lia97]. Among various kinds of pad conditioning types, diamond-impregnated abrasive disks are chosen to be the most effective ones. In order to stabilize the CMP process, initially a few blanket pilot wafers are processed to reach a stabilized material removal rate (MRR). This is done in order to open up the pores of the pad with DIW and conditioner and to start effectively distributing the slurry on the pad surface.

1.1.2.3 Slurry

CMP slurry is the key factor determining the process performance in terms of the material removal rate, surface quality. selectivity and global planarization. The slurry is fed to the system bu pumping, and it is carried to the wafer surface by the polishing pad grooves. Different materials and CMP processes require different formulations of CMP slurry, therefore, understanding both the physical and chemical aspects of the CMP slurry is very important. CMP processes such as interlayer dielectric (ILD) CMP, shallow trench isolation (STI) and metal CMP require different kinds of CMP slurries. For example, STI CMP requires the use of passivation agents for high selectivity and metal CMP requires oxidizers to form an oxidation layer on the surface to remove mechanically inert metal layers by the abrasives. Other than

these, the main function of the CMP slurry is to decreases the temperature on the wafer surface and to act as a lubricant and to serve as the carrier in order to remove the post polish by-products out of the wafer surface instantaneously. The type of abrasive particles used in the slurry, the size of the abrasives, concentration of the abrasives, surface charge of the abrasive particles, pH of the slurry, zeta potential of the slurry and the temperature of the slurry highly correlate to the removal rate mechanism.

The abrasive particles in the slurry provide mechanical component and selected among mostly alumina, silica, ceria or diamond. The weight percentage, particle size, shape and possible agglomerations due to the surface charge of the abrasive particles have effects on material removal rate and surface quality of the polished surface. As the previous literature indicates without the abrasive particles, or the presence of effective slurry chemistry there would not be any material removal [Coo90].

In this thesis, silica abrasives are used for chemical mechanical planarization (CMP) of Gallium Nitride (GaN). Silica abrasives are generally used to ILD, STI CMP and metal CMP. Two types of silica abrasives can be used; colloidal silica or fumed silica. Colloidal silica particles can be manufactured with a desired size, shape and homogeneous distribution through hydrolysis of metal organic precursors. Fumed silica on the other hand, is made by flame prolysis of silicon tetrachloride. It is inexpensive, it can provide high purity and it has a simple synthesis procedure. However, it has a higher tendency to agglomeration due to its network structure forming possibility in aqueous media because of the weak hydrogen bonding. The TEM images of both silica particles can be seen in Figure 1.1 [Zha12].

The size of the abrasive particles has an important effect on the surface quality of the wafer, where as the size of the abrasive particles increase, the possibility of scratches and defects on the wafer surface increases [Rem06]. However, there are contrasting findings on the effect of the size of the abrasive particles on the removal
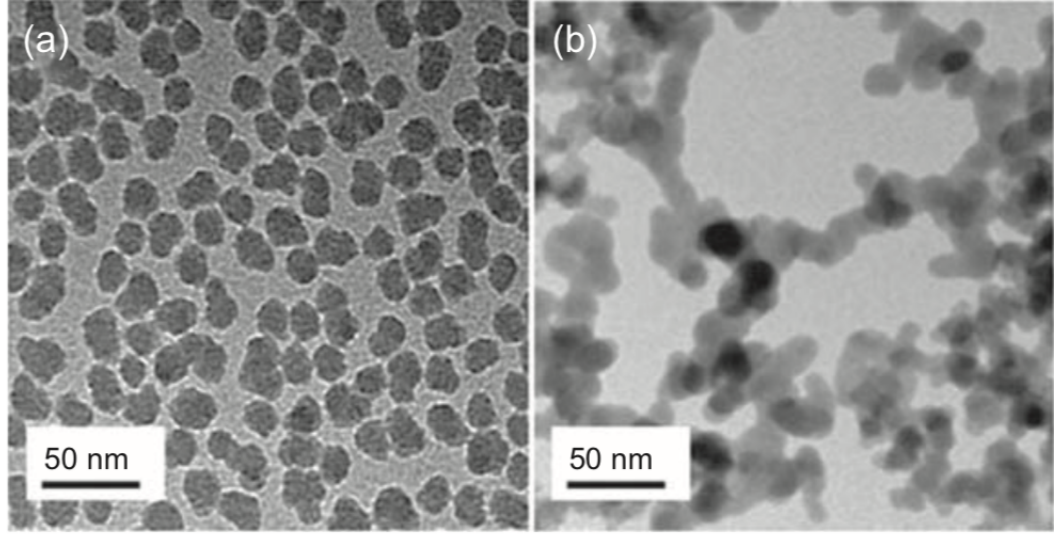
Figure 1.1: TEM images of (a) colloidal silica and (b) fumed silica [Zha12].

rate. Bielmann reported that the removal rate of Tungsten (W) film increases as the size of the abrasive particles decrease [Bie06]. On the other hand, Tamboli reported that the removal rate should increase as the size of the abrasive particles increase [Tam04]. However, as the permission for maximum number of defects decrease as the device dimensions decrease, smaller abrasive particles are selected in order to lower the number of defects on the wafer surface. In order to increase the material removal rate with smaller sized abrasive particles, higher concentration of particles are generally selected due to the relation of total area of contact (A) with solids concentration (C_o) and particle size (ϕ) as expressed in Equation (1.1) below [Bie98].

$$A \propto C_o^{1/3} \phi^{-1/3} \tag{1.1}$$

Zeta potential (ζ), is used as a measurement of stability of the particles. It is the electric potential at the slipping plane of a particle and it is not equal to Stern or surface potential, while they are measured at different locations than the zeta potential. Zeta potential is considered to be the effective charge on the particle, while during the transport process, ions are mostly carried within the slipping plane.
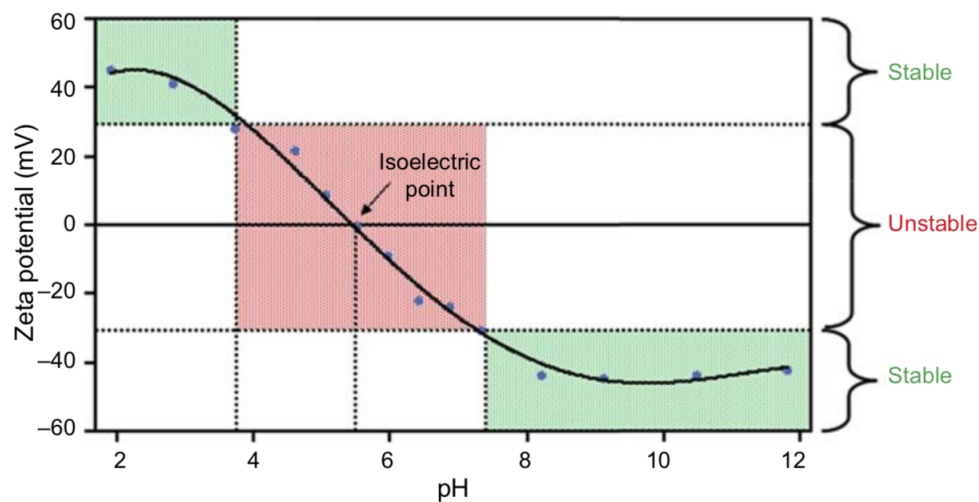
Figure 1.2: Zeta potential change with increasing pH [Bab16].

One should keep in mind that, altering the pH of a slurry, may provide benefits for the CMP process, however, it can also cause destabilization of the slurry, which may cause agglomeration; while the zeta potential of a particle changes with the pH of the medium. Figure 1.2 shows that the possible change of zeta potential with increasing pH. As it is seen on the graph, at the isoelectric point, when zeta potential is zero, the particles are no more stable [Bab16].

In addition to the aforementioned variables, slurry temperature affects the removal rate as well. During the CMP process, temperature may increase due to the heat generation via friction [Fra10], exothermic reactions between the material surface and the slurry chemicals [Cor03] and while pumping or mixing of the slurry. Temperature increase may cause non-uniform polishing and defects on the wafer surface by varying the pH of the slurry and surface charge of the abrasives. Therefore the temperature change should be observed and controlled during the CMP process.

1.1.3 Compound Semiconductors

A compound semiconductor is a semiconductor made up from two or more elements as the name implies. Common elements used for compound semiconductors are; gallium
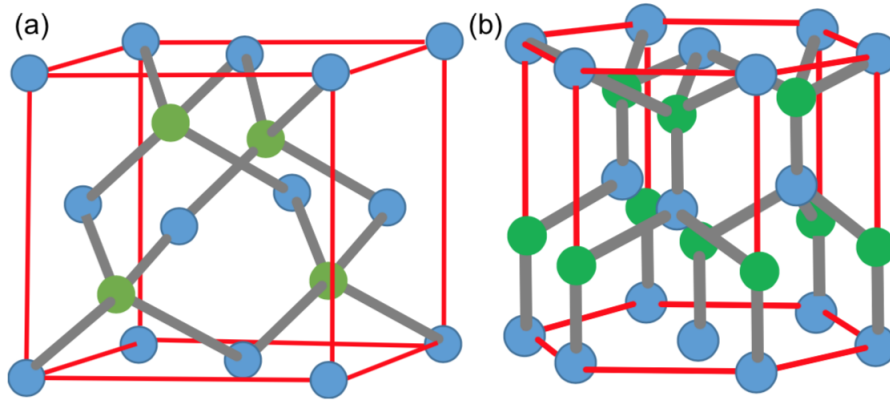
Figure 1.3: (a) Zincblende and (b) wurtzite structures [Hau16].

arsenide (GaAs), gallium nitride (GaN), indium phosphide (InP), zinc sulphide (ZnS), zinc selenide (ZnSe), silicon carbide (SiC) and silicon germanium (SiGe). Compound semiconductors are used in many applications were silicon is not sufficient due to its crystallographic orientation, while they have higher number of electrons, direct band gap and excellent thermal conductivity and they can sense and emit light and generate microwaves [Kue16]. The reason that it took very long time for compound semiconductors to be manufactured at high volumes is because of the difficulties in growing compound crystals, high number of defects in the crystals, higher fragility of the crystals and higher cost of manufacturing as compared to the silicon [Hau16].

The binary semiconductors are generally from Groups III-V and II-VI of the periodic table. Most of them have zincblende or wurtzite structures, which are shown in Figure 1.3.

Semiconductors are usually classified by their lattice parameters and band gaps. By using their similarities in chemical structures and properties, these materials can be grown on top of each other by a heteroepitaxial growth [Kue16]. The importance in growth of these materials is that the lattices of these materials should match and a minimal interfacial and surface defect level are obtained. Also, relative alignment of both the conduction and valence bands should be provided within the heterointerface.

1.1.4 Application of GaN in Electronic Devices

GaN is used for the high power, high temperature and high frequency microelectronics device manufacturing due to its wide bandgap energy and high electron mobility including heterojunction field effect transistors (HFETs) and its derivatives (Metal Oxide Semiconductor HFETs-MOSHFET and Metal Oxide Semiconductor Double HFETs- MOSDHFETs) as a barrier layer [Sim04], high electron mobility transistors (HEMTs) for power switching with AlGaN/GaN stacking as a buffer layer [McC04] as well as for the applications for heterojunction bipolar transistors (HBTs) and bipolar junction transistors (BJTs) [Pea00].

The advantageous property of GaN is that it has a hexagonal structure, which is called wurtzite, due to this structure, it is chemically stable and withstand high temperatures without decomposing into its components [Shu04]. In addition, GaN is suitable for photonics device manufacturing based on its direct bandgap. As the bandgap is related with the strength of the chemical bonds, these stronger bonds require more energy for an electron to jump from one site to another one. It is designed into the light emitting diodes (LEDs) and ultraviolet LED (UVLED) manufacturing as an active region [Wan11, Nak13]. Also, the high thermal conductivity of GaN makes it applicable for high power devices, where the material should be able to distribute the heat generated uniformly [Edg11].

GaN has wider band gap, higher critical electrical field capability and higher electron mobility than silicon as shown in Table 1.1. Therefore, using GaN transistors instead of silicon, improved devices in many ways; such as improvement of switching speed, less penalty in on-resistance and higher electron mobility. The increasing switching frequency enabled manufacturers to decrease the size of the devices keeping the efficiency of the device same [McC04].

The basis of the HEMT devices is the electron mobility in high concentration of electrons, which is created by depositing another layer on GaN layer. This can

Table 1.1: Comparison of GaN and Silicon [McC04].

Parameter	Silicon	GaN
Band Gap Eg [eV]	1.12	3.39
Critical Field E$_c$rit [MV/cm]	0.23	3.3
Electron Mobility [cm^2/V-s]	1400	1500
Thermal Conductivity [λ]	1.5	1.3

be achieved by depositing a thin layer of AlGaN on top of GaN. The deposition of AlGaN layer causes a shift in the atom placement, which causes a strain to form at the interface generating an electric field. This strain induces two dimensional electron gas (2DEG) and the higher the strain, the higher is the electric field [McC04].

1.1.5   Growth of GaN

The growth of thick and crystalline GaN films is very challenging due to the formation of the threading dislocations between the selected substrate and the GaN interface that can act as the short-circuit leakage paths [Shu04]. Furthermore, it is also known that GaN films tend to crack above a critical thickness, which can even lead to the film and the substrate to fracture into separate pieces [Etz01]. Many conventional deposition techniques fail to satisfy the defect free deposition of GaN on conventional substrates such as silicon. Therefore, substrates such as ZnO and SiC are experimented which have the same crystal structure as GaN (wurtzite) [Hel96, To98]. The Ga-rich face of GaN [0001], tends to grow on Zn and C on the ZnO and SiC substrates, respectively [To98]. Whereas, the N-rich face grows on the O and Si faces. Between these, SiC is a more suitable substrate for the commercial applications. The crystallographic polarity of the GaN affects the device properties as well as the chemical and mechanical response of the GaN surface in addition to the proper growth of the desired film [Hel98]. It is further reported that the N face GaN tends to be rougher as

compared to the Ga-face due to the nucleation mechanism driven by low atom mobility on the N-face as compared to the Ga-face during the deposition. The utilization of plasma assisted molecular beam epitaxy (PAMBE) deposition was investigated to optimize the surface smoothness of the N-face by implementing additional control parameters [To98]. Yet, it is clear that any investigation of the GaN surface treatment, such as CMP, has to take into consideration the polarity of the GaN substrates as well as the proneness of the GaN to fracturing under the applied forces.

1.1.6   Chemical Mechanical Planarization of Gallium Nitride

Gallium Nitride (GaN) is a III/V compound semiconductor material which can be used for manufacturing high power, high voltage and high temperature and wide range of microelectronics devices. It was introduced in high electron mobility transistors (HEMT) in 2004 by Eudyna Corporation by depositing GaN on SiC for radio frequency market (RF). Then in 2009, GaN field effect transistors (FET) were introduced as a power metal oxide silicon field effect transistor (MOSFET) replacement [Lid14].

The development of GaN can be divided into as bulk crystal growth technology and substrate processing technology where the produced bulk crystal is formed for device growth and later device-chip processing. The issue of producing bulk crystal GaN is almost resolved, whereas development of processing the bulk crystal growth is way behind, because the final atomic-level smoothness is hard to achieve. As the application of GaN in various transistor types require polishing and optimal planarization of the GaN layers, CMP is the method of choice due to its capability of enabling nanoscale smoothness on the wafer surfaces in addition to enabling material and topographic selectivity through advanced slurry formulations [Bas11]. Yet, the main problem in integration of GaN is related to the challenges in its defect free deposition and its hard and brittle nature, which makes it difficult to polish and planarize in an

integration scheme without creating surface defectivity (which can be defined as the elevated surface roughness, scratches, local pitting and protrusions, slurry particles and particles from the surroundings that might be left on the wafer surface).

1.1.6.1 Developments in CMP of GaN

Implementation of CMP on GaN planarization has long been studied with much better success as compared to the purely mechanical polishing methods [Wey97, Gon15]. Since the pure chemical dissolution rate of GaN is negligible, the mechanical removal provided by the submicron size abrasive particles was noted to be very critical for GaN removal after a chemically modified layer is formed on the surface [Gon15]. In 1996, bulk crystal GaN growth was done by Karpinski using a high temperature, high pressure synthesis which is called high pressure solution growth (HPSG) [Kar84]. At this time, the surface defects were removed by diamond particles and wet etching. Chu [Chu71] and Pankove [Pan72] implemented wet etching on GaN thin films and later on, Zhuang used wet etching for removing surface defects on bulk crystal GaN. However, the surface finish after wet etching process is limited by the rate of diffusion [Zhu05], and scratches were observed on the wafer surface, even though fine diamond abrasive grains were used [Bab16]. Although, using wet etching and mechanical abrasion techniques were sufficient for obtaining a flat surface, it was not possible to achieve an atomic-level flatness.

In 1997, Weyher published the first paper regarding a damage free flattening of GaN, where he combined wet etching and polishing to planarize crystal GaN using a KOH solution on a soft polishing pad [Wey97]. Later on, in 1998, Porowski, using the same method, polished GaN substrate which was produced by homoepitaxial growth. The material removal rate was 1.3 m/h at a 2-6 kg/cm^3 pressure [Por98]. However, the pressure found to be very high, and it was thought that mass production would be very limited due to this high pressure [Bab16]. Although dry etching results in higher

material removal rates, wet etching is a more favorable process then dry etching, because plasma induced damage occurs in dry etching.

In 2002, Tavernier focused on the CMP of GaN with colloidal silica slurry [Tav02]. During this time, it is observed that the dislocation density of GaN crystal can be estimated via CMP, while CMP slurry introduced etch pits at crystal dislocation positions [Xu03].

In 2008, bulk crystal GaN growth was established at a certain level by hydride vapor phase epitaxy (HVPE) growth, therefore a high demand has formed on the processing technology of GaN. Hayashi et al. reported a CMP procedure using alumina particles in an alkali solution, sodium-hypochlorite [Hay08]. Then in 2009, Yan et al. published a paper on CMP of GaN via diamond embedded soft pad with a KOH based alkali solution [Yan09]. As both diamond and alumina particles are harder than GaN, scratches were formed on the surface. On the other hand, in 2011, Aida et al. reported a CMP procedure employing colloidal silica slurry, which is softer compared to GaN [Aid11]. The preliminary investigations held by using silica based slurries and KOH or NaOH based pH adjustment of this study, have shown improved polishing rates as well as surface quality post material removal. A removal rate of 17 nm/h (2.83 Å/min) was reached with 0.1 nm of average surface roughness (Ra) after 40 hours of polishing [Aid11]. It was noted that the main challenge in reducing surface defectivity is driven by the initial poor surface quality of the substrate as the substrate surface quality strongly depended on the growth conditions. Furthermore, the polarity of the bulk and epitaxial GaN films was also outlined as the difference in driving the variability in the surface roughness post CMP. The Ga face of GaN is altered to form Ga_2O_3 on the surface, which is removed by the relatively harder slurry abrasive particles [Gon15]. By using acidic slurry (pH 2) and adjusting the slurry solids loading, 0.65 nm roughness (Ra) and 165 nm/h (27.5 Å/min) removal rates were obtained on the Ga-side. The removal mechanism on the N–side GaN is

also very well described as formation of nitrogen terminated layer with one negatively charged dangling bond on each nitrogen atom, adsorption of hydroxide ions, formation of oxides and dissolution and removal of the oxides [Tav02, Gon15]. Again by using silica-based slurry, the material removal rates were reported to vary from 400 to 1100 nm/h (66.7 to 183.3 Å/min) and the surface roughness values within 0.4–1.1 nm range (RMS–root mean square) were reached [Tav02]. Alumina based slurries in the presence of sodium hypochloride (NaOCl) on the other hand, resulted in residual particles to be left on the surface and required a buff step for post CMP cleaning while removal rates of 50 nm/min (8.3 Å/min) were obtained [Hay08]. More recent study comparing the alumina versus silica slurries in the acidic pH range in the presence of potassium permanganate ($KMNO_4$) as an oxidizer concluded that 39 nm/hr (6.5 Å/min) and 85 nm/hr (14.17 Å/min) removal rates were obtained with silica and alumina slurries, respectively. The root mean square (RMS) roughness values were reported to be 0.13 nm [Khu14]. By adjusting the slurry flow rate, the authors were able to improve the removal rates to 228687 nm/hr (380–114.5 Å/min) with a 1 nm RMS roughness obtained [Par17]. The use of metal (Fe^{+2}) catalyst, [Zou15] as well as conducting GaN CMP under UV light by using photocatalytic titania (TiO_2) nanoparticles as abrasives [Jie16] have been observed to increase the GaN removal rates on the Ga–face of the material.

1.1.7 Post CMP Cleaning

After the CMP process, slurry particles may remain on the surface of the wafer and cause defective devices due to electrical shorts and problems with the process integration. Mainly the larger size agglomerates of the primary slurry particles are the most concern due to the fact that they definitely kill the yield. Other than slurry particles, pad material and diamond particles from the conditioner may remain on the wafer surface and result in defects as well. The resulting defects tend to cause additional

problems in further processing steps which would affect the functionalization of the IC. Hence, post CMP cleaning to be implemented in order to reduce these defects. Post CMP cleaning has an important role in IC manufacturing since over 50 % of the yield loss is typically resulted from the contamination of the microelectronic devices on the processed wafers [Zha00].

There are four main contamination types, which are; particles, metallic, organic and other defects. These contaminations have different effects on wafer production. Particle contamination (i.e. silica) blocks photolithography by causing local roughness and cause short circuits by conductive particles. Metallic ions contamination (i.e. K^+, Ca^+) influences electrical characteristic of the device because the metal ions with high mobility, and noble metal ions may cause etching of Si and they also contribute to the doping of the materials. Organic contamination (i.e. salts, buffers, surfactants) affects wettability and surface energy of the surface to be planarized, therefore may result in poor adhesion of the deposited layer. The other process by-product contaminations, such as scratches and stress, cause nonplanar surface and serve as locations to deposit undesired molecules and materials [Zha99].

There are three main types of post CMP cleaning. The first one, batch cleaning is applied on a batch of wafer at the same time and usually there is no direct contact between the wafer surface and any cleaning apparatus. The second one, brush scrubbing is applied on a single wafer of a lot one by one, where a rotating brush comes in contact with the wafer surface with a lubricating chemical solution between them. Finally, the third one is megasonic cleaning, where the sound waves apply a drag force on the particles, without any direct contact by another apparatus. All three types of post CMP cleaning procedures are explained in the following.

16

1.1.7.1 Batch Cleaning

Batch cleaning utilizes a cassette of wafers names as a lot (one cassette generally contains 25 wafers), immersed in different tanks filled with different cleaning chemicals, in a specific order and time [Ker90]. Wet batch cleaning has some advantages and disadvantages. The advantage of using this method is that, the method comes with a low cost, a uniform contact of the cleaning chemical and both sides of the wafer is obtained and a good temperature control can be provided [Ruz06]. However, the disadvantage of this method, is that it requires high amount of chemicals and water consumption. Also, the method is mainly inadequate for removing particle contamination, although it is efficient for removing metallic impurities, organic contaminants, and soluble materials [Ker90]. On the other hand, in wet batching, impurities from the wafer cassette may be generated as well. This is tried to be prevented by replacing automatic wet benches by the manual ones [Kes15].

The regular process order in wet batch cleaning has four main steps and rinsing the wafer cassette with DIW is done between every step. The first step utilizes an alkali solution with a pH of 10-11. This alkaline pH, forms HO_2^-, which is a strong oxidant with the potential to remove organic contaminants from the wafer surface [Ola03, Zha01]. The second step uses an acidic solution with a pH less than 1. This acidic solution is used since it can dissolve any metal ion. After these steps, a thin oxide layer is formed due to oxidizing nature of the cleaning chemistries. To remove this oxide layer, dilute HF solution is used, which also removes metallic contamination inside this oxide layer. The last step is the drying process, which is done by placing wafers in isopropyl alcohol-water mixture at high temperatures [Ker90, Ker87].

Two main developments have been made on cleaning chemicals until now. The first one was implemented by Abbadie et al., in 2004, in automatic wet bench process. Two more cleaning procedures have been introduced by Abbadie, by utilizing ozone and acidic solution and the process is called HF–ozone process. The results show
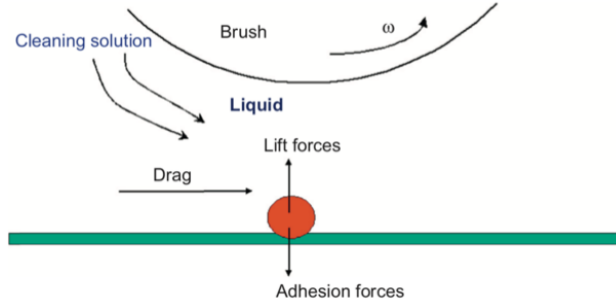
Figure 1.4: Brush Scrubbing [Tal90].

that a wafer surface protected by a chemical oxide, which is atomically flat, can be achieved with a reduced particle and contamination level. Also, they have proven that the particle contamination is reduced by the help of acidic media in the beginning of the cleaning process [Abb04]. The second development was introduced by Tseng et al. in 2003, by a hybrid cleaning process, where the wet batch cleaning using megasonic is combined with brush cleaning. They have shown that the hybrid cleaning process combining both acidic and basic solutions, results in 60 % reduction in CMP generated defects [Tse03].

1.1.7.2 Single Wafer Cleaning - Brush Scrubbing

Hydrodynamic removal is generated in brush scrubbing by the rotation of a nylon or a polypropylene brush rotating across the surface of the wafer to remove particulate contaminants and organic films. This type of cleaning can generate drag force and electrostatic double layer across the wafer surface [Che06]. The movement of the brush across the wafer surface generates a thin fluid film, which provides rolling of the particles. The fluid film prevents any scratches on the wafer surface that may occur during the contact of the brush [Bow95]. Also, the temperature gradient formed between the wafer surface and the particles generate forces against the adhesion forces of the particles. The figure 1.4 illustrates the forces generated on the particle [Tal90].

The disadvantage of brush scrubbing is that it is inadequate for particles smaller

than sub-micrometer sizes. However, the organic solvents used during brush scrubbing, help remove organic films and speed up the drying process. On the other hand, other than organic solvents, chemicals such as; water, surfactants, ammonium hydroxide solution, IPA, methanol and others can also be used in the cleaning process [Zha98, Xu04, Roy95].

The design of the brush is very crucial in brush scrubbing, while it determines the capability of the cleaning procedure on different geometrical features of the wafer surface. Improper design of a brush may cause clogging of the brush and damage to the wafer surface. Therefore, another disadvantage of the brush cleaning is that proper brush design is required and regular maintenance and replacement of the brushes should be done [Kes15].

The removal of the particle occurs in three modes; non-contact, semi contact and full contact [Bus02]. In non-contact mode, the brush does not come in contact with the particle, and it generates a fluid movement, where the velocity gradient is maximum at the brush surface and zero on the wafer surface due to no-slip condition. The generated flow of the fluid exerts a hydrodynamic force on the particle and causes rolling, and removal of the particle. In semi contact mode, the distance between the top surface of the particle and the bottom surface of the brush is zero, therefore their velocities are the same, and the particle moves with the brush. Finally, in full contact mode, the brush moves the particle by creating a rotational torque on the particle. However, scratches and defects are expected to form on the wafer surface during the full contact mode.

In 2004, Philipossian and Mustapha investigated the tribological aspect of brush scrubbing on thermally grown silicon dioxide films on Si wafers. They investigated effects of applied pressure on wafer, pH and flow rate of the cleaning solution [Phi04]. They explained tribological characteristic by the coefficient of friction (COF), which is known as the ratio of shear force to the normal force. Then, they compared COF
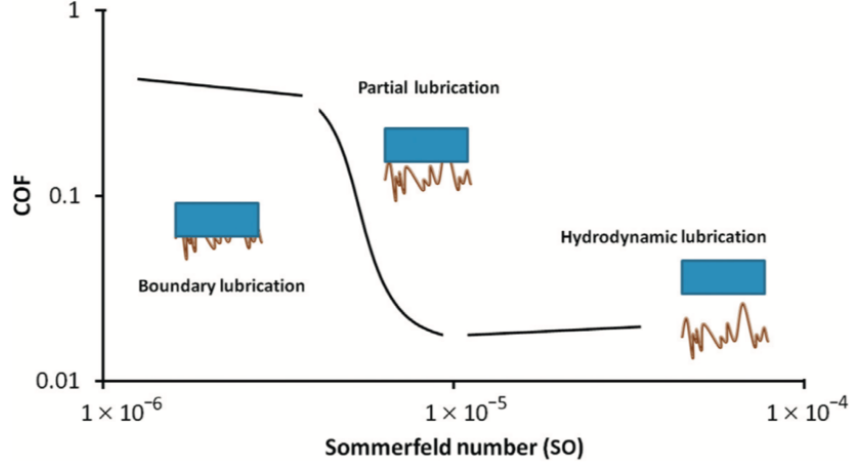
Figure 1.5: Sommerfeld Number [Tal90].

to a dimensionless number, which is called the Sommerfeld number (So) as shown below:

$$So = \frac{\mu * U}{P * h_{eff}} \qquad (1.2)$$

where, is the viscosity of the cleaning solution, is the relative of velocity between the brush and the wafer, is the applied pressure and is the effective thickness of the fluid film thickness between wafer and brush. The relationship between COF and So is shown in Figure 1.5.

As seen in the graph, at low So number, COF is high, which means the distance between the wafer and the brush is very low, with a very small amount of fluid between them. When the So number is at intermediate values, the distance between the wafer and brush is almost the same as the brush surface roughness. Finally, in hydrodynamic lubrication regime, the fluid layer thickness is much larger than the brush surface roughness, where there is almost no contact between the wafer and the brush.

To conclude, an optimum level of shear force is needed between the wafer and the brush in order to provide particle removal, while a low shear force will be inadequate to remove particles and a high shear force, which means high downward force, will

cause scratches and other types of defects on the wafer surface [Aid14]. In order to provide particle removal and smooth surface finish, high rotation speed of brush can be used at low downward forces.

1.1.7.3   Megasonic Cleaning

The demand on removal of particles from a polished surface without causing damage is critical and continuously increasing. However, the limitation of using aggressive chemicals to prevent material loss promotes using dilute chemicals. Therefore, the particles are tried to be removed by physical forces, such as drag force, instead of chemical reactions [Hat98]. In 1985, Schwartzman, Mayer and Kern introduced megasonic cleaning, where only a physical force is applied on particles without affecting the wafer surface mechanically [Sch85].

The most important benefit of megasonic cleaning is that it decreases the boundary layer thickness, which enables chemical reactions to take place at the interface, and within the boundary layer, the particles are forced to roll by the viscous forces.

In 1999, Moumen et al. focused on the power, temperature and time of the megasonic cleaning procedure applied on a polished thermal oxide wafer. It was proven that in the study using optimum parameters, a low defect cleaning procedure can be obtained. The wafers were polished with a silica based slurry and then cleaned in a megasonic tank with standard cleaning one (SC-1) solution at a frequency of 850 kHz. They modified the SC-1 solution, and used components in a ratio; $40(H_2O)$: $2(H_2O_2)$: $1(NH_4OH)$ [Mou99]. Their results showed that the cleaning procedure is not efficient when the cleaning time is higher than 8 minutes, and further experiments showed that the acoustic power they have used was above the threshold limit for the particle removal [Bus02]. On the other hand, the temperature was observed to be very effective on particle removal.

1.1.8   Experimental Optimization

The objective of the experimental optimization is to maximize the material removal rate and to minimize the surface roughness. In this thesis, experimental optimization is done via changing only one variable and keeping all the other variables the same. The advantage of experimental optimization is that it gives a correlation between the inputs and outputs, however it takes a longer time compared to mathematical optimization. In this thesis, inputs are selected to be; pH of the slurry, slurry solids loading, slurry flow rate, pressure, slurry temperature, chemicals added into the slurry. On the other hand, the outputs are selected as the material removal rate and the surface roughness. The variables are selected to be discrete while the number of experiments are limited by the number of samples. The minimum and maximum values of the input variables are determined due to available resources, such as abrasive particle concentration in the slurry and flow rate (where higher flow rates are provided by an external pump).

In order to reduce possible errors caused by the environmental factors, slurries are prepared by the same procedure at room temperature, the experiments are done in the same day, the polishing pad is cleaned every time (to minimize the possible defects because of the clogging of the polishing pad grooves.

1.1.9   Mathematical Optimization

To perform the mathematical optimization, the physico-chemical principles are initially investigated by the experimental optimization and developed into an equation according to these proven correlations. Using the constructed equation, rather than changing the input variables one by one, all of the input variables are changed simultaneously. By using mathematical optimization, the response of changing all the input variables at the same time is observed. Since the CMP procedure requires the maximization of material removal rate and minimization of the surface roughness, the

mathematical optimization brings the advantage of optimizing the input variables for both demands at the same time.

1.1.10 Modeling CMP

Although CMP is used in various steps in IC production, unexpected process performance results can be obtained for which numerical modeling can be implemented. There are various modeling approaches which focus on only one or two aspects of the CMP procedure. Most of them focus on the slurry flow behavior, the abrasive particles found in the slurry or the input variables, such as flow rate. Typically these modeling approaches are performed at micro-scales. Also, the Preston equation is widely used as the abrasive wear model in CMP modeling [Pre97]. However, Preston equation only takes the applied pressure and relative velocity into account, where many other variables such as, the chemicals used, consumption of polishing pad, slurry properties composed of nano-scale abrasives are neglected. That is why the MRR cannot be determined by this equation precisely. Therefore, Cook published a paper in 1990, explaining other factors affecting the CMP procedure [Coo90]. Cook stated that the polishing rate of glass is determined by five main factors, where he showed that the water diffuses into the glass surface, forming a dissolved surface, and this dissolved surface is removed by the abrasive surface.

1.1.10.1 Preston's Law

Many CMP models use the simplified equation of Prestons Law, where it evaluates material removal rate (MRR) function to be linearly proportional to applied pressure and velocity. However, this approach is not completely adequate for the CMP process, since it only covers the mechanical wear and does not include the chemical effects of the CMP procedure, such as bonds formed during the process, chemical etching and temperature sensitivity. It also neglects the fluid movement and its effects in between the pad and wafer surface.

The Preston equation is stated as in Equation (1.3);

$$\frac{dz}{dt} = -k_p pv \qquad (1.3)$$

where z is the film thickness removed, t is time, p is pressure, v is velocity and is the Preston coefficient [SM97]. Even if the Preston coefficient can stand for the surface and slurry chemistry and also all the other chemical reactions occurring during the CMP process, the equation assumes that the pressure applied is uniform among the wafer surface, however the experimental results show that there is a non-uniformity in the local pressure based on the wafer pattern. Therefore, it can be said that the CMP process cannot be modeled accurately based on such a simplified model.

1.1.10.2   Analysis of Fluid Flow Between the Wafer and the Polishing Pad

There are three possible forms in which the relative wafer and pad motion will occur. These are solid interaction, partially solid and partially hydrodynamic interaction and pure hydrodynamic interaction [Ste04]. In pure solid interaction, fluid flow occurs at a minimum level, therefore only mechanical forces act upon polishing. The temperature increases with the friction forces. In other cases, fluid flow differs by the pad wafer relative velocities. As mentioned before, if the pad wafer relative velocity is low, there would be partial solid and partial hydrodynamic behavior and if the relative velocity is high, hydrodynamic forces would be dominant. The thickness of the fluid layer determines if there is a contact between the wafer and the pad. If the roughness of the pad is the same as the fluid layer thickness between the wafer and the pad, then it is assumed that they are in contact. Also, the fluid is assumed to be continuous or partial in these two cases.
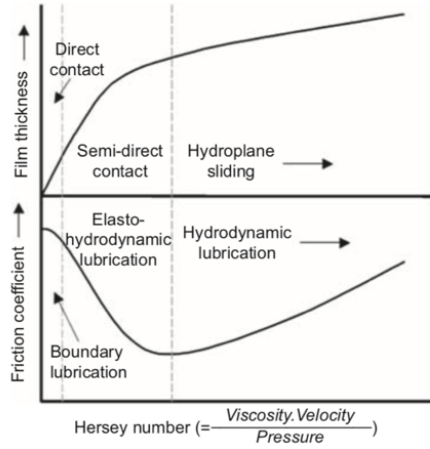
Figure 1.6: Stribeck Curve [Moo99].

1.1.10.3 Stribeck Curve

Stribeck curve (Figure 1.6) explains the relationship between the friction forces formed on the wafer surface and the fluid film thickness by relating this thickness to a constant called Hersey number. The equation of Hersey number is given below as in Equation (1.4) [Moo99].

$$\text{Hersey Number} = \frac{\text{Viscosity} \times \text{ Velocity}}{Pressure} \tag{1.4}$$

In Hersey number, viscosity stands for the fluid viscosity, velocity is the relative velocity of the wafer and the pressure is the applied down pressure by the head.

Stribeck curve shows that the friction coefficient decreases as the fluid film thickness increases when the relative velocity is increased. Stribeck curves can be interpreted within the removal rates in that as the film thickness increases (when the down pressure decreased or the relative velocity increased), the MRR tends to decrease due to the fact that there is less chance of wafer and pad asperities to interact [Bab16].

The boundary layer is formed between the wafer and slurry acts as a diffusion barrier and inhibits chemical reactions. Therefore, the boundary layer should be eliminated by CMP to accelerate chemical reactions. The boundary layer is defined as the thickness from the wafer surface to the layer where the velocity as at maximum. At the wafer surface, the velocity is assumed to be zero according to fluid dynamics, and increases as it goes away from the surface. The problem occurs, because the new slurry is at the layer where the velocity is maximum, therefore, the reactant molecule concentration is highest at this layer and it decreases as it goes to the wafer surface. The boundary layer thickness is given by the formula in Equation (**??**);

$$\delta = \frac{2}{3}L\sqrt{\frac{\mu}{\rho U L}} \tag{1.5}$$

where L is wafer length, is fluid viscosity, is fluid density and is maximum velocity of the fluid. However, this formula is valid for slurries without particle, the existence of particles would change the behavior of the boundary layer.

1.2   Summary

CMP was first introduced in 1950 for minimizing the surface defects on the silicon wafer utilized to manufacture the IC devices. However, as the device dimensions decreased, the capability of Si became insufficient due to its crystallographic orientation and material properties. Therefore, for applications requiring high temperature, high frequency and wider band gap, compound semiconductors are started to being used, which are generally composed of III/V or II/VI elements. Although, compound semiconductors are capable of providing the demands of new applications, most of them are chemically inert, mechanically hard and the growth of these semiconductors are more expensive and harder compared to Si. Therefore, the CMP procedure should be modified in order to be able to planarize the surface of the compound

semiconductors. The procedure is composed of the polishing pad, the chemically activated slurry containing abrasive particles, diamond pad conditioner and the head that holds the wafer to be polished. The wafer is pressed on to the rotating polishing pad with a constant pressure applied by the rotating head, and the polishing pad is conditioned by the diamond conditioner while the slurry is fed to the system by a determined flow rate. The type and the aging of the polishing pad plays a crucial role in determining the removal rate of the wafer, while the slurry is sent to the interface between the wafer and the polishing pad by the grooves of the polishing pad. The pH and the temperature of the slurry, types of abrasives used in the slurry, the concentration of the abrasives are important parameters for material removal rate and the surface quality while these parameters effect the stability of the slurry and the abrasive particles. This thesis focuses on the CMP of GaN. GaN is used in many applications such as microelectronics and photonics. However, polishing the surface of GaN without disturbing the single-crystal atomic arrangement is very hard due to it's unique properties. Also, the academic know-how on CMP of GaN is very low compared to Si, while understanding the surface processing properties of GaN was first established in 1996. Modeling approaches have been made for CMP procedure, although modeling approaches are not able to reflect the real life problems faced during the CMP procedure, while all the parameters could not be considered in the models. Therefore, gathering the information of the experimental procedures, analytical correlations between the inputs and outputs can be found to optimize the CMP process. On the other hand, as the device dimensions decrease, the permission of minimum surface defects decrease as well, therefore post CMP cleaning should also be considered. While removing particles from the surface during post CMP cleaning, the surface quality should be protected. There are various methods to conduct post CMP cleaning, however a new way of post CMP cleaning should be provided, while the current methods are insufficient.

CHAPTER II

PRELIMINARY SURFACE CHARACTERIZATION OF GAN WAFERS

2.1 *Introduction*

Preliminary surface characterization was conducted on the GaN wafers to observe material properties such as crystallographic orientation, material composition and wettability. The characterization of the wafer surface makes it possible to design a CMP procedure to optimize the process efficiency. Surface characterization methodology also allows to observing the changes occurring on the wafer surface after the CMP process as compared to the baseline film. The comparison of the surface characteristics before and after the CMP implementation makes it possible to explain the effects of polishing process on the wafer surface.

GaN bulk coupons were characterized on both Ga-rich and N-rich faces thoroughly in order to evaluate their CMP performances in terms of material removal rates as well as the pre and post polish surface quality. Both crystallographic faces were tested for wettability, surface energy and work of adhesion in addition to the FTIR/ATR surface scans and surface charge values, which were correlated to their CMP behavior as a function of the slurry pH and temperature as a preliminary evaluation.

In this chapter the GaN coupons were characterized for wettability, surface topology (root mean square rms) roughness), surface chemical composition and surface charge as a function of the crystallographic orientation.
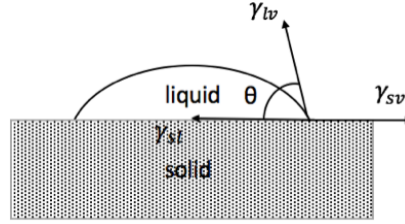
Figure 2.1: Sessile-drop contact angle method.

2.2   Experimental

2.2.1   Wettability Characterization

Surface wettability analyses were performed by using a KSV ATTENSION Theta Lite Optic Contact Angle Goniometer utilizing the sessile drop method. Contact angles of five drops of DI water were measured on each sample and the averages were reported with the standard deviation values. The drop images were stored by a camera and an image analysis system calculated the contact angle (Θ) from the shape of the drops. Surface free energy (SFE) and the work of adhesion (Wa) were calculated by using acid-base method after measuring contact angles with liquids of different polarity as given in the literature (ethylene glycol, formamide, glycerol and DI-water) [Bar09]. The surface free energy and the Wa are helpful in determining the propensity of particle adhesion on the wafer surfaces as well as the material removal potential based on surface chemical modification.

2.2.1.1   Contact Angle Measurements

Contact angle is defined as the angle at the intersection point of solid, liquid and gas phase, defining the wettability of a solid surface by a liquid phase also shown in Figure 2.1. Contact angle is divided into two phases; it is hydrophilic when $\Theta < 90^o$ and hydrophobic when $\Theta > 90^o$.

The most-known Young-Laplace equation (2.1), shows that the contact angle is

at equilibrium at a given temperature and pressure Equation (2.1) [Goo92].

$$\gamma_{lv}cos\theta_Y + \gamma_{sv} + \gamma_{sl} = 0 \tag{2.1}$$

In Equation (2.1), γ_{lv} stands for the surface tension of the liquid-vapor interface, stands for the surface tension of the solid-vapor interface and similarly, stands for the surface tension of the solid-liquid interface.

In this thesis, contact angle of Ga and N phases were measured with water droplets and the results are given in Figure 2.5.

2.2.1.2 Surface Free Energy and Work of Adhesion Calculations

Surface free energy and work of adhesion calculations were performed by acid-base method. This method requires the measurement of contact angle of different liquids having different polarities, which are given in literature [Bar09].

The total solid surface free energy is considered to be comprised by Lifshitz-van der Waals (LW) and polar acid-base (AB) components.

$$\gamma_s^{tot} = \gamma_s^{LW} + \gamma_s^{AB} \tag{2.2}$$

The acid-base component in equation (2.2) can be written in terms of γ^+, Lewis acid, electron acceptor and γ^-, Lewis base, electron donor.

$$\gamma_s^{AB} = 2\sqrt{\gamma_s^- \gamma_s^+} \tag{2.3}$$

The interfacial free energy at the contact of solid and the liquid substrate is given in below.

$$\gamma_{sl} = \gamma_s + \gamma_l - Wa \tag{2.4}$$

Work of adhesion (Wa) is the work required to separate two surfaces while they are in contact, and it can be written in terms of SFE.

$$Wa = 2\sqrt{\gamma_s^{LW}\gamma_l^{LW}} + \sqrt{\gamma_s^+\gamma_l^-} + \sqrt{\gamma_s^-\gamma_l^+} \tag{2.5}$$

2.2.2 Surface Topography and Roughness Characterization

The surface topographies of the GaN coupons were examined by Nanomagnetics Atomic Force Microscope (AFM) using contact mode. Surface roughness values were recorded on 5 x 5 μm scan area consistently and reported as an average of minimum three measurements taken on the samples. In order to determine the root mean square (RMS) surface roughness values properly, the line scans were also performed by excluding the major surface defectivity such as particles stacked on the surface or deep scratches when needed. Yet, the full AFM scans are presented since the surface slurry particles left on the wafers are related to the insufficient surface charge, which is also studied as delineated in the following section.

2.2.3 Surface Chemical Composition Analysis

The crystalline nature of the GaN surfaces was studied through FTIR analyses by using an ATR crystal to be able to focus onto the top surface film. A Bruker Tensor 27 FTIR was used to detect the GaN related peaks on both the Ga-face and the N-face of the bulk coupons. Furthermore, pre and post CMP FTIR analyses were conducted as a function of pH to determine the relative changes in the chemical bond intensities and the impact of polishing on the chemically modified top film during the CMP operations.

2.2.4 Surface Charge Analysis

In this thesis, surface charge and zeta potentials of GaN samples for both Ga and N faces were measured by using streaming current measurement technique with SurPASS Instrument by Anton Paar. For the analysis of the zeta potential, 1mM KCl solution was used as an electrolyte while 0.05 M HCl was used for the pH titration. The 10 mm^2 GaN samples were mounted to the adjustable gap cell by orienting two coupons with the same crystalline orientation to face each other within the required gap for the flow conditions.

2.2.5 Absorbance Experiment

Semiconductors and insulators have band-gaps, which is the energy difference between the beginning of the valence band and the end of the conduction band. The electrons in semiconductors are not permitted to stay in the band-gap, they have to stay either in the valence band or the conduction band [Oha11]. The energy required for an electron to move from the valence band to the conduction band is called the band gap energy. The band-gap energy of the semiconductors must be known for each application [Nag95].

To find the band-gap energy of semiconductors, there are various kinds of theoretical and experimental methods. In this thesis, absorbance experiments are conducted in order to find the band-gap energy. This method uses the absorption spectra to find the optical energy gap using the inter-band absorption theory by the relation given below in Equation (2.6) [Fah83];

$$\alpha h v = B(hv - E_g)^n \tag{2.6}$$

where, n is the empirical exponent index that characterizes the transition mode, α is the absorption coefficient, h is the Plank constant and E_g is the optical band-gap. By drawing a tangent line at the linearity of the $ahv)^n$ versus hv graph, the band gap energy is found by the corresponding hv value, where $(ahv)^n=0$, which is shown in Figure 2.2 [Cer17].
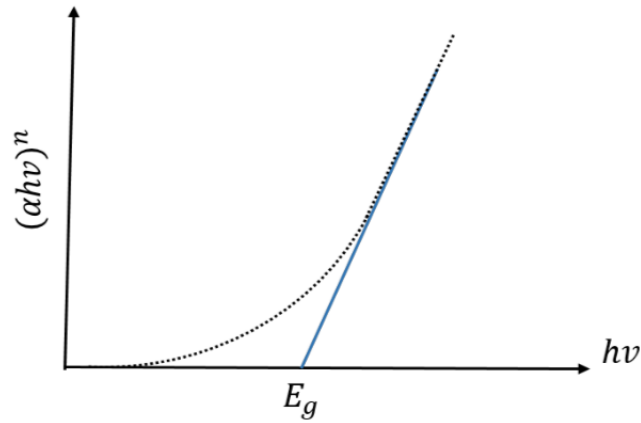
Figure 2.2: Absorption variation graph of $(ahv)^n$ versus hv [Cer17].

2.3   Results and Discussion

2.3.1   Surface Chemical Composition Analyses

In order to understand the effect of crystallographic orientation of bulk GaN coupons on CMP performance, initially the FTIR spectra were taken on both sides of the 0001 crystallographic orientation to identify the Ga-rich face [0001], and the N-rich face [000$\bar{1}$] of the bulk coupons [Hel98]. Figure 2.3 and Figure 2.4 shows the FTIR spectra of the N-face and Ga-face GaN with the primary peaks identifying the atomic vibrations related to the specific crystalline orientation. It can be seen in Figure 2.3. that the main peaks of G-N vibration are detected at 530 and 508 cm^{-1} wavelengths corresponding to the N-face, whereas the Ga-face shows in Figure 2.4, the intense H-Ga-Ga peak at 732 cm^{-1} wavelength that is missing in the N-face spectra [Ume15]. The additional Ga-N stretching is also seen on the Ga-face at 535, 497 and 475 cm^{-1} wavelengths in agreement with the literature findings [Ume15, Gan10, Wei13].
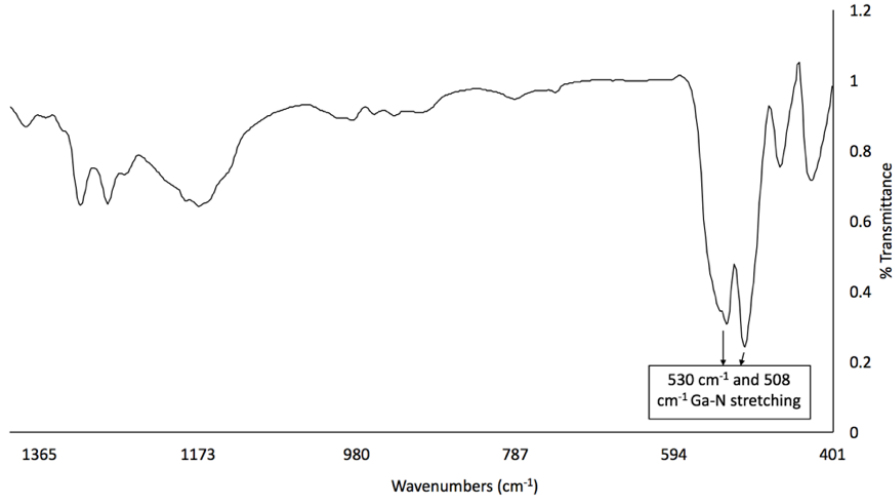
Figure 2.3: Surface FTIR analysis of N Face based on crystallographic orientation.
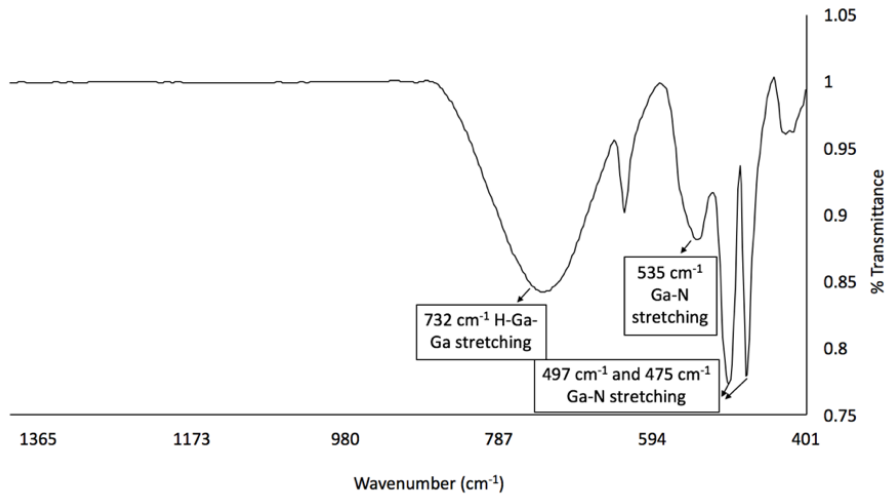
Figure 2.4: Surface FTIR analysis of Ga Face based on crystallographic orientation.

2.3.2 Contact Angle Measurements

Once the Ga-rich and N-rich surfaces were identified, wettability, surface energy and work of adhesion values were evaluated as can be seen in Figure 2.5. The image of the water droplet illustrated in Figure 2.5(a) shows a higher contact angle with the Ga-face, which is 107° and 10° higher than the N-face GaN. This statistically significant

34

difference between the contact angles of the two faces was found to be a useful tool in verifying the crystallographic orientations when needed. Although there is a difference between the wettability of the different sides, it is clear that the GaN shows a contact angle of 90° and higher that is an indicator of its hydrophobic nature. Furthermore, the work of adhesion (Wa) and surface free energies (SFE) were also measured (as per the procedure given by Bargir and co-workers) for both the orientations and reported in Figure 2.5(b) [Bar09]. The Wa values are beneficial in estimating the propensity of the surface to adhere other species and can be utilized in predicting the post CMP cleaning efficiency of the selected crystallographic orientations. In this case, the Ga-face had a lower Wa value (52.83 J/m^2) as compared to the N-face (69.62 J/m^2) indicating that the N-face is more prone to the attachment of particles post CMP. This characteristic was further verified by the surface charge measurement results as reported in Figure 2.6.
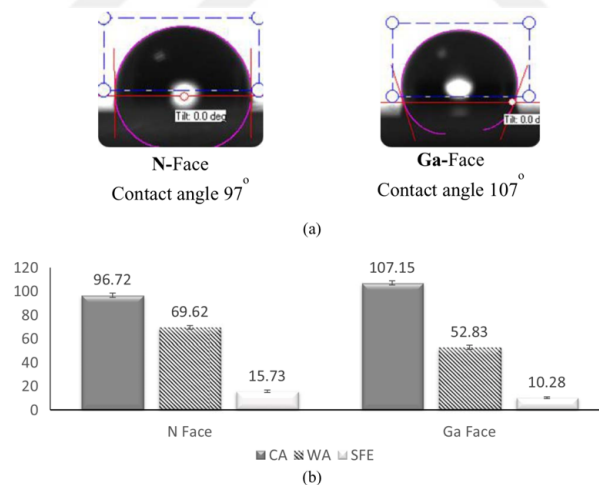
Figure 2.5: Surface characterization of the N-face and Ga-face of the GaN coupons through (a) contact angle measurements showing the DI-water droplets on the surfaces and (b) contact angle, work of adhesion and surface free energy values calculated by measuring the contact angle with liquids of varying polarity.
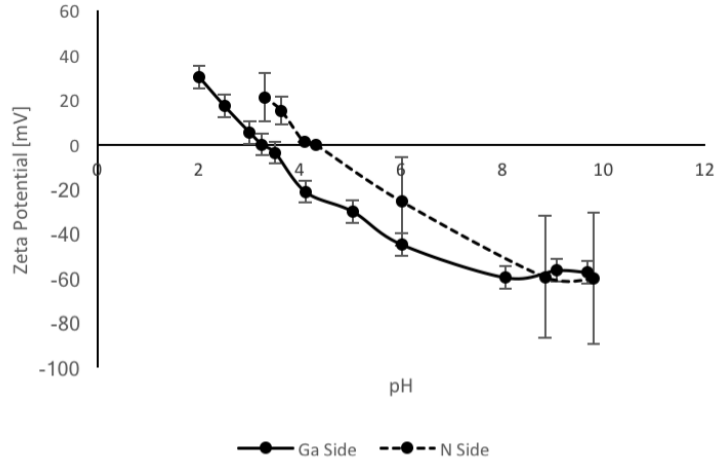
Figure 2.6: Surface charge measurements on the Ga-face and N-face of the GaN bulk coupons.

Furthermore, the surface energy values of 10.28 and 15.73 J/m^2 calculated on Ga-face and N-face, respectively indicate that the Ga-face is more stable as compared to the N-face, which is in agreement with the literature [To98, Hel98] indicating that the N-face decomposes more easily as compared to the Ga-face during the GaN growth. This observation is also consistent with the high standard deviations observed on the surface charge measurements of the N-face GaN as compared to the Ga-face.

2.3.3 Surface Charge Analysis

The isoelectric point (IEP) of both Ga and N-face results are given in Figure 2.6. The IEP of Ga-face was measured to be at pH 3.24, whereas the N-face was detected to be at pH 4.30. Hence at the given slurry pH of 6.4 the Ga-face is more negatively charged (–46 mV) as compared to the N-face (–23 mV). Consequently, the higher negative charge on the Ga-face results in more repulsive forces with the negatively charged silica particles (IEP of 2.2) and can be cleaned more easily.
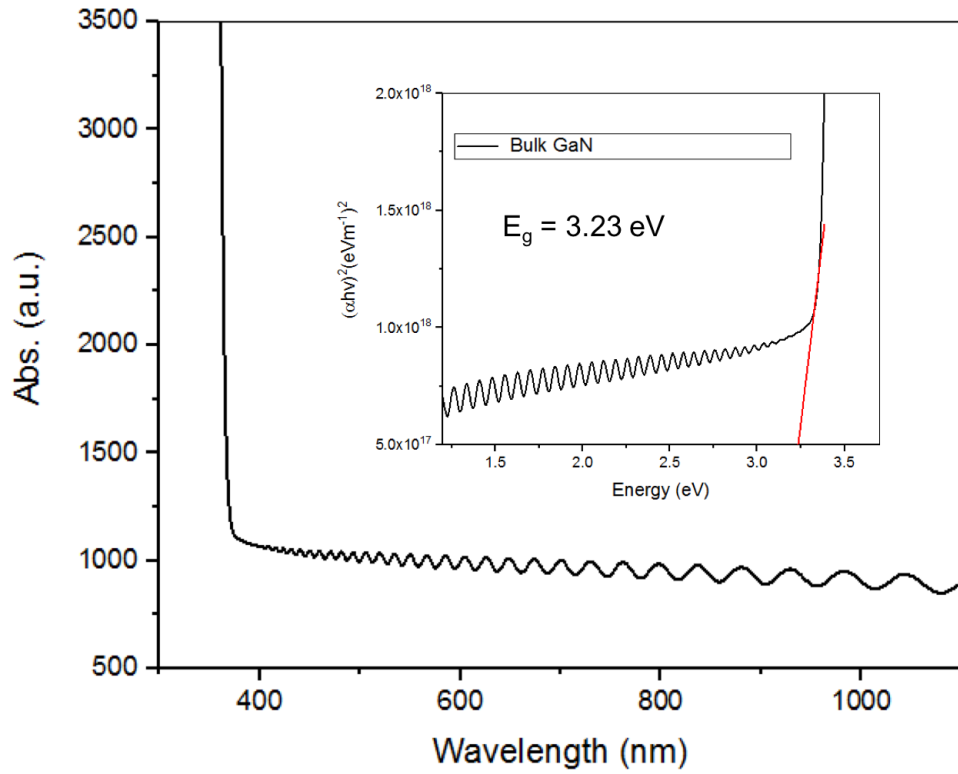
Figure 2.7: Absorbance graph of bulk GaN wafer.

2.3.4 Absorbance Experiments

The absorbance experiment of bulk GaN wafer is conducted in order to find the optical band-gap. The result is shown in Figure 2.7. A tangential line is drawn on where the $(ahv)^n$ versus hv graph starts to be linear and the corresponding hv value gives the optical band gap as 3.23 eV, the absorbance measurement was done using UV-VIS spectrometer.

2.4 Summary

The preliminary CMP analyses conducted on the GaN coupons as a function of the crystallographic orientation outline the differences of the Ga and N rich faces with

respect to wettability and surface energy as observed by the contact angle measurements. The pre and post CMP surface characterization of the wafers is critical in terms of understanding the chemical reactions taking place during the CMP process as well as the post CMP performance of the wafers in terms of the affinity of the particles to remain on the wafers.

CHAPTER III

DESIGN OF AN EFFECTIVE CHEMICAL MECHANICAL PLANARIZATION PROCESS FOR GALLIUM NITRIDE

3.1 Introduction

In this chapter, optimization of CMP process is discussed both experimentally and mathematically to enable high material removal rates and low surface defectivity for GaN processing. The experimental optimization was performed by changing the targeted process variables one at a time and keeping all the other variables constant. Once the selected variable was optimized, the optimal value was fixed and used for the optimization of the remaining variables by the following experiments. This approach was chosen to limit the number of experiments required for the optimization studies.

In mathematical optimization, the experimental data was used in order to find a correlation between the input and the output variables. The correlation was then used in order to do a convex optimization. The main difference between the experimental and the mathematical optimization is that, in mathematical optimization, all of the variables can be changed at the same time as desired to evaluate their interactions better.

CMP evaluations were performed on bulk GaN coupons with 10 x 10 mm dimension and 1 mm thickness. Bulk GaN coupons with (0001) orientation were selected on purpose to prevent any defectivity driven by the dislocation threads originated from the GaN/substrate interface. Both Ga-face and the N-face were available on the bulk substrates. A baseline silica slurry with uniform particle size distribution and 0.1 μm mean particle size provided by BASF SE, Germany was used for the CMP experiments. Slurry pH was stable at pH 6.42 and it was adjusted by adding HCl and

NH_3 as needed. Slurry stability was checked through particles size measurements by using static light scattering technique with Coulter LS 13 320 Instrument Universal Liquid Module. Background DI water pH and temperature were adjusted as needed to maintain the slurry conditions during the particle size measurements and evaluate the stability precisely. IC 1000/Suba IV stacked pads were used after aging for 100 hours to accomplish a soft pad/wafer interface and promote removal rates as per our observation in the earlier studies [Kar15].

3.2 Experimental

CMP experiments were conducted on a tabletop Struers Tegrapol-31 polisher. Figure 3.1(a) illustrates the polisher set up with the modifications made to form a slurry pool (which is utilized as a part of the new slurry feeding methodology) and the single wafer holder. Figure 3.1(b) and Figure 3.1(c) show the standard polishing platen with 3M conditioner and the multi-wafer coupon holder to adjust the applied pressure by changing the number of wafers placed during the polishing experiments. CMP tests were conducted at 30 N downforce, which is equivalent to $\sim$ 43 psi pressure on 10 x 10 mm sample size. To adjust the pressure to lower values, the multi-wafer holder was utilized and 3.3, 6.2, 8.7, 14.5 psi polishing performances were also evaluated. GaN samples were polished for 5 minutes and the material removal rates were reported as Å/min through weighing the samples pre and post polish by Swiss Made ES125SM model precise scientific balance (five digits after the decimal point, 0.01 mg accuracy). All samples were cleaned in ultrasonic bath with pH-adjusted water at pH 9 for 5 minutes and dried with nitrogen gas before they were characterized. Slurry pH was evaluated at pH 3, 6 and 9, solids loading was tested at 5,10, 15, 20 and 25 %wt, and the flow rate values of 20, 50 and 100 ml/min were experimented to optimize the material removal rates.
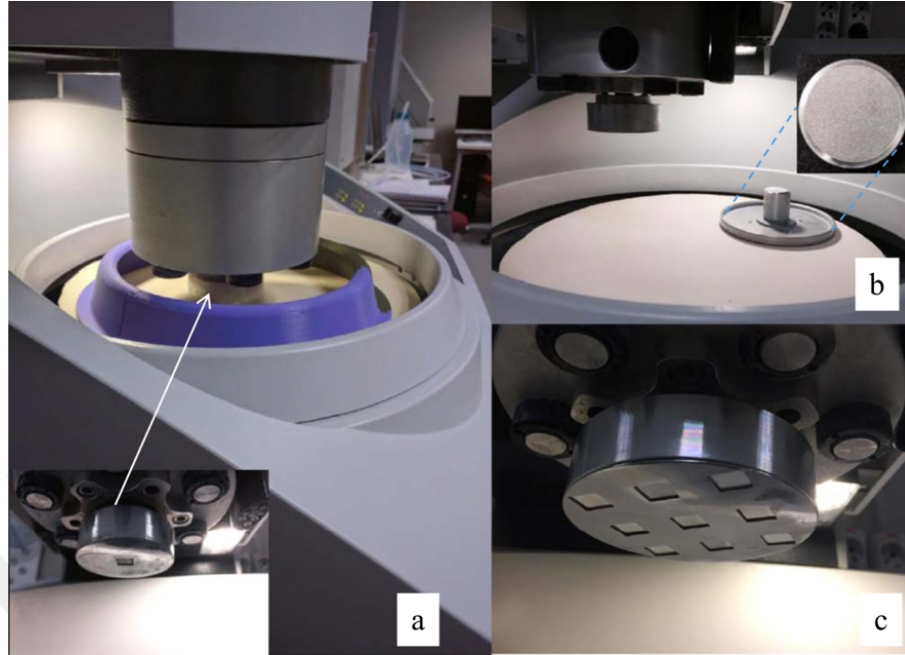
Figure 3.1: Desktop Struers Tegrapol-31 polisher (a) with the standard single wafer holder and slurry pool adopted (b) platen and the conditioning disk for the standard CMP testing and (c) multi-wafer holder designed to reduce pressure by adjusting the downforce through changing the number of wafers held during the polishing experiments.

The experiments were done under three evaluation methods, pH evaluations, mechanical composition and chemical compositions. During pH evaluations, both Ga and N rich faces are compared in terms of material removal rate. On the other hand, the tendency of particle agglomeration is considered due to surface charge of silica particles formed by different pH values. Mechanical composition includes, solids loading of abrasive particles in the slurry, slurry flow rate and applied down force. Finally, the chemical composition includes the pH adjustment and the temperature of the slurry. After optimizing all these components of CMP, a tool design is conducted. A pool is designed in order to reduce the amount of slurry, therefore reduce the cost.

3.2.1   pH Evaluations

pH evaluations were done as the first analysis in order to conduct other evaluations at a specific pH value. First of all, the pH of the 10 %wt silica slurries were adjusted by adding NH3. Then, the slurries were kept in the stirrer for 24 hours and 20 minutes in the ultrasonic bath, in order to make sure the slurry is homogeneous. Before the CMP process, size analyses were conducted on the slurries at pH 3, 6, and 9, as the pH value of the slurry, effects the particle agglomeration. Particle size measurements were conducted by light scattering technique using Coulter LS-13 320 Laser Diffraction Particle Size Analyzer (Beckman Coulter ALM-aqueous Liquid Module Instrument). The background water was adjusted to corresponding pH value while measuring particle size. CMP of both Ga and N rich faces were done with slurries at different pH values at the same day, in order to prevent any errors that may be caused by the environmental factors. After CMP process, the wettability analysis, FTIR analysis and topography analysis were conducted.

3.2.2   Slurry Solids Loading

According to the results obtained in the pH evaluations, the optimum pH value is determined as pH 9, which gives the highest MRR value with the lowest RMS value. Therefore, solids loading experiments were conducted at pH 9, 30 N downforce, 20°C and 20 ml/min flow rate at varying solids loading; 5, 10, 15, 25 %wt. The original slurry was 30 %wt, which is diluted by DIW and then adjusted to pH 9. All the slurries were kept on the stirrer for 24 hours and 20 min of ultrasonic bath.

3.2.3   Slurry Flow Rate

The results obtained in the solids loading evaluations, the optimum solids loading of the slurry was found to be 10 %wt. Therefore, the flow rate experiments were conducted with a 10 %wt silica based slurry adjusted to pH 9. Downforce was 30 N and the flow rates were; 20, 50 and 100 ml/min. The pumps which are already on the

CMP machine are insufficient for flow rates above 20 ml/min, therefore an external pump is used for flow rates at 50 ml/min and 100 ml/min. This external pump is connected to the machine with an external pipe, which is mounted at the original pipe location of the CMP machine.

3.2.4 Pressure (Down-force)

During flow rate analysis, 20 ml/min was found to be the optimum flow rate, therefore, downforce experiments were conducted with a 10 %wt silica based slurry adjusted to pH 9 at 20 ml/min flow rate. The minimum downforce applied by the CMP machine was 30 N, therefore a multi-wafer holder is designed to increase the area, thus to decrease the pressure. According to the demanded pressure, the number of dummy wafers were changed, where the dummy wafers have the same thickness as the polished GaN wafer.

3.2.5 Slurry Chemistry

The experiments conducted to observe the MRR and RMS changes according to the change in slurry chemistry were conducted in two ways. In the first one, 0.1 M HCl was fed to the system at 2 ml/min flow rate, where the silica slurry used was at pH 9 and in the second one, 0.1 M NH_3 was fed to the system at 2 ml/min flow rate, where this time, the silica slurry used was at pH 3. The objective of adding an acid and base externally was to keep pushing the reaction forward, therefore increase the polishing rate.

Although, before conducting the experiments, particle size analysis was conducted for the silica slurry, while the tendency of silica particles to agglomerate changes with varying pH value.

Table 3.1: Mean particle size of silica particles in pH 3, 6 and 9.

pH Value	Mean Particle Size [nm]
pH 3	106
pH 6	105
pH 9	74

3.2.6 Temperature

Temperature evaluation experiments were done at 10 %wt silica slurry adjusted to pH 9 at 20 ml/min flow rate and 10 N downforce at 20°C and 4°C. The temperature of the slurry was checked continuously during polishing time and the slurry was kept in an insulating cup to prevent any heat exchange.

3.3 Results and Discussion

3.3.1 pH Evaluations

The first analysis done before CMP with different pH values was the particle size measurement. The results of particle size measurements are given in Table 2 and Figure 3.2. The mean particle size measurement results are, 106 nm, 105 nm and 74 nm at pH 3, 6 and 9, respectively. As these results show, the decrease in pH results in agglomeration due to the reduction of the surface charge of silica particles. The results of the particle size analyses confirm the formation of soft agglomerates (due to coagulation) in the slurry, based on larger mean particle size of the slurries at lower pH, which tends to mechanically abrade the surface and generate higher levels of defectivity.
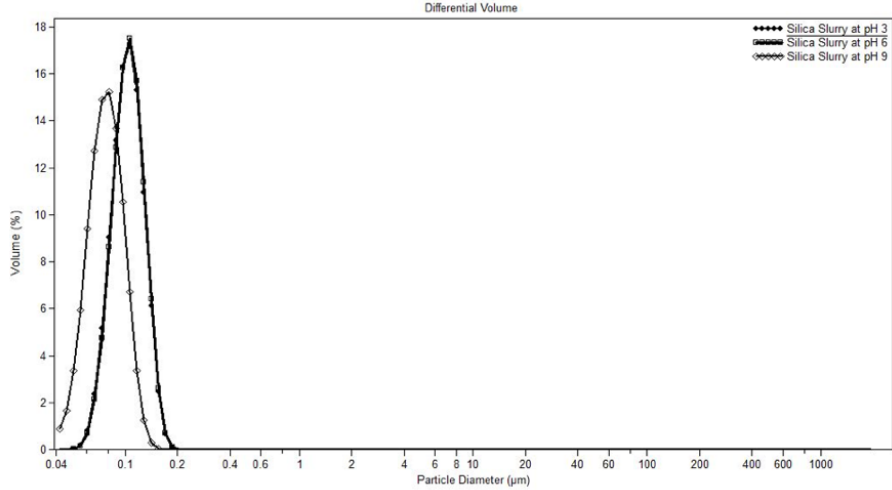
Figure 3.2: Particle size distribution analysis by volume% for silica slurry at pH 3, 6 and 9.

Table 3.2 summarizes the material removal rate (MRR) results on the N-face and Ga-face of GaN coupons at 30 N downforce and 10 ml/min slurry flow rate at pH 3, 6 and 9 without using a conditioner. The effect of conditioner can be seen when they are compared with the resulting MRR results shown in further in this chapter, where conditioner is used. The use of conditioner increases the material removal rate, while the slurry is distributed in a more homogeneous way. It can be seen that the increase in pH results in increasing MRR values on both sides of GaN. However, the Ga-rich side has removal rates that are at least an order of magnitude higher as compared to the N-rich side. This can be attributed to the nature of material removal on the Ga-rich face, which occurs through formation of Ga_2O_3 on the wafer and its removal by the relatively harder slurry abrasive particles [Gon15]. On the other hand, the N-side GaN requires the formation of a nitrogen terminated layer with one negatively charged dangling bond on each nitrogen atom followed by the adsorption of hydroxide ions leading to the formation of oxides and dissolution and removal of the oxides [Tav02, Pec12]. Therefore, the CMP performance optimization

studies were focused on the N-rich face where the MRR is limited and needs to be improved mainly for the applications in LEDs.

Figure 3.3 and Figure 3.4 summarizes the material removal rates and the surface roughness values of the N-face GaN at pH 3, 6 and 9. It can be seen that the increasing pH promoted the MRR values as it helps providing additional hydroxide ions required for activating the material removal on the N-face. The MRR values increased from 47 Å/min at pH 3 to 110 and 142 Å/min at pH 6 and pH 9, respectively. As the material removal is enabled by increased pH, the surface roughness was also observed to decrease as can be seen in Figure 3.4.

Table 3.2: Material removal rate evaluations as a function of pH, for N face and Ga face with 10% wt Silica slurry for 5 minutes with 30 N downforce.

Slurry pH Value	N Face MRR [Å/min]	Ga Face MRR [Å/min]
pH 3	47.2	1313.9
pH 6	110.06	1887.6
pH 9	141.55	2269.6
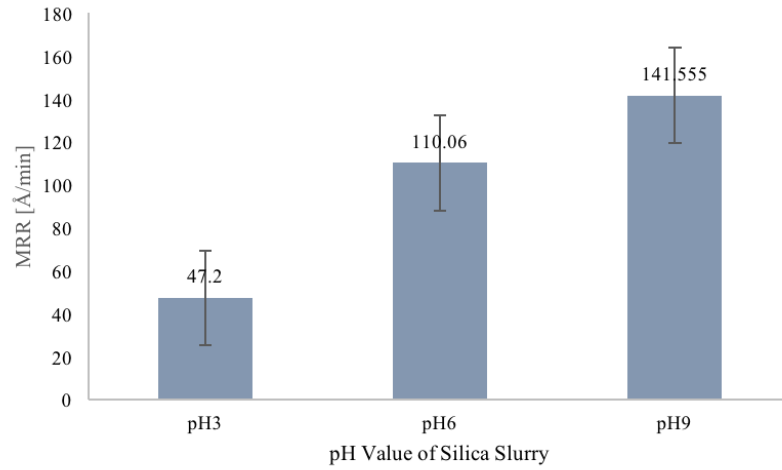
Figure 3.3: Material removal rate results of post CMP of N-face GaN as a function of pH.
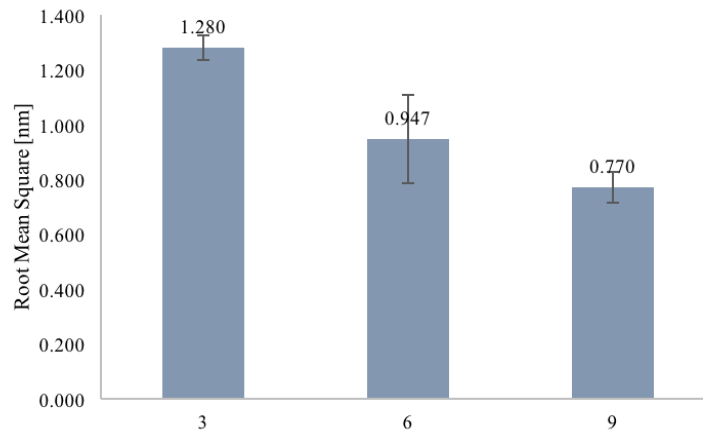
Figure 3.4: Root mean square (roughness) results of post CMP of N-face GaN as a function of pH.
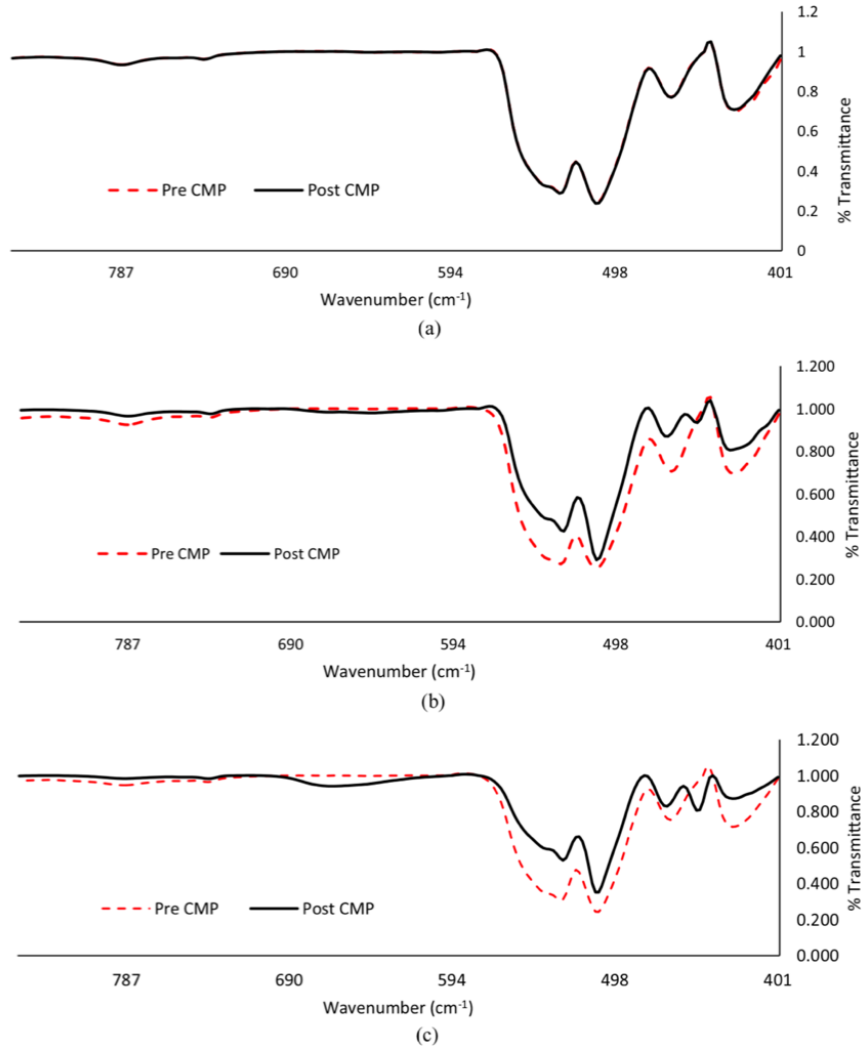
Figure 3.5: FTIR spectra of pre and post CMP as a function of pH (a) pH 3 (b) pH 6 (c) pH 9.

The increase in the chemical activity resulting in GaN removal was further verified with the FTIR spectra collected pre and post CMP as a function of pH as it can be seen in Figure 3.5. While the FTIR spectra exactly overlapped for the GaN coupons pre and post CMP polished at pH 3 Figure 3.5(a), the Ga-N vibration peaks at 530 and 508 cm^1 wavelengths were observed to decrease post CMP at pH 6 and pH 9 indicating removal of GaN.

In terms of surface quality performance, the decrease in the surface roughness with

the increasing pH can be explained based on two phenomena. First of all, the decrease in the slurry pH results in agglomeration due to the reduction of the surface charge of the silica particles (IEP of pH 2.2), which are shown in Figure 3.2. Furthermore, Figure 3.6 compares the surface free energy and the work of adhesion values pre and post CMP conducted at pH 3, 6 and 9. It is clearly seen that, polishing in general increases both the surface free energy and work of adhesion due to the opening of fresh surface layers. Yet, the work of adhesion is the highest when the CMP is conducted at pH 3 meaning that the propensity of the slurry particles to adhere on the surface increases.
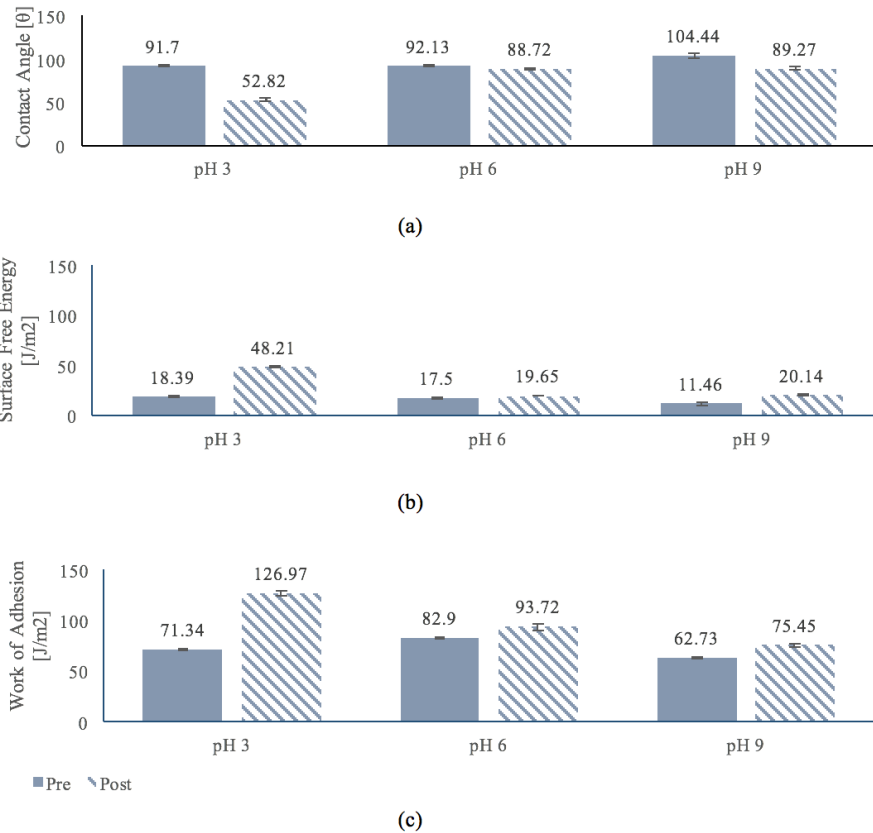
Figure 3.6: Pre and post CMP results of (a) contact angle, (b) surface free energy and (c) work of adhesion.

49

The AFM results show that the particles tend to agglomerate at pH 3 and 6, and also as it can be seen from the Figure 3.7 and Figure 3.8, that they tend to stick on the wafer surface at low pH values, even though the post CMP cleaning procedure is applied. Figure 3.10 shows the possible silica particle that is stuck on the surface. The pit observed on the wafer surface can be treated as a silica particle, while it almost has a spherical shape and the roughness value is much higher than the other surface points around that area.
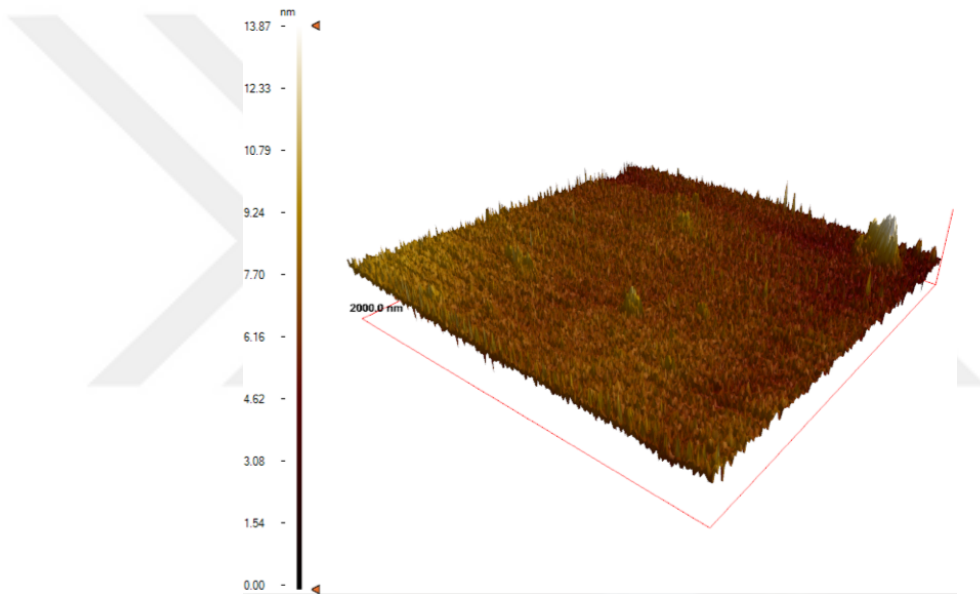
Figure 3.7: 3D view of GaN N Face after CMP at pH 3.
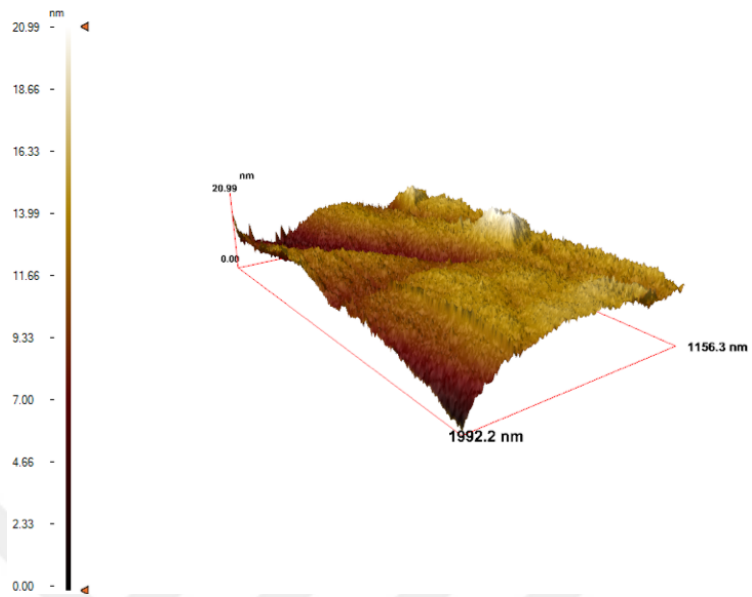
Figure 3.8: 3D view of GaN N Face after CMP at pH 6.
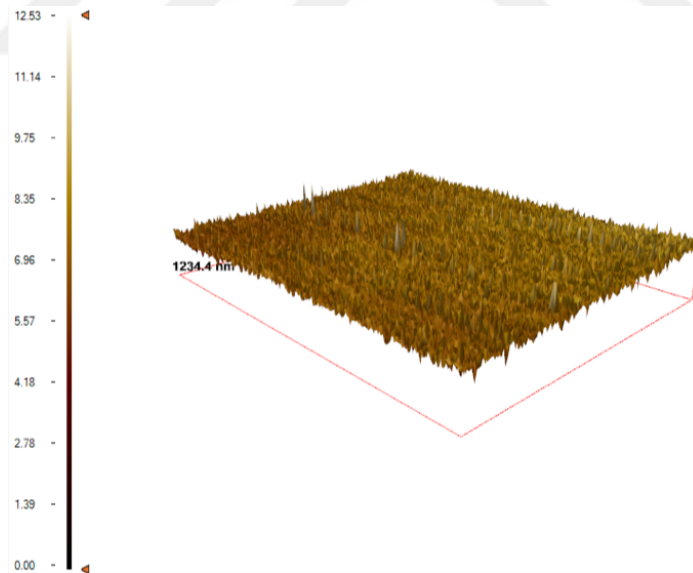
Figure 3.9: 3D view of GaN N Face after CMP at pH 9.
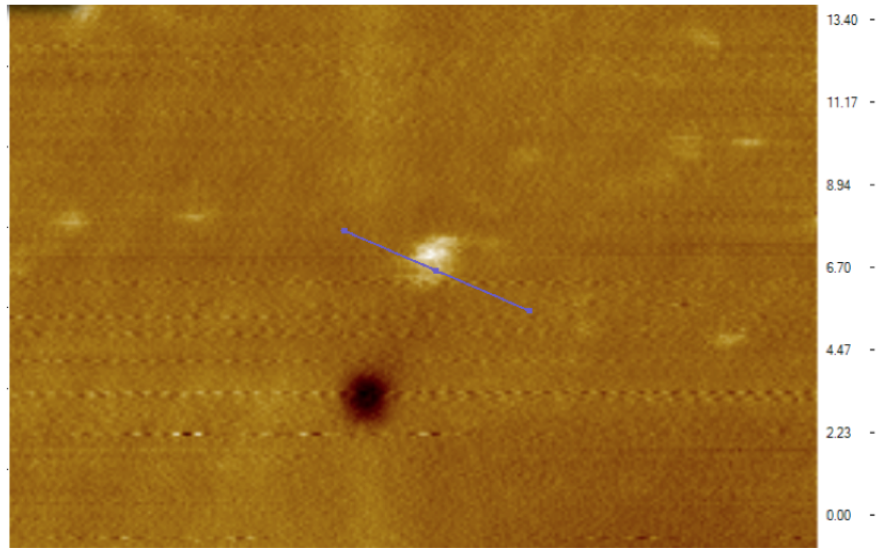
(a)
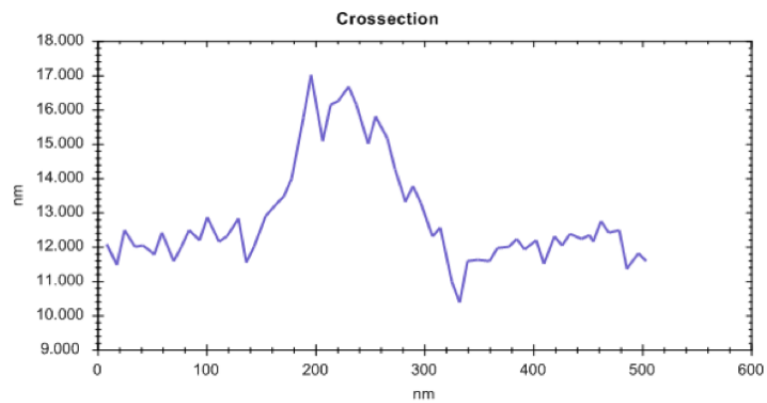
(b)

Figure 3.10: 2D view of the silica particle on the N face (a) and the corresponding cross-section view (b).

3.3.2 Slurry Solids Loading

The slurry solids loading was experimented at 5, 10, 15, 20 and 25 %wt as illustrated in Figure 3.11. It was observed that the highest removal rate was achieved at 10 %wt slurry solids loading, which was 220 Å/min at 30 N downforce. The use of pad conditioner also increased the MRR value significantly from 141.6 Å/min (Figure 3.3)
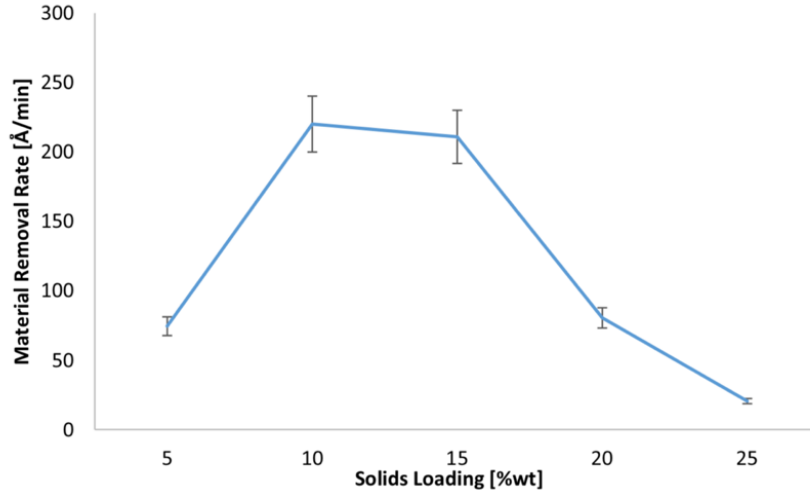
Figure 3.11: Material removal rate as a function of solids loading.

up to 220 Å/min. Beyond 10 %wt, the MRR values tend to decrease, which can be attributed to the surface saturation of particles resulting in the rolling action of the abrasive particles on the surface and hence decreasing the efficacy of the mechanical abrasion, known as the contact area based material removal mechanism promoting chemical activity and demoting mechanical abrasion [Bas11]. The decrease in the MRR as the solids loading increase can also be attributed to the increase in number of particles, therefore decreasing the pressure applied on each particle.

3.3.3 Slurry Flow Rate

Following the slurry solids loading optimization, the slurry flow rate impact was evaluated at 20, 50 and 100 ml/min as seen in Figure 3.12. It was also observed that beyond 20 ml/min, the excessive slurry flow rate did not affect the material removal rate and even decreased the MRR at 100 ml/min of slurry flow. This trend can also be explained based on the contact area based material removal to become more pronounced as observed in the effect of slurry solids loading.
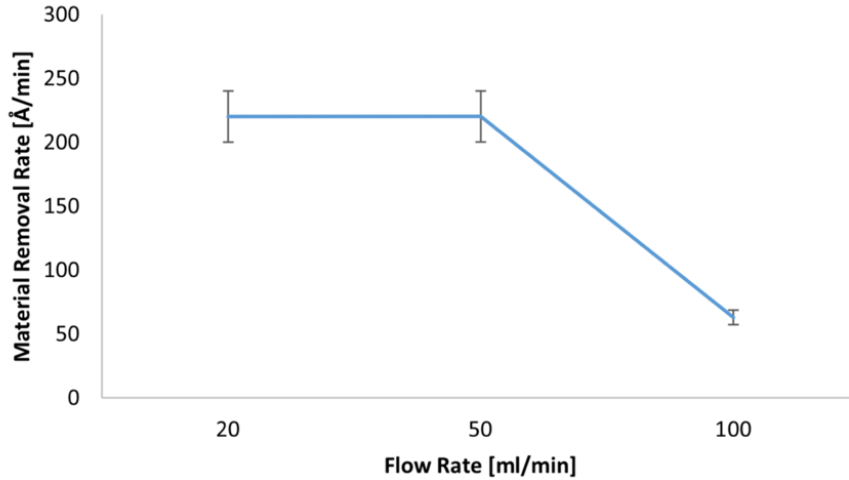
Figure 3.12: Material removal rate as a function of flow rate.

3.3.4 Pressure (Down-force)

Figure 3.13 illustrates the impact of downforce which was experimented by using 10 %wt slurry solids loading at 20 ml/min slurry flow rate by using the multiple-wafer sample holder illustrated in Figure 3.1. In this case, it was observed that the highest removal rate (346 Å/min) was obtained at 10N downforce, which corresponded to 14.5 psi pressure. The effect of pressure on the removal rate response can be explained in two ways; (i) the higher the pressure, the load per particle increases which promotes the mechanical action of the abrasives on the surface and expected to promote the removal rates, and (ii) the higher the pressure it becomes more difficult for the abrasive particles (slurry) to be fed in between the sample and the polishing pad, reducing the chemical activity and the total surface area of particles in contact with surface, demoting the removal rates. Hence, the high pressure tends to result in more mechanically driven removal mechanism reducing the number of particles engaged in polishing by reducing the total contact area. In this case, 10 N downforce seems to be the optimal to promote both the chemical and the mechanical actions and increase the removal rates.
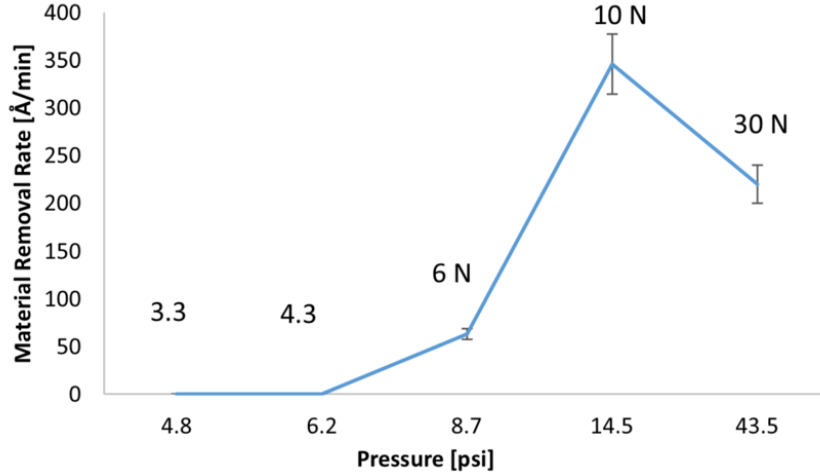
Figure 3.13: Material removal rate as a function of pressure.

3.3.5 Slurry Chemistry

The chemical reaction that defines the GaN dissolution for the N-rich surface is given in equation (3.1) as described by Weyher and co-workers [Wey97]. Based on this reaction, the chemical decomposition of GaN results in formation of ammonia (NH_3) in the products. Although the high pH values obtained by adjusting slurry pH to 9 by NH_3 addition helps increasing the material removal rates by promoting the hydroxyl ion formation, the resulting NH_3 in the products tend to push the reaction backwards resulting in a decrease in the material removal rates. Therefore, a series of experiments were conducted intending the neutralization of the ammonia in the reaction product.

$$GaN + OH^- + 3H_2O \rightarrow Ga(OH)_4^- + NH_3 \tag{3.1}$$

Figure 3.14 illustrates the material removal rate response for the slurry adjusted to pH 9 by NH_3 addition as compared to the in-situ neutralization of NH3 on the pad surface by adding 0.1 M HCl through the secondary slurry flow line (20 ml/min slurry flow at 30 N downforce without conditioner). It can be seen that the MRR value of 157 Å/min increased to 189 Å/min by in-situ neutralization of the NH_3 in the

products pushing the dissolution reaction forward. Any ammonium chloride (NH_4Cl), which may be forming out of this reaction may slightly increase the ionic strength as a salt that is highly soluble in water. In order to prove the concept, the same experiment was conducted by using a HCl adjusted acidic slurry at pH 3 and adding NH_3 through the secondary slurry flow line as can be seen in Figure 3.14(b). However, the MRR values further decreased when the neutralization was performed by using a base in the acidic slurry. Hence, it can be concluded that the initial impact of NH_3 is necessary to form the hydroxyl ions on the surface as a reactant in equation (3.1), whereas, the addition of HCl on the pad surface can neutralize the excessive NH3 and further help pushing the reaction forward. Furthermore, the same CMP tests were also conducted on the silica wafers yet resulted in no material removal rate indicating that this chemical promotion is specific to the GaN polishing. However, this is an indicator that GaN can be selectively removed against silica by using this specific process.
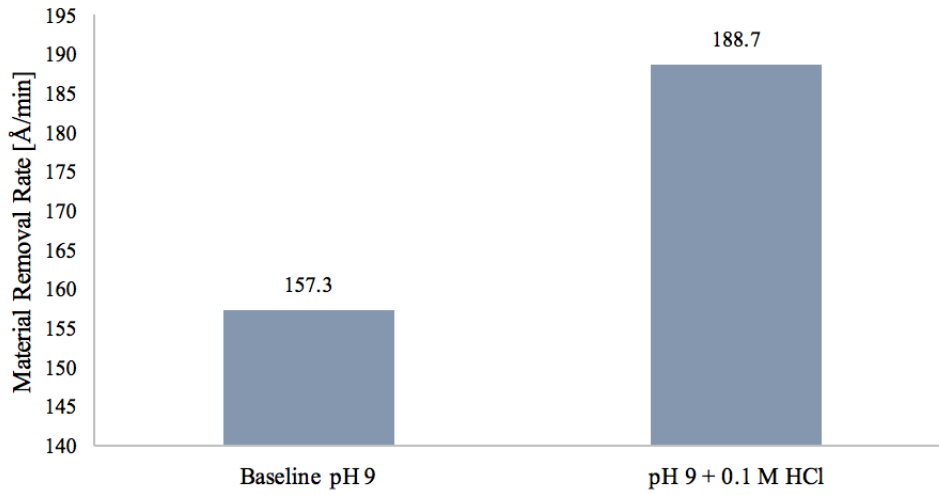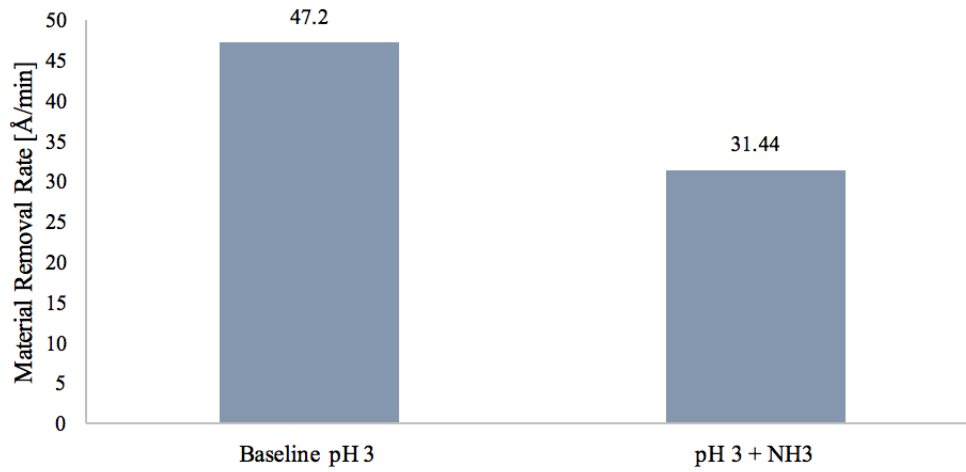
Figure 3.14: Material removal rate as a function of slurry chemistry by pushing the chemical reaction forward through (a) neutralizing the basic slurry with an acid and (b) neutralizing the acidic slurry with a base.

Although the MRR increases by in-situ neutralization the basic slurry with an acid, the particle size measurement by using volume% distribution in Figure 3.15 shows that slurry neutralization with HCl increases the particle mean size which is
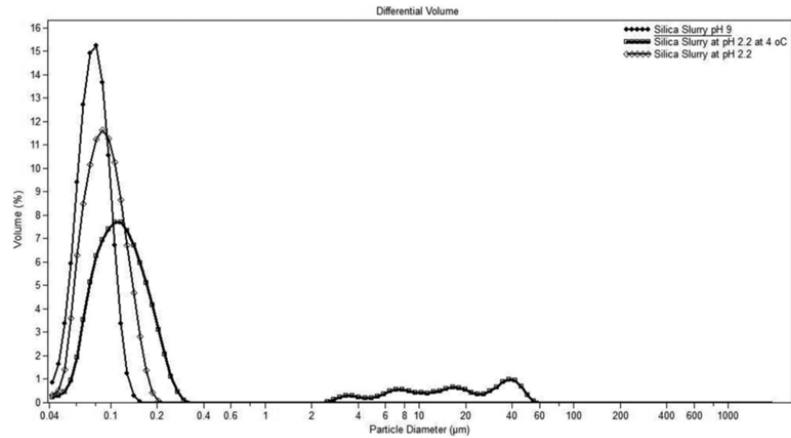
Figure 3.15: Particle size measurement in volume% for silica slurry at pH 9, for neutralized basic silica slurry with 0.1 M HCl and neutralized slurry at 4^oC.

suspected to be due to agglomeration of the particles with the decreased pH.

3.3.6 Temperature

As an additional chemical modification, the effect of temperature was also evaluated on the material removal rate responses. Table 3 compares the material removal rates of the wafers polished with CMP slurry at pH 9 with and without the addition of 0.1 M HCl to the pad surface at 4^oC and 20^oC (ambient). It can be seen that the lowered temperatures helped increasing the material removal rates by 2 to 3 times. As the GaN CMP generates heat as a reaction product, the cooling of the platen surface also helps promoting the removal rates by pushing the reaction forward. Consequently, MRR values of 500 Å/min were achieved on the N-face GaN coupons by using a slurry at 4^oC in combination with the HCl neutralization in-situ. However, the particle size analyses conducted with Coulter LS 13 320 (by using volume% distribution) to detect any agglomeration have shown that a severe agglomeration was observed at 4^oC slurry temperature as can be seen in Figure 3.15. Therefore, the surfaces were found to be more defective when lower temperature slurry was used for the processing as illustrated in Figure 3.16 and Figure 3.17, although the removal rates

Table 3.3: The effect of slurry temperature on the MRR.

Slurry Chemistry	4^oC	20^oC
pH 9	475.0 Å/min	158.5 Å/min
pH 9 + 0.1 M HCl	503.2 Å/min	188.7 Å/min
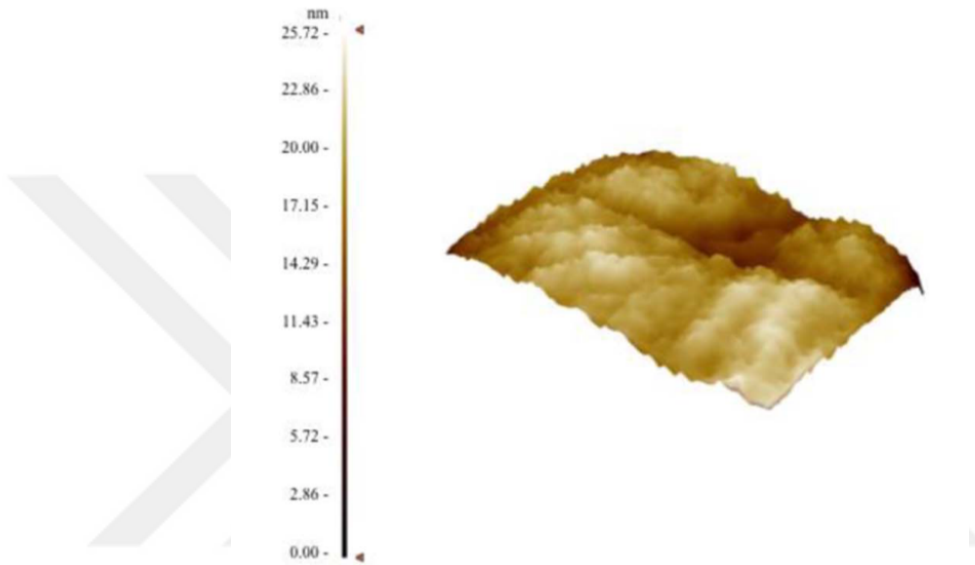
Figure 3.16: Surface quality analysis through AFM images of GaN N-rich face at 20^oC polished with neutralized silica slurry at pH 9 with 0.1 M HCl.

were improved significantly. Hence, the trade-off between improving the removal rates and maintaining the surface quality still remains with configurations in process set-up required.

3.4   Optimized CMP Tool Set Up and Process Configurations

Based on the improvement of the material removal rates of the N-face GaN with the in-situ addition of HCl, a new tool configuration was also experimented by adopting a slurry collector pool around the polishing platen as can be seen in Figure 3.1(a). In this configuration, the pool was filled with the slurry (200 ml) and the CMP was performed with and without flowing 0.1M HCl solution at 20 ml/min flow rate. By
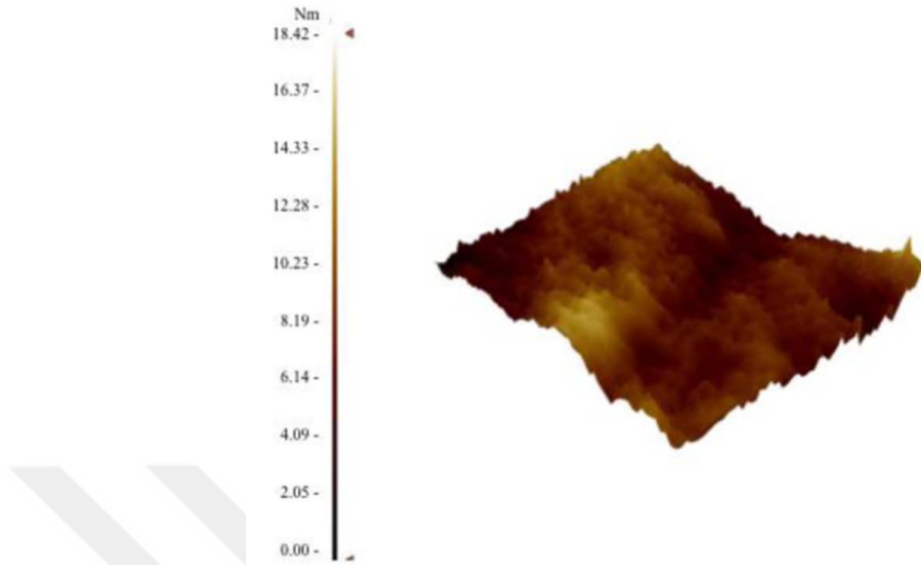
Figure 3.17: Surface quality analysis through AFM images of GaN N-rich face at 4°C polished with neutralized silica slurry at pH 9 with 0.1 M HCl.

using the slurry pool configuration, it was observed that the removal rate without the HCl addition was 94.35 Å/min as the generated NH3 forced the dissolution reaction to go backwards. However, when the HCl flow was on, MRR value of 157.22 Å/min was reached which was equivalent to the polishing with just the pH 9 slurry by continuously flowing the slurry at 20 ml/min flow rate and at 30N downforce. This configuration may help conserve slurry for the bulk GaN polishing, which can be followed by a buff process by using fresh slurry.

In order to finalize the optimization, the best processing conditions including the mechanical and the chemical improvements were tested on the N-face GaN coupons. By using 10 %wt slurry solids loading at pH 9 and 4°C temperature and 20 ml/min flow rate with 0.1M HCl flown through the secondary slurry feeder at 10N downforce and in-situ conditioning CMP experiments were conducted. The tests resulted in 880 $\pm$ 110 Å/min MRR and 0.8 $\pm$ 0.4 nm surface roughness value.

3.5 Mathematical Simulation Based Optimization

The experimental optimization performed as presented above provides sufficient data in order to find a correlation between the input variables and the resultant output factors. In addition to the experimental optimization a mathematical optimization was conducted to find the correlation between the input and the output variables and optimize the CMP process by the capability of changing all the variables simultaneously.

Least square error (LSE) optimization aims to find a $\vec{p}$ vector which minimizes the error between the input variable, x, and the output variable, y [Yor69]. The $\vec{p}$ vector, which minimized the squared sum of errors is found by the following equation;

$$y_n = px_n + e_n \tag{3.2}$$

where, y_n is the set of measurements (dependent variable), x_n is the set of variables (independent variable), and e_n is the set of measurement errors; y_n, p and e_n are vectors and X is a matrix. The objective function of the optimization problem is written as equation (3.10).

$$min(p) \sum_{n=1}^{N} (y_n - px_n)^2 \tag{3.3}$$

There are three different ways to solve this problem. One of them is to solve it analytically, by setting the derivative of the error expression with respect to p is equal to zero and solve for p, where the solution would be found by Equation (3.4).

$$p_{opt} = \frac{\vec{y}^T \vec{x}}{\vec{x}^T \vec{x}} \tag{3.4}$$

The second method uses a geometrical approach, where a scale factor p is aimed to be found, such that px would be close as much as possible to y. This solution method can be expressed as Equation (3.5).

$$p_{opt}\vec{x} = (\vec{y}^T \hat{x})\hat{x} = \frac{\vec{y}^T \vec{x}}{||\vec{x}||^2}\vec{x} \tag{3.5}$$

61
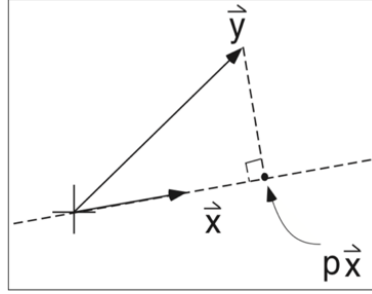
Figure 3.18: 2nd Method in Optimization [Sim17].
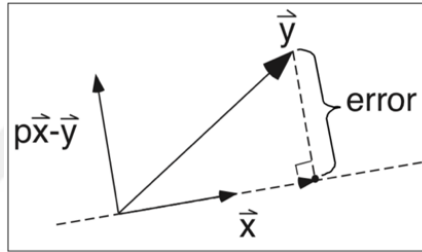
Figure 3.19: Orthogonality Method in Optimization [Sim17].

This method can be shown graphically as in Figure 3.18.

The third method uses the orthogonality principle. A scaled version of $\vec{x}$ is searched so that it comes as close as possible to $\vec{y}$. This would be expressed as Equation (3.6) and can also be shown graphically as in Figure 3.19.

$$\vec{x}^{T}(\vec{y} - p_{opt}\vec{x}) = 0 \qquad (3.6)$$

The aim of least square error optimization is to minimize the p vector and call the optimal value as p_{opt}. If the columns of matrix X is composed of the independent vectors, then the optimization problem can be written as equation (3.7);

$$min(p)||\vec{y} - X\vec{p}||^{2} \qquad (3.7)$$

where, the vector $X\vec{p}$ is the sum of independent variables, which then it would be possible to say that if $\vec{y}$ is equal to $X\vec{p}$, then p_{opt} would be minimum as possible.

In addition, if one would like to define a reliability for an experiment, then there is a need to use the weighting method. In order to apply weighting method, a W

62

matrix should be formed, where it has N columns and N rows, and the diagonals should tell the reliability of the experiments. The diagonals should sum up to 1, and all the other elements of the matrix should be zero. With the weighting method, the optimization problem can be written as equation (3.8).

$$min(p)||W(\vec{y} - X\vec{p})||^2 \tag{3.8}$$

Finally, p_{opt} would be multiplied by x_n to get y_n, which would give a correlation function between the independent and the dependent variables [Sim17].

The important input variables for CMP optimization were selected as the slurry solids loading (the number of abrasive particles in the colloidal silica solution), slurry flow rate and the applied downforce by the head polishing head on the wafer. On the other hand, the output variables were determined as the material removal rate (MRR), being the most important factor to improve for GaN CMP as the MRR values tend to be very limited for this very hard material. The MRR values were calculated by weighing the GaN coupon before and after the CMP process to determine the change in mass and dividing this value by the surface area and the duration of the experiment. Initially the experimental optimization was performed by changing only one variable, and keeping the other variables constant. Afterwards the variable, which maximizes the MRR, was selected as the optimal value and kept constant for the following experiments. The input and output variables were determined as below;

- X_1 = Slurry solids loading (% wt)

- X_2 = Slurry flow rate (ml/min)

- X_3 = Pressure (psi)

- X_4 = Temperature (^{o}C)

- Y_1 = Material removal rate (Å/min)

These factors were selected to run a linear optimization. However, as it can be seen in Figure 3.11 and Figure 3.13 solids loading and pressure graphs are not linear. In order to solve a linear problem, the first data representing the effect of solids loading on MRR in Figure 3.11 and the last data in Figure 3.13 showing the effect of pressure on MRR were neglected. Yet, these data points would not have been neglected if they were maximizing the MRR value.

While conducting LSE, weighting method was also utilized in order to assign some coefficients for each experiment, depending on the reliability of the experimental conditions and the obtained results. In order to include weighting, a W matrix was defined, where the diagonals are the coefficients of each experiment, meaning that if an experiment is multiplied by a higher coefficient, it is more trustworthy as compared to the other experimental values. The diagonals of W matrix were determined as (nth diagonal corresponds to nth experiment); 0.02, 0.02, 0.02, 0.02, 0.074, 0.074, 0.074, 0.074, 0.074, 0.074, 0.074, 0.2, 0.2, respectively. The sum of the diagonals should make 1 according to the literature [Sim17].

In order to visualize the number of experiments and the value of the parameters, a systematic was formed as shown in Table 5.

Based on Table 3.4 experiments from 1 to 4 represent the solids loading, only X_1 value has been changed and the other variables were kept constant in the simulation. Then, selecting the X_1 value, which gives the highest MRR value, slurry flow rate has been changed on the experimental evaluations from 5 to 7. Then, the same procedure was applied for pressure and temperature as the input variables.

The correlation found by the LSE optimization method is given in Equation (3.9). This equation shows that, a p matrix is found, having a 4x1 dimension, with elements, 1.8227, 0.1521, 3.0592 and 0.2481, which minimizes the error between the input and the output variables.

$$y = 0.3470x_1 - 0.2058x_2 + 2.7970x_3 - 2.9928x_4 \qquad (3.9)$$

64

Table 3.4: Experimental visualization for LSE optimization method.

Experiment No	X_1	X_2	X_3	X_4	Y_1
1st	10	20	43.5	20	220.1
2nd	15	20	43.5	20	210.8
3rd	20	20	43.5	20	80.5
4th	25	20	43.5	20	20.4
5th	10	20	43.5	20	220.1
6th	10	50	43.5	20	220.0
7th	10	100	43.5	20	62.9
8th	10	20	4.8	20	0
9th	10	20	6.2	20	0
10th	10	20	8.7	20	62.9
11th	10	20	14.5	20	345.9
12th	10	20	14.5	4	475.0
13th	10	20	14.5	20	158.5

In order to compare the experimental findings to the LSE simulations, graphical comparisons were performed where the pink lines illustrate the LSE results and orange lines illustrate the experimental values. Figure 3.20 shows that the experimental data of slurry solids loading graph has a decreasing slope, whereas the data found by the mathematical optimization has a slightly increasing slope. The same problem was observed in slurry flow rate (Figure 3.22) and temperature graphs (Figure 3.23) as well. In order to solve these inconsistent results weighting was applied as well in combination with the LSE method.

65
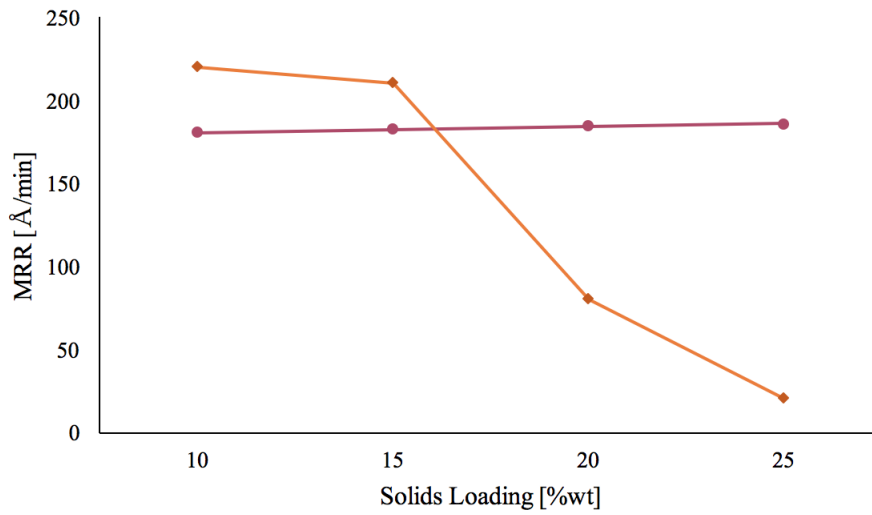
Figure 3.20: Comparison of the experimental values of MRR with the results obtained by the LSE method for solids loading.
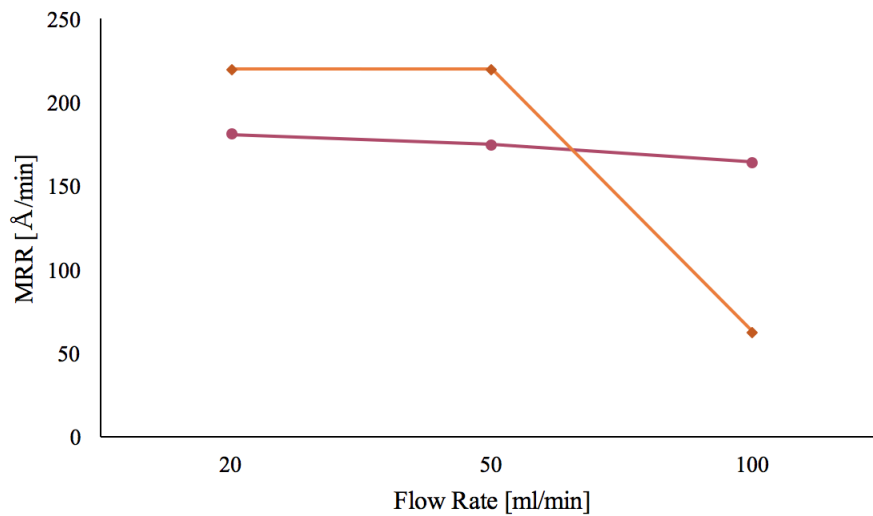
Figure 3.21: Comparison of the experimental values of MRR with the results obtained by the LSE method for flow rate.
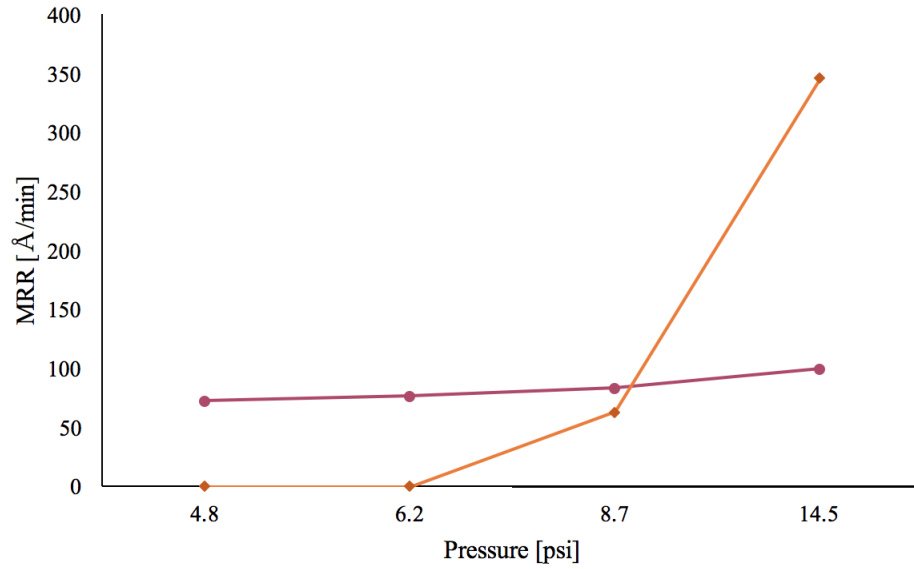
Figure 3.22: Comparison of the experimental values of MRR with the results obtained by the LSE method for pressure.
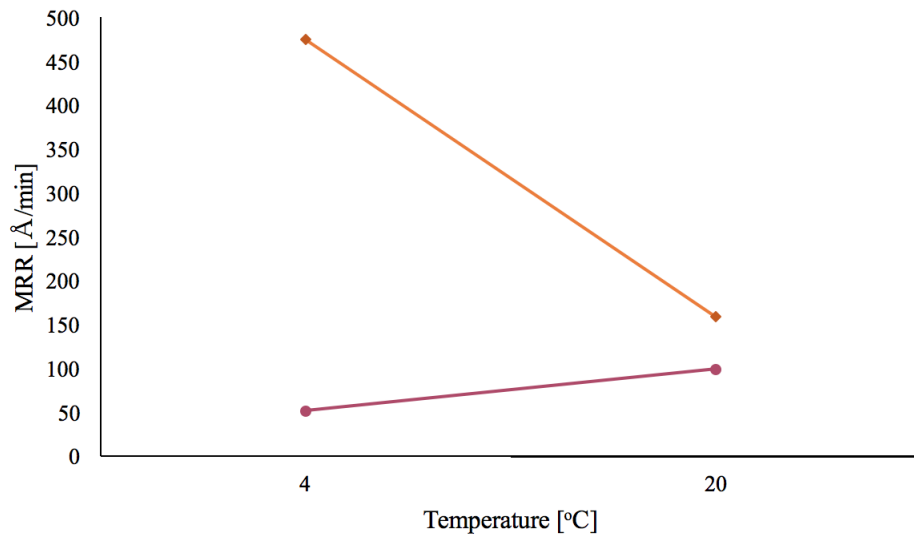
Figure 3.23: Comparison of the experimental values of MRR with the results obtained by the LSE method for temperature.

The correlations obtained based on combining weighting with LSE is given in

Equation (3.10). The graphs constructed by including weighting in the optimization are also presented in Figure 3.24 to Figure 3.27. The orange, pink and green lines represent experimental, optimization and optimization conducted with weighting data, respectively.

$$y = 50.7439x_1 - 1.3239x_2 + 3.0559x_3 - 19.5343x_4 \tag{3.10}$$

As it can be seen from these figures, when weighting was integrated, slope of the optimization curves became parallel to the experimental values, except for the solids loading correlation. The reason behind the problem with solids loading graph might be neglecting the first value in order to make the problem linear. The solids loading of the slurry affects the MRR by a change in the removal mechanism from a indentation mechanism to a contact area driven mechanism. At low solids loadings where the particles tend to gauge on the material surface through a 2-body friction mechanism, more defectivity is observed and the MRR values are also lower. When the percent solids of the CMP slurry is increased, there are more particles available to interact with the wafer surface in a 3-body friction mode and lower defectivity and higher removal rates can be obtained. Yet, the mathematical simulation requires boundary conditions to be able to account for these two mechanism and falls short to represent the removal response as a function of slurry solids loading with the current conditions and assumptions.

Figure 3.24: Comparison of the experimental values of MRR with the results obtained by the LSE method and with the weighting method for solids loading.
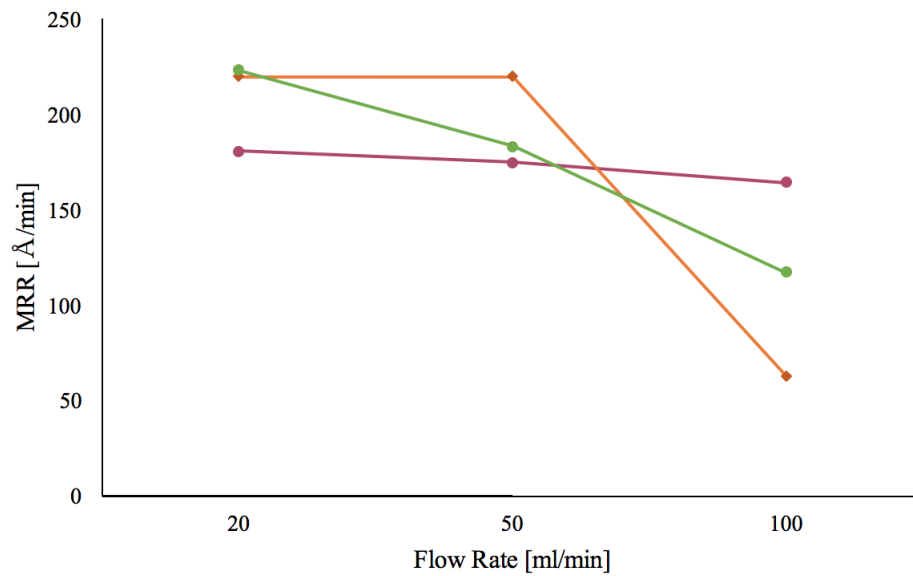
Figure 3.25: Comparison of the experimental values of MRR with the results obtained by the LSE method and with the weighting method for flow rate.

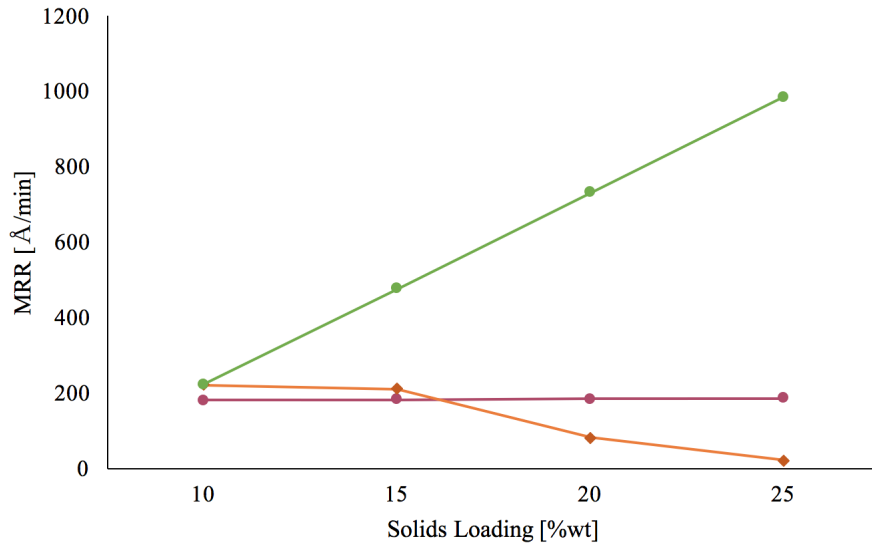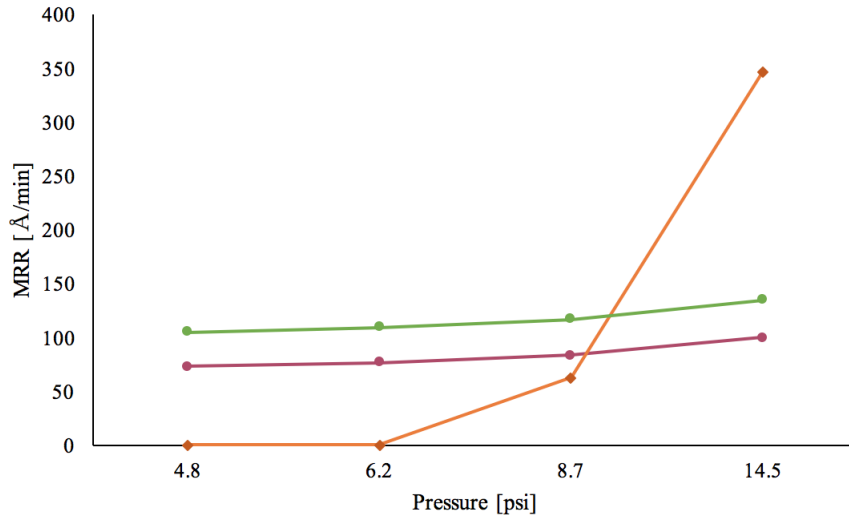**Figure 3.26:** Comparison of the experimental values of MRR with the results obtained by the LSE method and with the weighting method for pressure.
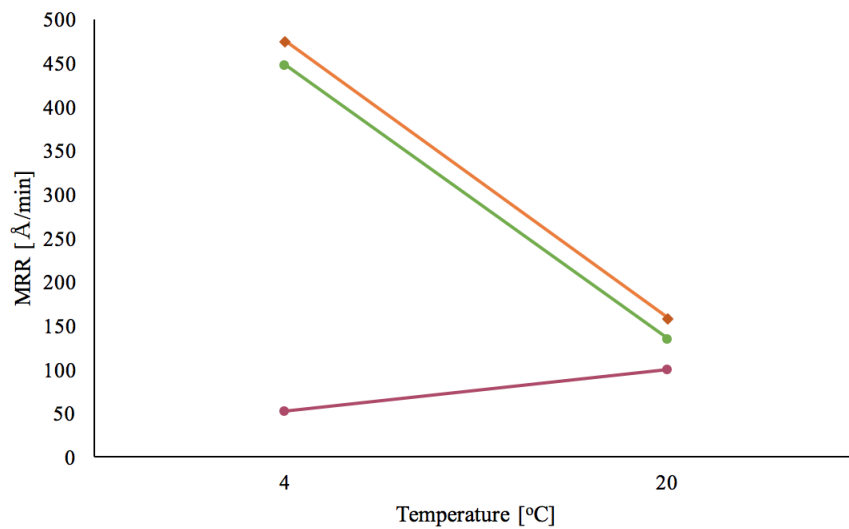
Figure 3.27: Comparison of the experimental values of MRR with the results obtained by the LSE method and with the weighting method for temperature.

Also, as for integrating surface roughness in mathematical optimization as well, pH evaluation experiments were selected. The input variables for pH experiments are

solids loading, flow rate and downward force, which are 10 %wt, 20 ml/min and 30 N respectively, which were not changed during the experiments, and lastly pH value of the slurry, which are 3, 6 and 9. The output variable was selected as surface roughness which are 1.280 nm, 0.9467 nm and 0.770 nm for pH 3, 6 and 9 respectively. The result of LSE gave an estimated result of 7.25 nm, 6.75 nm and 6.25 nm for pH 3, 6 and 9. As a result, the LSE of surface roughness should be developed and a trade-off between the surface roughness and the material removal rate should be done.

3.6   Summary

Experimental optimization was performed by changing the targeted the process variables one at a time and keeping all the other variables constant. Once the selected variable was optimized, the optimal value was fixed and used for the optimization of the remaining variables by the following experiments. This type of optimization requires high number of experiments, and therefore mathematical optimization is also conducted based on the physico-chemical knowledge gained from the experimental optimization. CMP evaluations were performed on bulk GaN coupons with 10 x 10 mm dimension and 1 mm thickness. During experiments, the effect of conditioner, pH value of the slurry, concentration of abrasive particles in the slurry, slurry flow rate, pressure applied on the wafer, chemistry of the slurry and temperature of the slurry was evaluated. Also a new tool set-up was developed in order to reduce the amount of slurry used. The use of conditioner showed an increase in the material removal rate, while it enables homogeneous slurry flow, and preserving the roughness of the polishing pad. During the pH evaluations, it is observed that the Ga-rich side has at least an order of magnitude higher removal rate compared to N-rich side. This is because of formation of Ga_2O_3 on the wafer surface and its removal by the relatively harder slurry abrasive particles. On the other hand, N-rich side requires the formation of a nitrogen terminated layer with one negatively charged dangling bond

on each nitrogen atom followed by the adsorption of hydroxide ions leading to the formation of oxides and removal of the oxides. Therefore, after the pH evaluations, CMP of N-rich side has been the focus of the study. pH evaluations showed that the material removal rate increased as the pH of the slurry increased, due to addition of hydroxide ions required for activating the material removal rate on the N-face. Also, the roughness values decreased as the pH of the slurry increased, which can be attributed by the tendency of silica particles to agglomerate at lower pH values. As a result, it is observed that the both surface free energy and work of adhesion values increased after polishing due to opening of fresh surface layers. During the slurry solids loading and slurry flow rate experiments, it is observed that the higher concentration of abrasive particles and higher flow rate detriments the material removal rate. This can be explained by the rolling of particles as higher number of particles exist between the polishing pad and the wafer surface. On the other hand, greater downforce values cause a decrease in material removal rate by inhibiting the number of particles to exist between the polishing pad and wafer interface. After the mechanical aspects were evaluated, the chemistry of the slurry is modified. As a result, addition of 0.1 M HCl contributed in removal rate by neutralizing the resultant NH_3 in-situ and pushing the reaction forward. The addition of 0.1 M HCl increased the MRR value from 157 Å/min to 189 Å/min. As a chemical modification, temperature of the slurry was also investigated. At 4°C, the MRR increased to 500 Å/min. This is because the GaN CMP reaction is an exothermic reaction which generates heat, and cooling the polishing pad by the slurry promotes the removal rate by pushing the reaction forward. However, although the MRR increased by the addition of 0.1 M HCl and decreasing the temperature of the slurry, the surface roughness values increased. This is because of the agglomeration of the particles at lower pH values and temperatures. Therefore, a trade-off should be made between the MRR and surface roughness of the wafer. Finally, a new pool configuration was developed and 157.22 Å/min MRR

was found, which is the same MRR value found by polishing with pH 9 slurry at 20 ml/min flow rate at 30 N downforce. As a result of the experimental optimization, 10 %wt slurry was used at pH 9 and 4^oC and 20 ml/min flow rate with 0.1 M HCl flown through the second slurry feeder at 10 N downforce in-situ conditioning CMP experiments were conducted. 880 ± 110 Å/min material removal rate with 0.8 ± 0.4 nm surface roughness were obtained.

By using the results of these experiments, mathematical optimization was performed. Using least square error method, the correlations between the selected input and output data are found. Weighting method was also used to determine reliabilities of the experiments. It is observed that when weighting method is used, the results of mathematical optimization got closer to the results of experimental values. The correlations between the input and output variables can give insight of the CMP procedure. Mathematical optimization can gather all the information gathered by experiments, and therefore reduce the number of experiments. The mathematical optimization approach conducted in this chapter is a preliminary work and can be developed by considering other parameters affecting the CMP procedure such as surface roughness. A trade off can be made by the mathematical optimization between the material removal and the surface roughness.

CHAPTER IV

CHARACTERIZATION AND IMPROVEMENT OF POST CMP CLEANING THROUGH SURFACE ANALYSES

4.1   Introduction

Chemical mechanical planarization is a well-established process in semiconductor manufacturing utilized for planarization of deposited metal or dielectric films to enable photo-lithography and multi-layer-metalization (MLM). The wafer surface is held by a holder and exposed to a polymeric pad under applied pressure as the head and the platen carrying the polishing pad rotate within a mismatch velocity. In the meantime, polishing slurry is flown on the pad surface, which is made of nano-meter sized abrasive particles and chemical agents to activate the wafer surface chemically. Hence, CMP has both mechanical and chemical components to achieve planarization and material removal spontaneously. The wafer surface is cleaned from the excessive chemicals and the slurry particles post CMP operations through utilization of the fundamentals of colloids and surface chemistry. The problem of attachment of the slurry particles on the wafer surface is becoming a more severe with the microelectronic device dimensions decreasing continuously.

In order to address the challenges of the post CMP cleaning, this chapter focuses on the correlation of the changes in the surface energy of the wafer post CMP to the particle count remaining on the wafer surface for the oxide surfaces as a model. To study the effects of surface nature of the substrate, surface roughness, contact angle, surface energy, and surface charge measurements of the glass slides were measured and compared to the particle count on the wafers post CMP cleaning treatment. In order to study the particle retention on the surface, particle removal experiments were
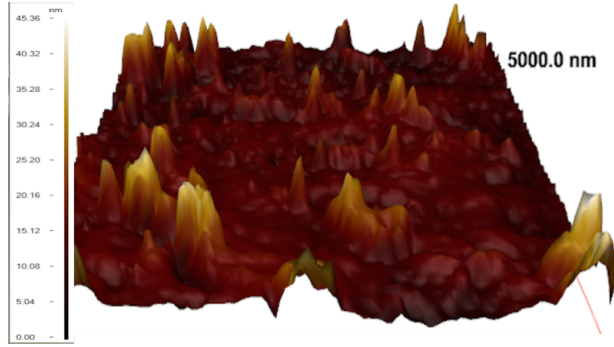
Figure 4.1: The glass slide surface cleaned by ultrasonication treatment at pH 9.

conducted in a rinsing flow cell and a siphoning flow cell by implementing impinging jet (rinsing) flow and siphoning flow, respectively. Consequently, better post CMP cleaning formulations were suggested for the oxide based CMP applications with optimal surface energy conditions fulfilled.

The post CMP cleaning procedure described in detail in Chapter 3 is implemented by rinsing the wafer surface in DIW, followed by the wafer treated in the ultrasonic bath in pH adjusted DIW at pH 9 for 10 minutes, then rinsed with DIW again and finally dried with Nitrogen gas. However, this process is found to be insufficient for removing particles from the wafer surface as it can be seen in Figure 4.1. The protruded regions on the glass slide are the remaining particles from the CMP treatment demonstrating the insufficient removal with the described procedure.

4.2   Glass Slide Experiments

The objective of this study is to analyze the relationship between the contact angle and the surface roughness to determine the optimum conditions for an easier post CMP cleaning scheme. The glass slides were utilized as a model to represent the silica based CMP applications such as oxide and STI CMP, yet the results of the systematic study can be implemented on to other surfaces such as GaN studied in this thesis in detail. An optimal post CMP cleaning procedure must be able to

remove the particles from the wafer surface effectively without damaging the surface. Therefore, the particle adhesion on glass surface was studied which is dominated by the van der Waals forces for particles in micron size range. The number of particles attached on the glass surface was observed by dynamic light scattering experiments.

The size of the abrasive particles in the CMP slurry has an important effect on the polishing rate and the surface quality. As the particle size increases, the polishing mechanism is more dominated by the 2-body friction as the larger particles are held by the pad and gauge against the wafer surface leading to more mechanical removal and elevated surface roughness. The change in slurry abrasive particle size can help modulate the surface roughness. Therefore, in order to obtain variation in surface roughness, abrasive particles with 60 nm, 1 μm, 3 μm, 6 μm and 9 μm particle sizes were used to obtain different surface roughness values on the glass slides.

4.2.1 Evaluation of the CMP Results for Correlation to Post CMP Performance

Glass slides were polished in order to obtain varying surface roughness values. All the experiments were conducted under the same conditions consecutively. Polishing conditions were set to 30 N downforce, 20 ml/min flow rate, 20 %wt slurry solids loading and 150 rpm rotational velocity for both the wafer holder and the polishing pad (same direction) with 20 seconds of CMP duration. IC-1000 pad was used with a diamond pad conditioner. Polishing slurries with silica and 1 μm, 3 μm, 6 μm and 9 μm sized diamond abrasives were used. For every type of slurry, five samples were polished in order to obtain a standard deviation. Polishing rates of the glass slides are determined by weighing the samples before and after the CMP process and finding the removed volume by the density formula based on the sample area and then dividing the removed thickness by the polishing duration. The surface roughness values were obtained via AFM measurements in contact mode.
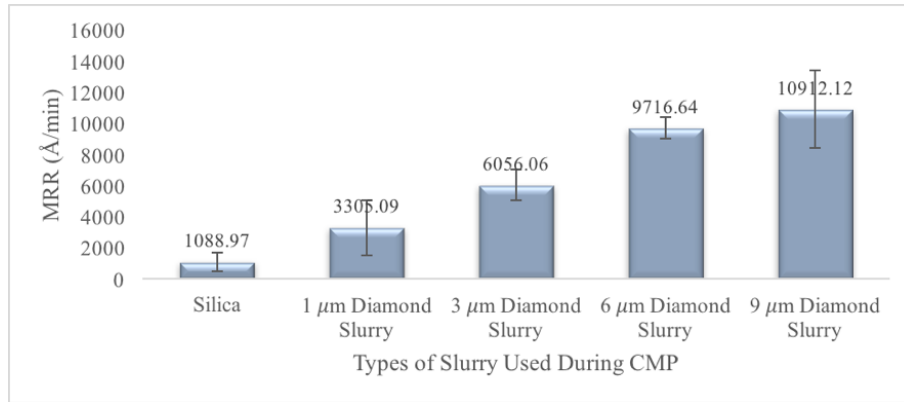
Figure 4.2: MRR results of the polished surfaces.
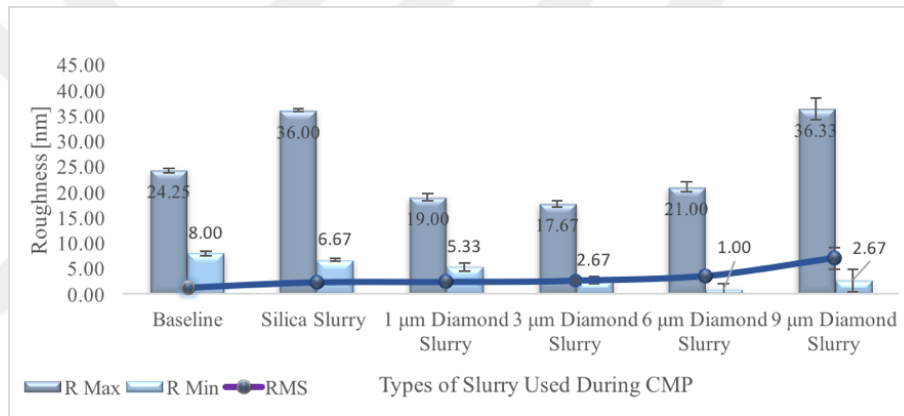
Figure 4.3: Roughness graph of the polished surfaces.

Figure 4.2 shows that the CMP MRR results as a function of slurry particle size. The CMP polishing rate increases as the particle size increases. The error bars were obtained by conducting the same experiment with 3 different glass slide samples. Figure 4.3 shows the corresponding surface roughness values in root mean square (RMS). It can be seen that the roughness values increase with the increasing particle size. The relatively higher R_{max} values observed with the CMP conducted by using the baseline slurry and 1 μm diamond slurry were caused by the silica particles remained stuck on the surface that can be seen in the Figure 4.5. Figure 4.5 through Figure 4.9 show the AFM images of the surfaces polished with different types of abrasives in the CMP slurry.
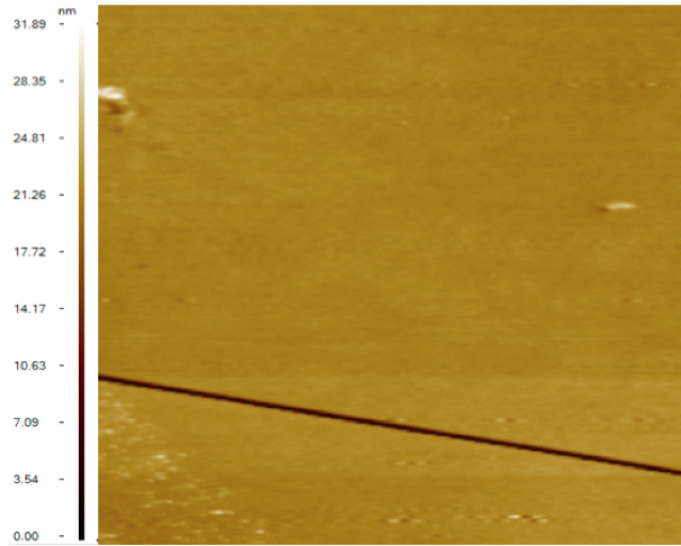
(a)
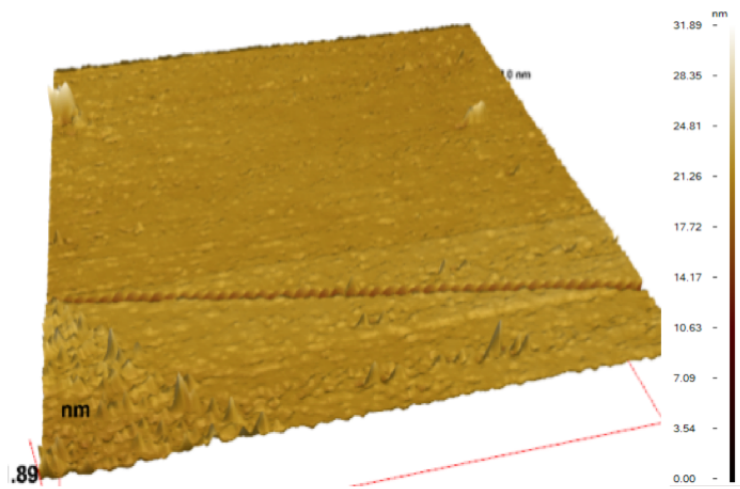
(b)

Figure 4.4: AFM images of the glass slide surface before polishing (a) 2D and (b) 3D.
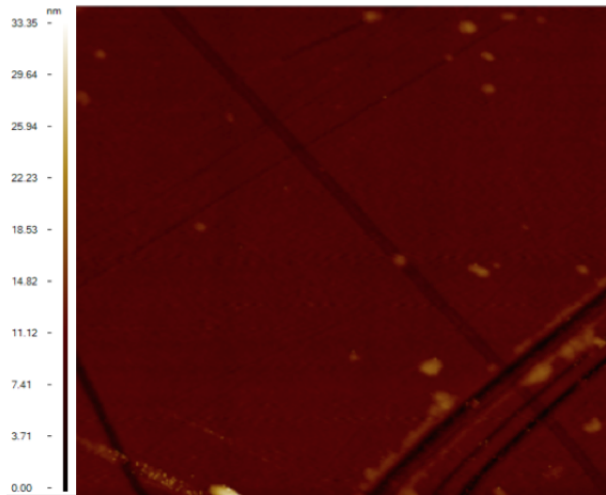
(a)
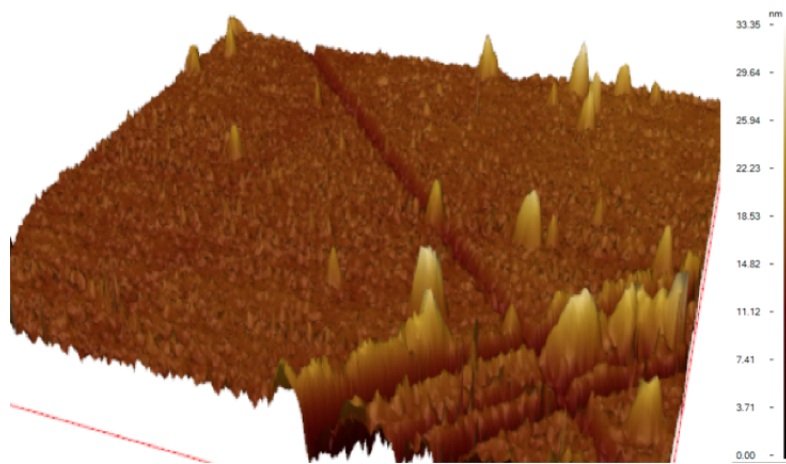
(b)

Figure 4.5: AFM images of the glass slide surface after polished with 20 %wt silica slurry (a) 2D and (b) 3D.
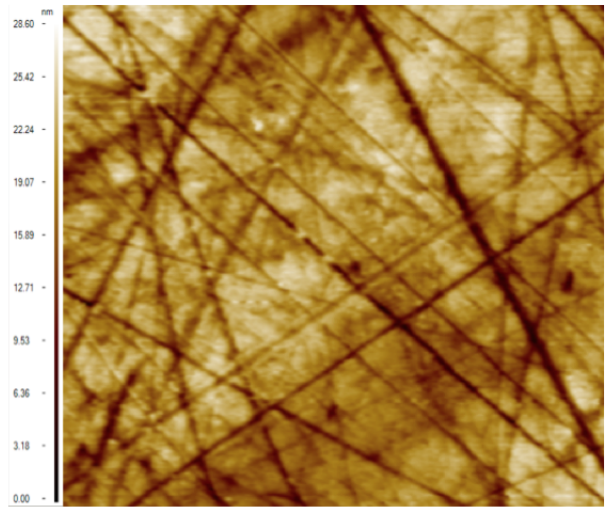
(a)
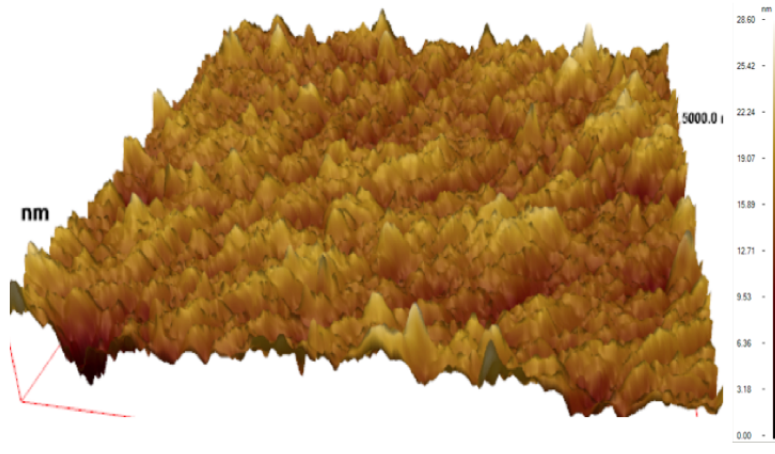
(b)

Figure 4.6: AFM images of the glass slide surface after polished with 20 %wt diamond slurry with particle size of 1 μm (a) 2D and (b) 3D.
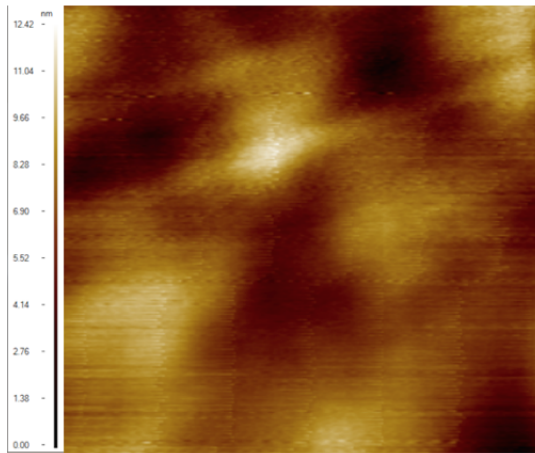
(a)
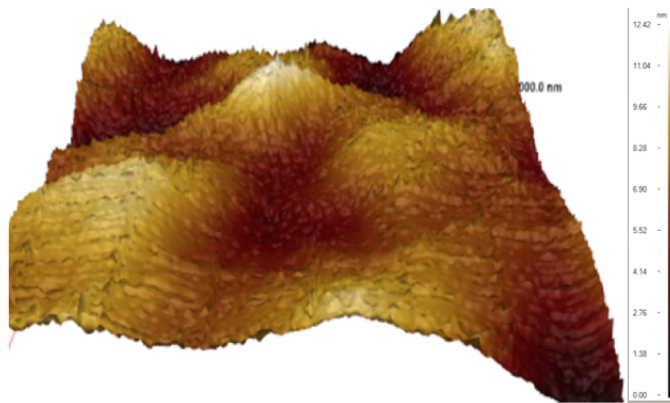
(b)

Figure 4.7: AFM images of the glass slide surface after polished with 20 %wt diamond slurry with particle size of 3 μm (a) 2D and (b) 3D.
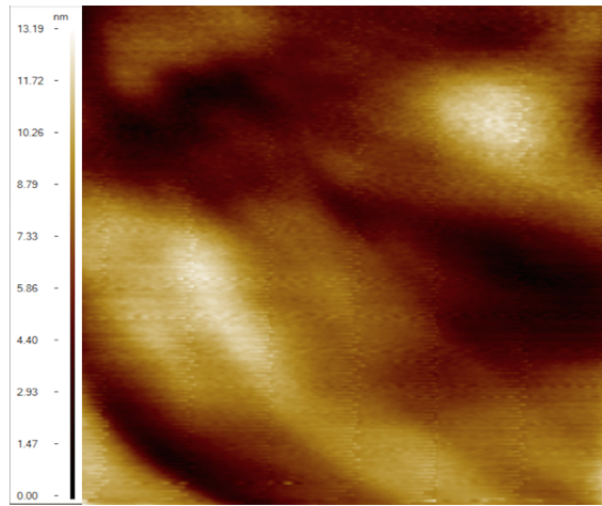
(a)
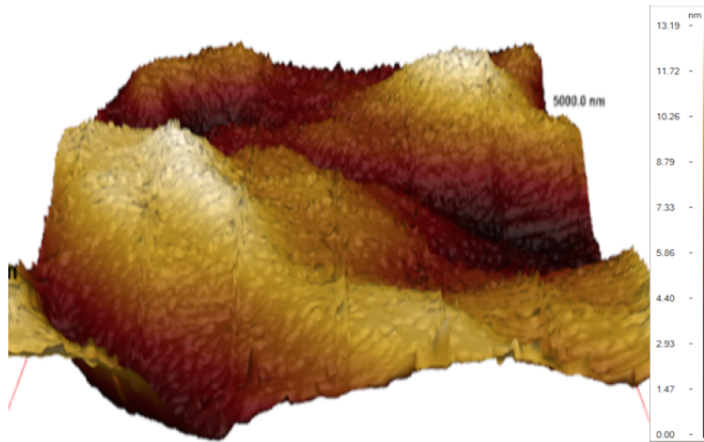
(b)

Figure 4.8: AFM images of the glass slide surface after polished with 20 %wt diamond slurry with particle size of 6 μm (a) 2D and (b) 3D.
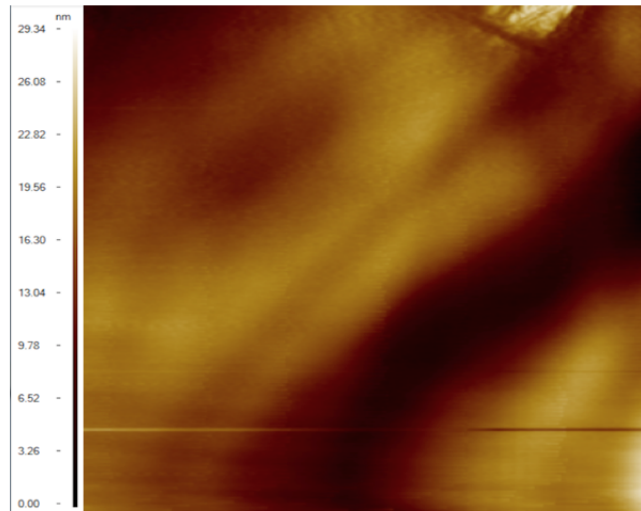
(a)
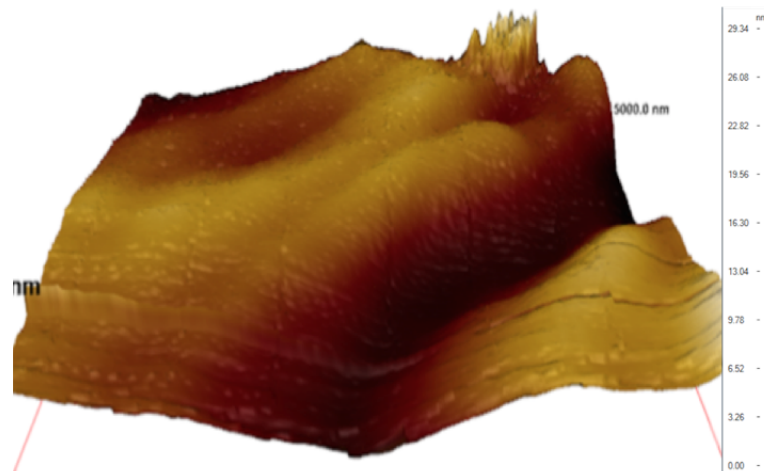
(b)

Figure 4.9: AFM images of the glass slide surface after polished with 20 %wt diamond slurry with particle size of 9 μm (a) 2D and (b) 3D.

In an attempt to improve the post CMP cleaning, the wettability of the surface is a very critical factor as it determines the tendency of the particles to get stuck on the wafer surface. Therefore, contact angle measurements and surface free energy

and work of adhesion calculations were conducted for the glass slide surfaces polished with different slurry abrasives sizes. Figure 4.10 shows the contact angle measurement results of the unpolished (baseline) and polished surfaces. Unpolished surface has a contact angle of 66.85^o, which is already a hydrophilic surface, and as the polishing was performed the contact angle values decreased dramatically, indicating that the surfaces became more hydrophilic. The contact angle results correlate to the surface roughness measurements in that as the surface roughness increases the wettability also increases. In Figure 4.11, it is observed that as the surface roughness increases, the work of adhesion also increases meaning that the propensity of particle attachment to the surface has increased and higher amount of work should be applied to detach a solid and a liquid substrate.
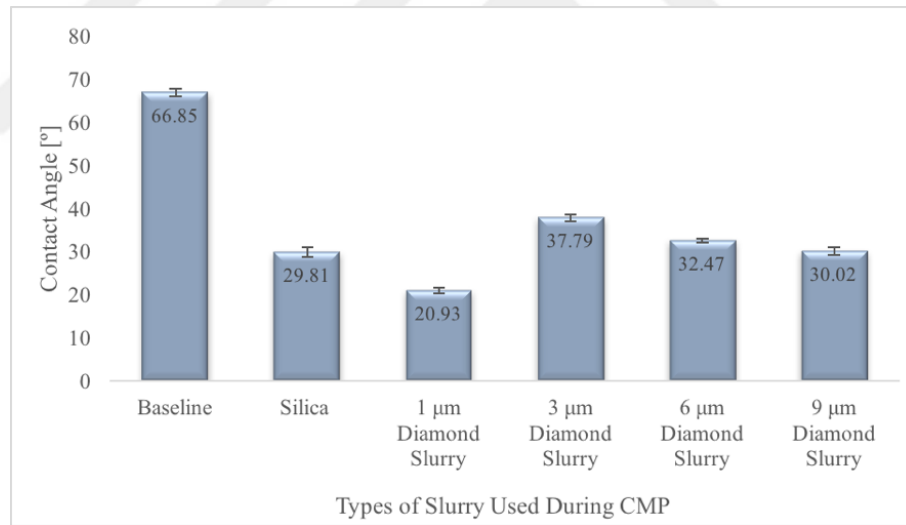
Figure 4.10: Contact angle results of the polished surfaces.
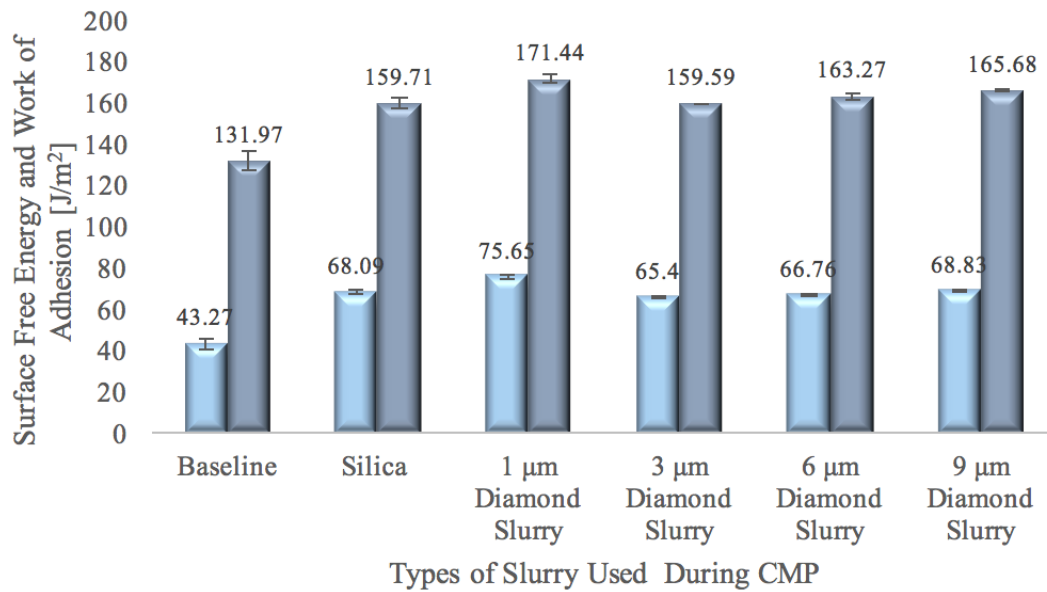
Figure 4.11: Surface free energy and work of adhesion calculations of the polished surfaces.

4.3 Post CMP Cleaning Evaluations by Using Viscoelastic Fluids

Removing particles from the surface, while maintaining the surface quality is important in various applications, such as aerospace, pharmaceuticals [Kas97] and optical lenses. In integrated circuit fabrication, over 50% of the yield losses occur because of the insufficient cleaning of the wafers [Zha00]. In order to clean the surfaces post processing, there are numerous methods available including physical and chemical methods as discussed in Chapter 2. The use of strong chemicals like hydrogen peroxide and hydrochloric acid may be preferable, however, one should consider the environmental effects of the chemicals used while removing particles from the surface particularly for high volume manufacturing applications such as microelectronics production [Ker90, Ita93].

Particles can be removed from the surfaces by chemical etching [Kum06], and also

by applying external physical forces. The physical removal of particles is achieved by weakening the adhesion forces between the particles and the surface and then applying an external force during this spontaneous detachment of the particles [Vis95]. As an external force, hydrodynamic forces via application of flow is also considered. Most of these applications utilize simple shear flows generated by channel flows [And11, Yia95] or rotating the surface while it is dipped into a liquid [Bus93]. Also, jet flows are considered by Gim et al. and Soltani and Ahmadi [Gim95, Sol94, Hir06]. However, all these applications can be conducted preferably by using a Newtonian fluid [Hir06] and water has been shown to be effective only when the adhesion forces are weak. Therefore, in this work, post CMP cleaning by viscoelastic polymer solutions was studied which was studied and proven to be effective by Walker 2013 [Wal13].

Walker et al. focused on two different flow methods, siphoning flow and jet flow by using two different fluids as shown in Figure 4.12 [Wal13]. In both flow cases, the glass substrate coated with silica particles are coated with a polymeric solution. In siphoning flow, the polymeric fluid is vacuumed from the glass surface, and in the jet flow a water jet flow is applied on the surface. In this study, only siphoning flow was implemented since it is important to reduce the possibility of reattachment of particles on the surface and also because of the fact that it is a simpler method as compared to the jet flow where two fluids with different viscosities need to be considered.

The previous studies on particle removal by hydrodynamic forces proposed that the particles might be rolling, sliding or lifted from the surface during removal. The particles might be sliding on the surface caused by the Stokes drag force or rolling because of the shear force formed by the torque applied on the particles during the cleaning procedure. These two mechanisms will be discussed to explain the cleaning performance in the presence of the viscoelastic fluids.
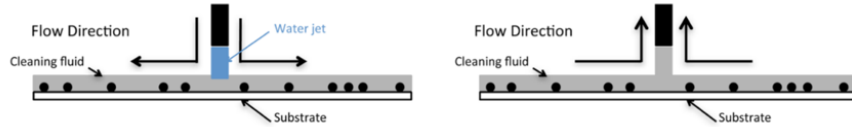
Figure 4.12: Visualization of jet flow and siphoning flows, the figures are not drawn to scale [Wal13]

.

4.3.1   Polymeric Solution

PAM (polyacrylamide) and PEO (polyethyleneoxide) polymers were chosen to study viscoelastic flow and 7% weight concentration of PAM solution was prepared for the post CMP cleaning experiments. Separan AP-273 (Dow Chemical Co.) is an anionic polyacrylamide in neutral or alkaline solutions with sodium as its counter ion. In the molecular formula for the linear polyelectrolyte, [CH2CH(CONH2)]x [CH(CONa)]y, the ratio x:y is 77. The average molecular weight of Separan AP-273 is estimated to be 6 x 106 daltons, but the weight ranges from under 3 x 105 to over 4 x 107 daltons [Col87] Separan AP-273 was mixed with water in order to generate 7% weight concentration solution.

4.3.2   Rheology Test Results

Rheology tests for 0.7 %wt PAM solution were conducted with 60 mm 1° cone. The degree of cone expresses the angle between the cone and the plate surface. The reason behind using a small angle cone is that it requires small amount of sample, the temperature rise is very small, the sample can be kept between the cone and the plate easily and the shear rate and shear stresses are uniform.

Dynamic rheology tests of the solution were conducted in order to find G', G" and G* values, which are; storage modulus, loss modulus and complex modulus. The storage modulus represents the elastic part of the viscoelastic fluid and it indicates

the stress energy which is stored temporarily during the test, and can be recovered after the test is finished. The loss modulus represents the viscous part of the fluid and it indicates the energy required to initialize the flow, which is irreversibly converted to shear heat [Kre00].

In the dynamic tests conducted in this chapter, an oscillating strain is applied with an assigned frequency. Dynamic tests provide data on viscosity and elasticity responses of the sample in time.

First of all, the oscillation amplitude test was done at isothermal conditions at 25°C. The angular frequency was selected to be 1 rad/s, strain limits are between 1 x 10-5% and 10.0% and points per decade as 5. Figure 4.13 shows the results of the first test demonstrating that the linearity is at 5% strain. Therefore, 5% strain was applied for the 2nd experiment.

The second test performed was the oscillation frequency testing, which was conducted also under the isothermal conditions of 25°C temperature. Strain level was selected to be 5% with angular frequency limits between 0.01 rad/s to 100 rad/s and points per decade was chosen to be 5 again. The result of the second experiment is represented in Figure 4.14 shows the intersection point of G and G. It can be seen that there are two different intersection points, and the one where the phase angle increased too much was neglected.
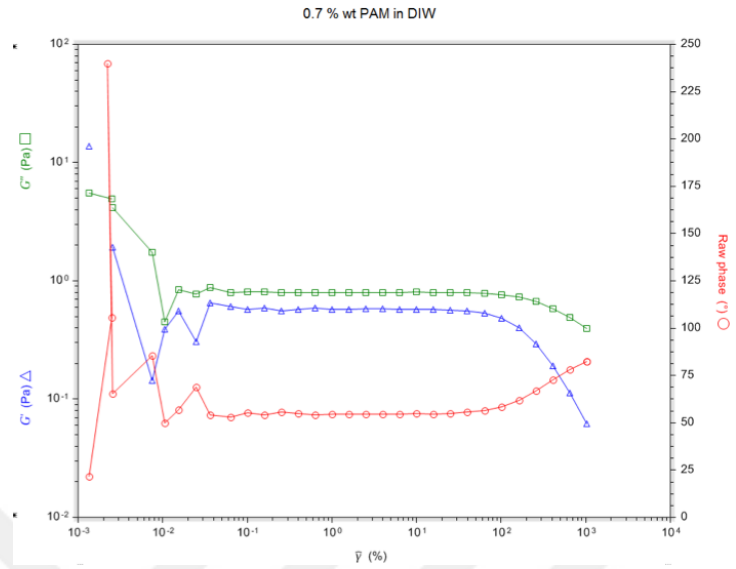
Figure 4.13: Results of Oscillation Amplitude for 0.7 %wt PAM solution.
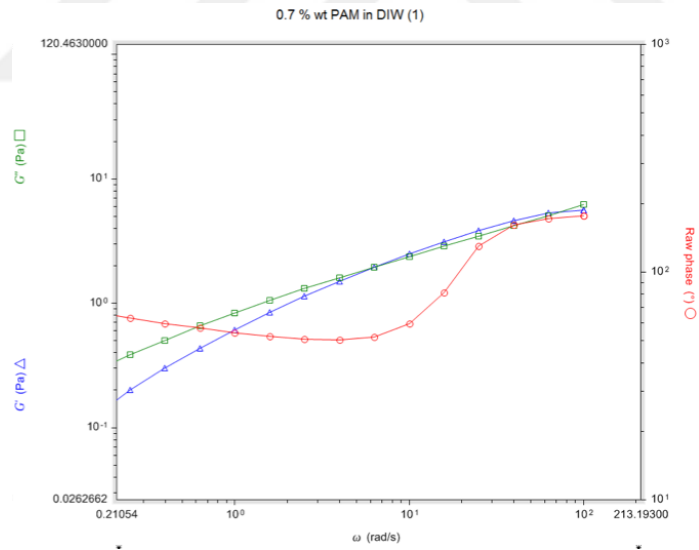
Figure 4.14: Results of Oscillation Frequency Test for 0.7 %wt PAM solution.

The third experiment performed was the flow sweep (shear rate) test (Figure 4.15) which was done between the shear rate limits of 0.01 /s to 100.01 /s and under isothermal conditions at 25°C for consistency.
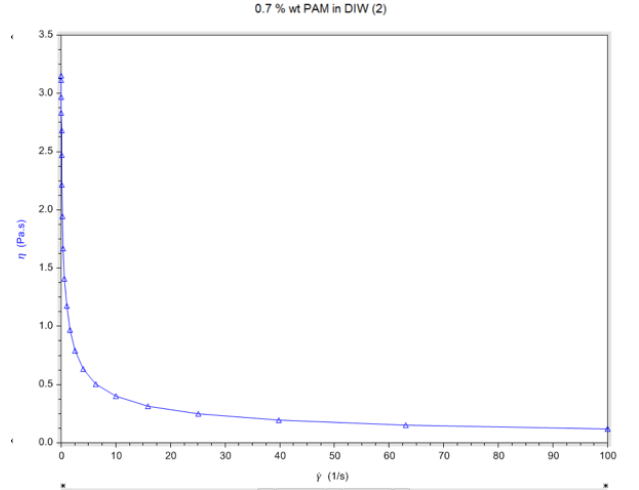
Figure 4.15: Results of Shear Rate Test for 0.7 %wt PAM solution.

The rheology tests in the presence of 0.5 wt% PEO solution were conducted with 60 mm 1° cone as well. The first test was the oscillation amplitude, which was performed at isothermal conditions at 25^oC. The angular frequency was determined as 1 rad/s, and strain limits determined between 0.01% to 10.0% and the points per decade is chosen as 5. The results of this test showed that the linearity is at 6.3% (Figure 4.16).
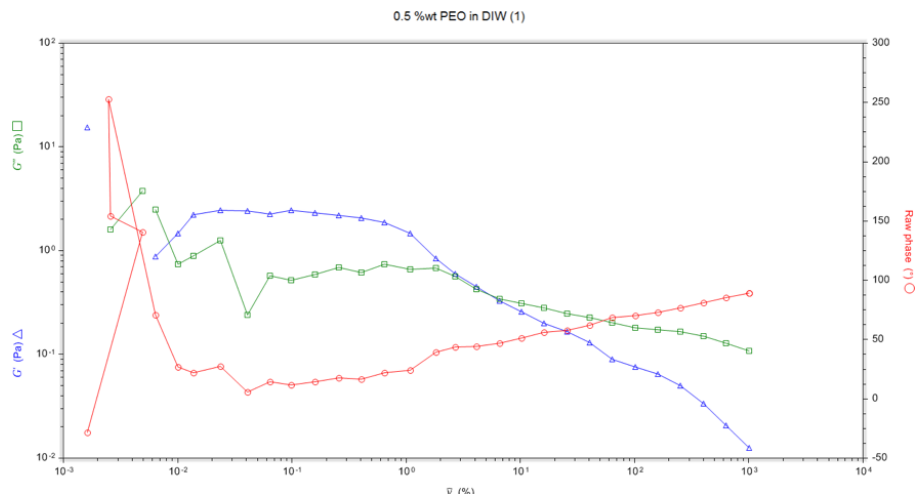
Figure 4.16: Results of Oscillation Amplitude Test for 0.5 %wt PAM Solution.
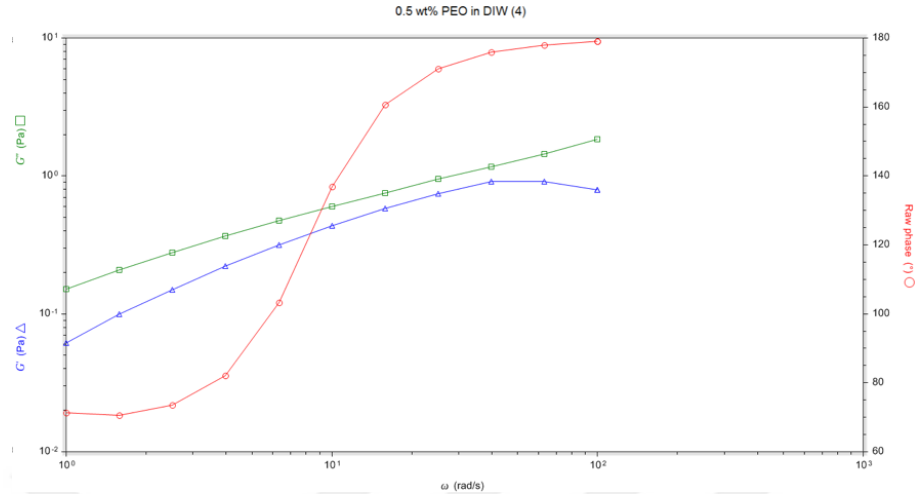
Figure 4.17: Result of Oscillation Frequency Test for 0.5 %wt PEO Solution.

The second test was the oscillation frequency done at isothermal conditions at 25°C. The strain percentage is selected to be 6.3% as a results of the oscillation amplitude test. The angular frequency limits were between 0.01 rad/s to 100 rad/s. An intersection point of G and G is not observed in this test as shown in Figure 4.17.

In these tests, it is observed that the viscosity of 0.7 %wt PAM solution decreases as the shear rate increases, indicating a shear thinning behavior. The oscillation frequency test for 0.7 %wt PAM solution, shows that the loss modulus is higher than the storage modulus up to critical frequency, where they intersect. However, above this frequency, the viscous and elastic parts of the solution are almost equal, as it is for 0.5 %wt PEO solution.

4.3.3 Silica Coating of the Glass Slides

There are various ways to coat the glass slide by the silica particles to study their effective removal methods. One method is using an atomizer to spray the silica solution on the glass slide, another alternative may be immersing the glass slide in the silica solution at a high temperature or spin coating as alternatives. In this study, the glass slides were coated by sonication method. The aim of this procedure was to

force particles to attach on the surface by the sound waves generated by the sonication tip.

First of all, a silica solution with ethanol was prepared (the details of this solution is given in the following section). Then this solution was sonicated at amplitude of 30 for 1 min. Then the glass slide was mounted with a clamp in the solution beaker perpendicular to the bottom of the beaker as shown in Figure 4.18. While mounting the glass slide, the back of the sample should not be covered. After mounting, the sonication tip was turned on at an amplitude of 30 and glass slide was kept in the solution with the sonication tip on for 15 minutes. The beaker or the glass slide were kept stand still during the coating operation. The glass slide was kept in the beaker with the sonication tip on for 15 minutes more. When the sonication was stopped, glass slide was heated on a pre-heated hot plate until the ethanol was fully evaporated. This enables attachment of silica particles on both sides of the glass slide, however, the surface which is closer to the sonication tip has more particles coated on it. The surface which had less particles is cleaned since the remaining silica particles on the backside of the analyzed surface would cause reflection and misleading particle counts.
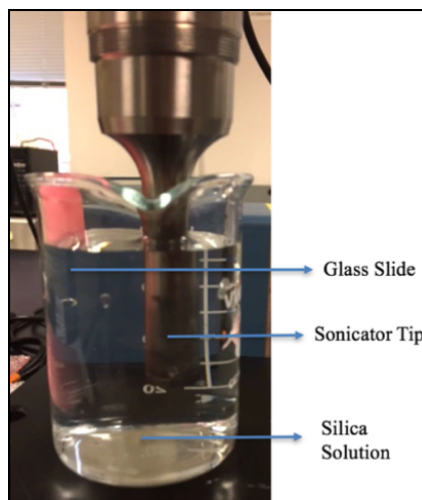
Figure 4.18: Setup for Coating with Sonication Tip.

4.3.4 Optimum Concentration of Silica Solution

In order to determine the optimum concentration of the silica solution, which is used to coat the glass slides, 6 different concentrations were experimented.

- 0.001 %wt

- 0.005 %wt

- 0.01 %wt

- 0.025 %wt

- 0.05 %wt

These solutions were prepared by using ethanol and dry silica particles. Due to the agglomeration tendency and enabling uniform distribution of the particles, 0.025 %wt silica was chosen as the optimum concentration. Figure 4.19 shows comparison of different methods of coating silica particles on the glass slide. The image on the left shows the particle distribution of silica on the glass slide coated with the silica solution by sonication, and the image on the right shows the particle distribution of silica particles on the glass slide coated by spraying the silica solution with an atomizer. As it can be seen clearly, spraying particles on the glass surface causes severe agglomeration of the particles and homogeneous distribution cannot be obtained. Hence the sonication method is much more preferable to evaluate post CMP cleaning performance.
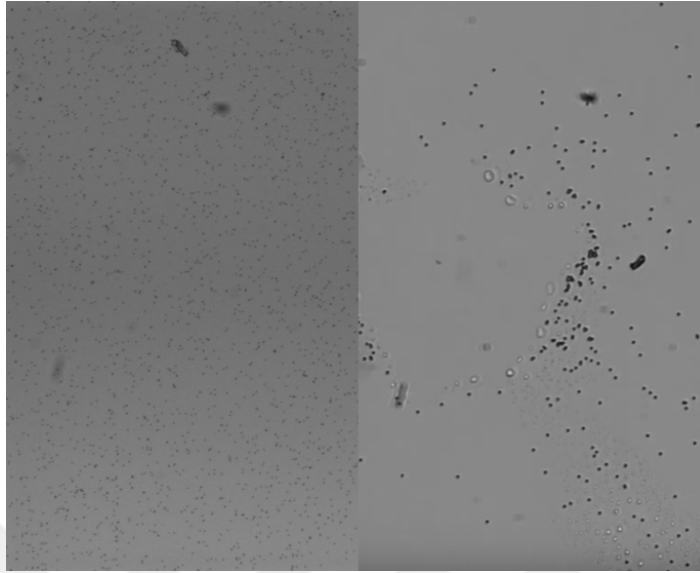
Figure 4.19: Comparison of Different Methods of Silica Coating.

4.3.5 Background Subtracting

While there was some background noise because of the microscope lenses, the background image should be subtracted from the final images analyzed. First of all, subtraction by using Image J was tried, however, it was insufficient. Therefore, a MATLAB code was generated in order to subtract background image from the image of the glass slide. The code returns the subtracted image and the particle density. Figure 4.20 shows the images before and after background subtraction.
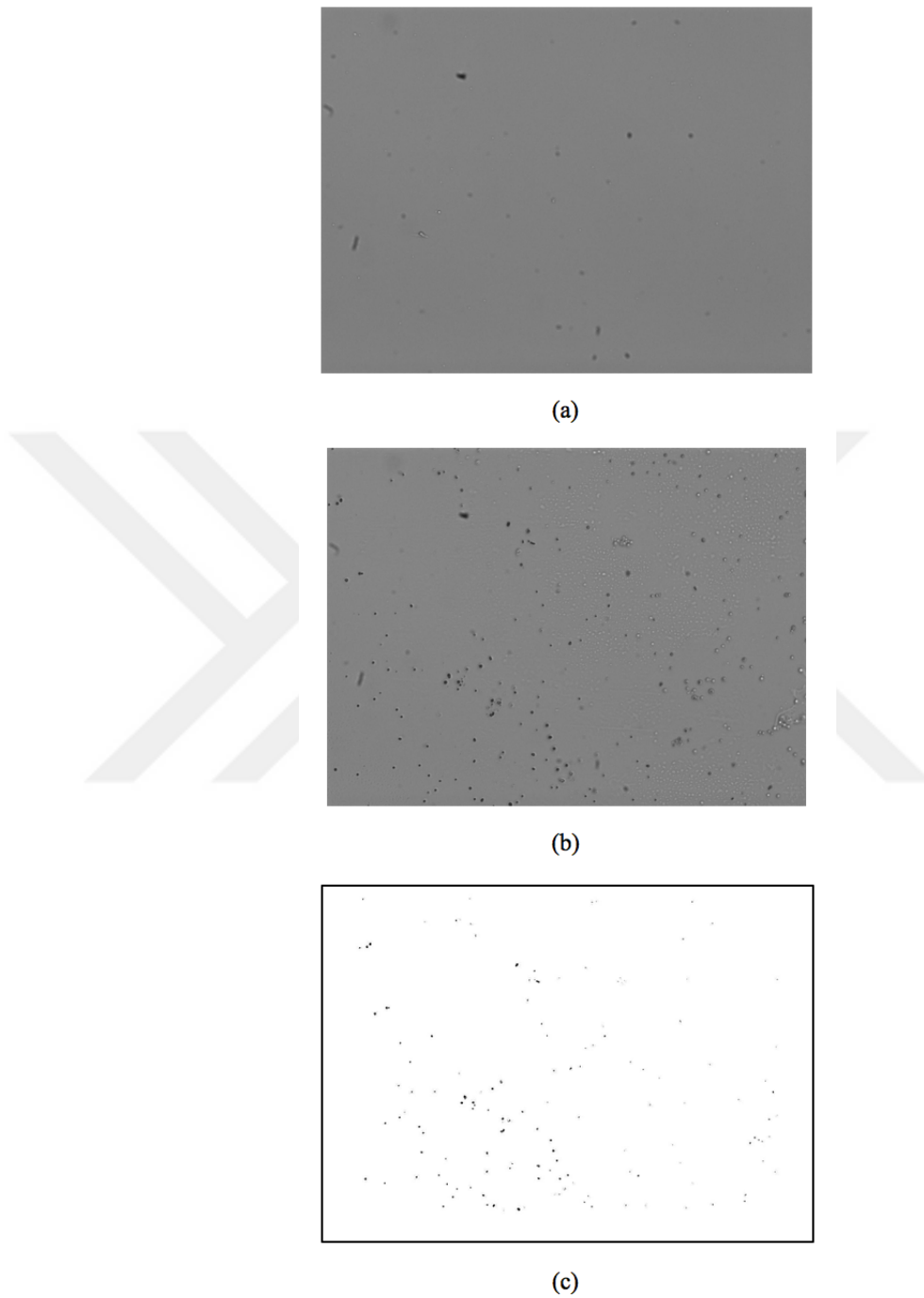
Figure 4.20: Images of (a) background, (b) before background subtraction, (c) after background subtraction

4.3.6 Experimental Parameters

In order to conduct siphoning flow experiments to represent the cleaning of the surface from the attached particles, an air vacuum, a Florence flask, and a siphon tube were utilized. The air vacuum was connected to the Florence flask, which enables collecting the silica particles and the polymeric solution into the Florence flask.

To conduct the experiment, a holder was used which enables to conduct the experiment without changing the position of the glass slide with reference to the microscopic lens. This holder was mounted on the automated stage, where the automated stage could move in x and y directions. The importance of the automated stage was that it enabled observing the surface as a whole through taking pictures simultaneously at different locations. 10X magnifier lens was used in order to be able to observe a larger area of the surface, while the aim was to evaluate the difference between the number of particles on the glass slide, before and after siphoning flows. Figure 4.18 shows the siphoning flow set-up.

While conducting the siphoning flow experiments, polymeric solutions were used as prepared earlier. These were 0.7 %wt PAM solution and 0.5 %wt PEO solutions. For either of these solutions, the glass slides had to be fully coated for the siphoning flow to be generated appropriately. The optimum amount of polymeric solution was determined as 40 ml, according to the experimental results. To determine the flow rate of the air vacuum, the time it takes to siphon 100 ml of polymer solution was measured. The flow rate was measured to be 42.1 ml/sec during the experiments.

In siphoning flow experiments, the tip of the nozzle was 1 cm above the substrate and the inner diameter of it was 3.2 mm. First of all, the polymer was poured onto the glass substrate, where the substrate was in a holder so that the polymer was not spilled and a film thickness could be obtained. Then, the siphoning experiments were conducted. After conducting the siphoning flow experiment, multiple images were taken at 30 FPS (frames per second) and these images were aimed to be stitched

together in order to build up another bigger picture to be able to conduct particle removal analyses. Stitching was possible when two images overlapped. To provide this overlap, velocities for both x and y motors were determined.

The automated stage was moving with the help of two motors (one in x direction and the other is in y direction). These motors moved the stage in such a way that, almost every part of the glass slide could be seen. For the first iteration, 75% overlap in x direction and 25% overlap in y direction was chosen. To ensure the set-up configuration the images were taken at 30 FPS while both motors were moved with a 0.1 mm/s velocity.

Another issue with the images were the inhomogeneous distribution of silica particles over the glass slide. The coating procedure with the sonication worked well in terms of homogeneity and distribution, yet the sides of the glass slide could not be coated by sonication method. That is why, the images were taken mostly by avoiding the edges of the glass slides. Because of this, the optimum starting point was determined as (7.5, 4.5).

4.3.7 Correlation of Distance with Particle Removal

In this part, a correlation in the distance between the siphon tube and the particle removal efficiency was tried to be achieved. First of all, a center was defined and the siphon tube was kept at this center. Then, 10 points were determined and using the motor controller pictures were taken at each determined point. Afterwards, the siphoning flow was done at the determined center and pictures were taken again from the same points after the siphoning flow. Finally, background subtraction was performed for each image and particle count was done by using ImageJ program. The results of this experiment are shown in Figure 4.21 indicating that the particle removal decreases as the distance between the siphon tube and the particle increases.
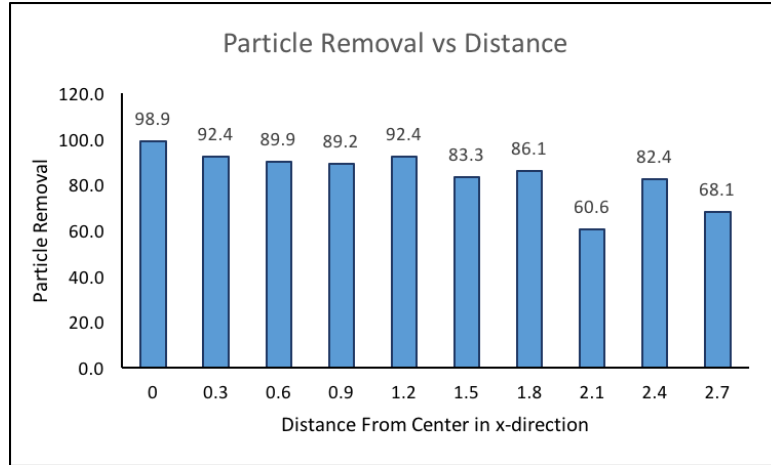
Figure 4.21: Distance vs Particle Removal Experimental Result.

4.4 Summary

In this chapter, the surface free energy and work of adhesion values were correlated with the surface roughness values. It is shown that the larger abrasive particle size contribute to higher material removal rates, however, they cause the surface roughness values to increase as well. It is observed that as the surface roughness values increase, the surface free energy and work of adhesion values increase as well. This is directly related with post CMP cleaning, where as the surface free energy increases, it will be higher to remove particles from the surface without damaging the surface quality. As shown in Chapter 3, the surface free energy of GaN surface increase after polishing, because of opening of the fresh surface layers. As the surface free energy increases, it is harder to remove particles from the surface. Therefore, water becomes insufficient for removing these particles. Acidic solutions can be used for post CMP cleaning, however these strong chemicals would cause damage on the wafer surface due to etching. Therefore, a new method of post CMP cleaning is proposed in this chapter. It is observed that using viscoelastic fluids increases the removal of particles, due to the Stokes drag force applied on the particles by the viscoelastic fluids. The cleaning

98

method can be improved by applying it on different surfaces with different roughness values, which are obtained by different abrasive particle sizes.

CHAPTER V

CONCLUSION

5.1   *Summary*

This thesis focused on the characterization of GaN surface, CMP of GaN and post CMP cleaning development. CMP was first introduced in 1950 for minimizing the surface defects on the silicon wafer utilized to manufacture the IC devices. However, as the device dimensions decreased, the capability of Si became insufficient due to its crystallographic orientation and material properties. Therefore, for applications requiring high temperature, high frequency and wider band gap, compound semiconductors are started to being used, which are generally composed of III/V or II/VI elements, such as GaN. Although, GaN is capable of providing the demands of new applications, it is chemically inert, mechanically hard and the growth of GaN is harder compared to Si. Therefore, polishing the surface of GaN without disturbing the single-crystal atomic arrangement is very hard due to it's unique properties. Also, the academic know-how on CMP of GaN is very low compared to Si, while understanding the surface processing properties of GaN was first established in 1996. Modeling approaches have been made for CMP procedure, although modeling approaches are not able to reflect the real life problems faced during the CMP procedure, while all the parameters could not be considered in the models. Therefore, gathering the information through the experimental procedures, analytical correlations between the inputs and outputs can be utilized to optimize the CMP process. On the other hand, as the device dimensions decrease, the permission of minimum surface defects decrease as well, therefore post CMP cleaning should also be considered. While removing particles from the surface during post CMP cleaning, the surface quality should be

protected. There are various methods to conduct post CMP cleaning, however a new way of post CMP cleaning should be provided, while the current methods are insufficient.

The preliminary CMP analyses conducted on the GaN coupons as a function of the crystallographic outline orientation outline the differences of the Ga and N rich faces with respect to wettability and surface energy as observed by the contact angle measurements. The pre and post CMP surface characterization of the wafers is critical in terms of understanding the chemical reactions taking place during the CMP process as well as the post CMP performance of the wafers in terms of the affinity of the particles to remain on the wafers.

In experimental optimization results, it is observed that the use of conditioner increases the material removal rate, while it enables homogeneous slurry flow, and preserves the roughness of the polishing pad. During the pH evaluations, it is observed that the Ga-rich side has at least an order of magnitude higher removal rate compared to N-rich side. This is because of formation of Ga_2O_3 on the wafer surface and its removal by the relatively harder slurry abrasive particles. On the other hand, N-rich side requires the formation of a nitrogen terminated layer with one negatively charged dangling bond on each nitrogen atom followed by the adsorption of hydroxide ions leading to the formation of oxides and removal of the oxides. Therefore, after the pH evaluations, CMP of N-rich side has been the focus of the study. pH evaluations showed that the material removal rate increased as the pH of the slurry increased, due to addition of hydroxide ions required for activating the material removal rate on the N-face. Also, the roughness values decreased as the pH of the slurry increased, which can be attributed by the tendency of silica particles to agglomerate at lower pH values. As a result, it is observed that the both surface free energy and work of adhesion values increased after polishing due to opening of fresh surface layers. During the slurry solids loading and slurry flow rate experiments, it is observed that the

higher concentration of abrasive particles and higher flow rate detriments the material removal rate. This can be explained by the rolling of particles as higher number of particles exist between the polishing pad and the wafer surface. On the other hand, greater downforce values cause a decrease in material removal rate by inhibiting the number of particles to exist between the polishing pad and wafer interface. After the mechanical aspects were evaluated, the chemistry of the slurry is modified. As a result, addition of 0.1 M HCl contributed in removal rate by neutralizing the resultant NH_3 in-situ and pushing the reaction forward. The addition of 0.1 M HCl increased the MRR value from 157 Å/min to 189 Å/min. As a chemical modification, temperature of the slurry was also investigated. At 4°C, the MRR increased to 500 Å/min. This is because the GaN CMP reaction is an exothermic reaction which generates heat, and cooling the polishing pad by the slurry promotes the removal rate by pushing the reaction forward. However, although the MRR increased by the addition of 0.1 M HCl and decreasing the temperature of the slurry, the surface roughness values increased. This is because of the agglomeration of the particles at lower pH values and temperatures. Therefore, a trade-off should be made between the MRR and surface roughness of the wafer. Finally, a new pool configuration was developed and 157.22 Å/min MRR was found, which is the same MRR value found by polishing with pH 9 slurry at 20 ml/min flow rate at 30 N downforce. As a result of the experimental optimization, 10 %wt slurry was used at pH 9 and 4°C and 20 ml/min flow rate with 0.1 M HCl flown through the second slurry feeder at 10 N downforce in-situ conditioning CMP experiments were conducted. 880 $\pm$ 110 Å/min material removal rate with 0.8 $\pm$ 0.4 nm surface roughness were obtained.

By using the results of these experiments, mathematical optimization was performed. Using least square error method, the correlations between the selected input and output data are found. Weighting method was also used to determine reliabilities of the experiments. It is observed that when weighting method is used, the results

of mathematical optimization got closer to the results of experimental values. The correlations between the input and output variables can give insight of the CMP procedure. Mathematical optimization can gather all the information gathered by experiments, and therefore reduce the number of experiments. The mathematical optimization approach conducted in this chapter is a preliminary work and can be developed by considering other parameters affecting the CMP procedure such as surface roughness. A trade off can be made by the mathematical optimization between the material removal and the surface roughness.

In Chapter 4, the surface free energy and work of adhesion values were correlated with the surface roughness values. It was shown that the larger abrasive particle size contribute to higher material removal rates, however, they cause the surface roughness values to increase as well. It is observed that as the surface roughness values increase, the surface free energy and work of adhesion values also increase. This is directly related to the post CMP cleaning performance, where as the surface free energy increases, it will be harder to remove particles from the surface without damaging the surface quality. As shown in Chapter 3, the surface free energy of GaN surface increase after polishing, because of opening of the fresh surface layers. As the surface free energy increases, it is harder to remove particles from the surface. Therefore, water becomes insufficient for removing these particles. Acidic solutions can be used for post CMP cleaning, however these strong chemicals would cause damage on the wafer surface due to etching. Therefore, a new method of post CMP cleaning is proposed in this study. It is observed that using viscoelastic fluids increases the removal of particles, due to the Stokes drag force applied on the particles by the viscoelastic fluids. The cleaning method can be improved by applying it on different surfaces with different roughness values, which are obtained by different abrasive particle sizes.

5.2 Recommendations For Future Work

The findings of this thesis can be applied to other compound semiconductors composed of III/V or II/VI elements in the periodic table, which tend to have similar properties to GaN. These findings can also be applied to other materials, which are chemically inert and mechanically hard and hence hard to remove and planarize such as SiN, AlN, etc.

The mathematical optimization is a preliminary work and can be developed to obtain more realistic correlations between the input and output variables and this can be performed by adding new input variables depending on the material of choice.

The post CMP cleaning procedure using viscoelastic fluid can be further studied on GaN and alternative wafers. This procedure can also be implemented in a way to be integrated with the conventional post CMP cleaning methods in-situ for high volume manufacturing applications.

APPENDIX A

SOME ANCILLARY STUFF

A.1 Background Subtraction

```
clear all;

close all;

I = imread('background.jpg');

Y = imread('after background.jpg');

X = imabsdiff(I,Y);

X = ceil((1 - X / max(max(X)))*255);

imshow(X)

imbinarize(X);

hold on

size(X);

density = 0;

for row = 1:964

for column = 1:1292

if X(row, column)== 0

density = density +1;

else

end

end

end

disp(density)
```

A.2 Least Square Error Optimization

clear all close all

% X Matrix X = [10 20 43.5 20; 15 20 43.5 20; 20 20 43.5 20; 25 20 43.5 20; 10 20 43.5 20; 10 50 43.5 20; 10 100 43.5 20; 10 20 4.8 20; 10 20 6.2 20; 10 20 8.7 20; 10 20 14.5 20; 10 20 14.5 4; 10 20 14.5 20];

% Y Vector Y = [220.1; 210.8; 80.5; 20.4; 220.1; 220.0; 62.9; 0; 0; 62.9; 345.9; 475.0; 158.5];

% X Transpose B = X.';

% X inverse Xinv= (inv((B*X))*B);

W = [0.02 0 0 0 0 0 0 0 0 0 0 0 0;0 0.02 0 0 0 0 0 0 0 0 0 0 0;0 0 0.02 0 0 0 0 0 0 0 0 0;0 0 0 0.02 0 0 0 0 0 0 0 0 0;0 0 0 0 0.074 0 0 0 0 0 0 0 0;0 0 0 0 0 0.074 0 0 0 0 0 0 0;0 0 0 0 0 0 0.074 0 0 0 0 0 0;0 0 0 0 0 0 0 0.074 0 0 0 0 0;0 0 0 0 0 0 0 0 0.074 0 0 0 0;0 0 0 0 0 0 0 0 0 0.074 0 0 0;0 0 0 0 0 0 0 0 0 0 0.074 0 0;0 0 0 0 0 0 0 0 0 0 0 0.2 0;0 0 0 0 0 0 0 0 0 0 0 0 0.2];

% p vector without weighting p = (inv(B * X)) * B * Y

% p vector with weighting p.w.opt = inv(X'*W'*W*X)*X'*W'*W*Y

Est = X * p

Est.W = X * p.w.opt

Bibliography

[Abb04]   A. Abbadie. Advanced wet cleanings post-cmp: application to reclaim wafers. *J. Electrochem. Soc.*, 151:G57, 2004.

[Aid11]   H. Aida. Chemical mechanical polishing of gallium nitride with colloidal silica. *J. Electrochem. Soc.*, 158:H1206–H1212, 2011.

[Aid14]   H. Aida. Surface planarization of GaN-on-sapphire template by chemical mechanical polishing for subsequent GaN homoepitaxy. *ECS Journal of Solid State Science and Technology*, 5(3):163–168, 2014.

[And11]   V. A. Andreev. Silicon-wafer cleaning with aqueous surfactant-stabilized gas/solids suspensions. *JECS*, 158:H55–H62, 2011.

[Bab16]   S. Babu. *Advances in Chemuical Mechanical Planarization CMP*. Woodhead Publishing, 2016.

[Ban08]   G. Banerjee. Chemical mechanical planarization historical review and future direction. *ECS Transactions*, 13(4):1–19, 2008.

[Bar09]   S. Bargir. The use of contact angle measurements to estimate the adhesion propensity of calcium carbonate to solid substrates in water. *Applied Surface Science*, 255(9):4873, 2009.

[Bas11]   G. B. Basim. *Engineered Particulate Systems for Chemical Mechanical Planarization*. Lambert Academic Publishing, 2011.

[Bie98]   M. Bielmann. Chemical mechanical polishing of tungsten. Master's thesis, University of Florida, Gainsville, 1998.

[Bie06]   M. Bielmann. Effect of particle size during tungsten chemical mechanical polishing. *Electrochem. Solid State Lett.*, 153:401–403, 2006.

[Bon77]   A. C. Bonora. Flex-mount polishing of silicon wafers. *Solid State Technol.*, pages 55–62, 1977.

[Bow95]   R. A. Bowling. An analysis of particle adhesion on semiconductor surfaces. *J. Electrochem. Soc.*, 132:2208, 1995.

[Bus93]   A. Busnaina. Measurements of adhesion and removal forces of submicron particles on silicon surfaces. *J. Adhes. Sci. Technol.*, 7:441–445, 1993.

[Bus02]   A.A. Busnaina. Particle adhesion and removal mechanisms in post-cmp cleaning processes. *IEEE Trans. Semicond. Manuf.*, 15:374, 2002.

[Cer17]   A. Cerhan. Development of nano structured photo-catalytic textile materials. Master's thesis, Ozyegin University, Istanbul, 2017.

[Che06] R. Chein. Modeling of particle removal using non-contact brush scrubbing in post- cmp cleaning processes. *J. Adhesion*, 82:555, 2006.

[Chu71] T. L. Chu. Gallium nitride films. *J. Electrochem. Soc.*, 118:1200–1203, 1971.

[Col87] P. B. Coleman. Effects of a drag-reducing polyelectrolyte of microscopic linear dimension (separan AP-273) on rat hemodynamics. *Journal of the American Heart Association*, 61(6), 1987.

[Coo90] L. Cook. Chemical processes in glass polishing. *J. Non-Cryst. Solids*, 120:152–171, 1990.

[Cor03] J. Cornely. In situ temperature measurement during oxide chemical mechanical planarization. *Mater. Res. Soc. Symp. Proc.*, 767, 2003.

[Dav89] B. Davari. A new planarization technique, using a combination of rie and chemical mechanical polish (CMP). *IEEE, IEDM Technical Digest*, 89:341–344, 1989.

[Doy04] T. K. Doy. Impact of novel pad groove designs on removal rate and uniformity of dielectric and copper (CMP). *Journal of Electrochemical Society*, 151(3):G196–G199, 2004.

[Edg11] J. H. Edgar. *Properties of Group III Nitrides*. Electronic Materials Information Service (EMIS), London, 2011.

[Etz01] E. V. Etzkorn. Cracking of gan films. *Journal of Applied Physics*, 89(2):1025, 2001.

[Fah83] A. L. Fahrenbruch. *in: Fundamentals of Solar Cells.* Academic Press, New York, 1983.

[Fra10] S. Fransilla. *Introduction to Microfabrication.* Hoboken, New Jersey, 2010.

[Gan10] V. Ganesh. Syntheis and characterization of nanicrystalline gallium nitride by nitridation of Ga-EDTA complex. *Journal of Alloys and Compounds*, 498, 2010.

[Gim95] R. Gim. *Fluid dynamics of liquid jets used for particle removal from surfaces in: Particles on Surfaces, Detection, Adhesion and Removal.* Marcel Dekker, 1995.

[Gon15] H. Gong. Investigation of cmp on gan substrate for led manufacturing. *In Planarization/CMP Technology (ICPT) 2015 International Conference*, page 1, 2015.

[Goo92] R. J. Good. Contact angle, wetting, and adhesion: a critical review. *J. Adhesion Sci. Technol.*, 12(6):1269–1302, 1992.

[Hat98] T. Hattori. *Ultraclean Surface Processing of Silicon Wafers. Secrets of VLSI Manufacturing.* Springer-Verlag, Berlin, 1998.

[Hau16] J. W. Haus. *Fundamentals and applications of nanophotonics.* Woodhead Publishing, 2016.

[Hay08] S. Hayashi. Chemical mechanical polishing of gan. *J. Electrochem. Soc.*, 155:H113–H116, 2008.

[Hel96] E. S. Hellman. Growth of ga-face and n-face gan films using zno substrates. *MRS Internet Journal of Nitride Semiconductor Research*, 16(1), 1996.

[Hel98] E. S. Hellman. The polarity of gan: a critical review. *MRS Internet Journal of Nitride Semiconductor Research*, 3(11), 1998.

[Her99] J. Hernandez. Chemical mechanical polishing of Al and SiO2 thin films: the role of consumables. *Electrochem Soc.*, 146(12):4647–4653, 1999.

[Hir06] H. Hirano. Damage-free ultradiluted hf/nitrogen jet spray cleaning for particle removal with minimal silicon and oxide loss. *Electrochem. Solid-State Lett.*, 9:G62–G65, 2006.

[Hon17] J. Hong. Removal rate and surface quality of the GLSI Silicon substrate during the CMP process. microelectronic engineering. *Microelectronic Engineering*, 168:76–81, 2017.

[Ili17] F. Ilie. Chemical-mechanical impact of nanoparticles and pH effect of the slurry on the CMP of selective layer surfaces. *Lubricants*, 5(15), 2017.

[Ita93] M. Itano. Particle removal from silicon wafer surface in wet cleaning process. *IEEE Trans. Semicond. Manuf.*, 6:258–267, 1993.

[Jie16] W. Jie. Effect of photocatalytic oxidation technology on GaN CMP. *Applied Surface Science*, 361, 2016.

[Kar84] J. Karpinski. Equilibrium pressure of n2 over gan and high pressure solution growth of gan. *J. Cryst. Growth*, 66:1–10, 1984.

[Kar15] A. Karagoz. Chemical mechanical planarization studies on gallium nitride for improved performance. *In Planarization/CMP Technology (ICPT)*, page 1, 2015.

[Kas97] I. Kashkoush. Particulate removal from silicon substrates in megasonic-assisted dilute SC1 chemistry. *Mater. Res. Soc. Symp. Proc.*, 477:21–26, 1997.

[Ker87] W. Kern. *Chemistry of the Semiconductor Industry.* Chapman and Hall, New York, 1987.

[Ker90]   W. Kern. The evolution of silicon wafer cleaning technology. *J. Electrochem. Soc.*, 137:1887, 1990.

[Kes15]   M. Keswani. *in: Developments in Surface Contamination and Cleaning Volume VIII Wet and Dry Cleaning Methods.* William Andrew, 2015.

[Khu14]   A. Khushnuma. Effect of polishing parameters on chemical mechanical planarization of c-plane (0001) gallium nitride surface using sio2 and al2o3 abrasives. *ECS Journal of Solid State Science and Technology*, 3(8):277, 2014.

[Kre00]   A. Kreiba. The rheological properties of aqueous polyacrylamide solutions. Master's thesis, Concordia University, Montreal, Quebec, Canada, 2000.

[Kue16]   T. F. Kuech. III-V compound semiconductor. *Progress in crystal growth and characterization of materials*, 62:352–370, 2016.

[Kum06]   G. Kumar. Undercut removal of micrometer-scale particles from surfaces. *J. Electrochem. Soc.*, 153:G175–G181, 2006.

[Lia97]   H. Liang. Wear phenomenon in chemical mechanical polishing. *Wear*, 211:271–279, 1997.

[Lid14]   A. Lidow. *GaN transistors for efficient power conversion.* John Wiley and Sons, 2014.

[Lid15]   A. Lidow. *GaN Transistors for Efficient Power Conversion.* John Wiley and Sons, West Sussex, 2015.

[Lin04]   J. F. Lin. Analysis of the tribological mechanisms arising in the chemical mechanical polishing of copper-film wafers,. *Journal of Tribology*, 126, 2004.

[McC04]   L. S. McCarty. High voltage AlGaN/GaN heterojunction transistors. *Int. J. High Speed Electron.*, 14(1):225, 2004.

[Mit06]   E. Mitani. Mass production of high voltage gaas and gan devices. *CS Mantech Conference Vancouver B.C. Canada Apr.*, pages 24–27, 2006.

[Moo99]   Y. Moon. Mechanical aspects of the material removal mechanism in chemical mechanical polishing CMP. Master's thesis, University of California, Berkeley, 1999.

[Mou99]   N. Moumen. The effect of relative-humidity on particle adhesion and removal. *Proc. 22nd Annual Meeting of the Adhesion Society*, 1999.

[Nag95]   B. R. Nag. Direct band-gap energy of semiconductors. *Infrared Phys. Technol.*, 36:831–835, 1995.

[Nag07] K. Nagayama. *A Computational Study on Slurry Flow Between a Wafer and CMP Pad with Grooves, In: Towards Synthesis of Micro-/Nano systems.* Springer, London, 2007.

[Nak13] S. Nakamura. History of galliumnitride-based light-emitting diodes for illumination. *Proceedings of the IEEE*, 101(10):2211, 2013.

[Oha11] Y. Ohama. *Application of Titanium Dioxide Photocatalysis to Construction Materials.* Springer, 2011.

[Ola03] G. A. Olah. *Hydrocarbon Chemistry.* Wiley-Inter Science, New York, 2003.

[Oli04] M. Oliver. *Chemical-Mechanical Planarization of Semiconductor Materials.* Springer, 2004.

[Pan72] J. I. Pankove. Electrolytic etching of gan. *J. Electrochem. Soc.*, 119:1118–1119, 1972.

[Par17] P. Parthiban. Influence of slurry flow rate on material removal rate on material removal rate and topography of chemical mechanically planarizaed c-plane (0001) gan surface. *ECS Journal of Solid State Science and Technology*, 6(4):113, 2017.

[Pea00] S. J. Pearton. Fabrication and performance of GaN electronic devices. *Mater. Sci. Eng. R-Rep.*, 30(3–6):55, 2000.

[Pec12] S. L. Peczonczyk. Wet chemical functionalization of iiiv semiconductor surfaces: Alkylation of gallium arsenide and gallium nitride by a grignard reaction sequence. *Langmuir*, 28(10):4672, 2012.

[Phi04] A. Philipossian. Tribological attributes of post-cmp brush scrubbing. *J. Electrochem. Soc.*, 151:G456, 2004.

[Por98] S. Porowski. Bulk and homoepitaxial gan-growth and characterization. *J. Cryst. Growth*, 189:153–158, 1998.

[Pre97] F. W. Preston. The theory and design of plate glass polishing machine. *J. Soc. Glass Technol.*, 11:214–256, 1997.

[Rem06] E. E. Remsen. Analysis of large particle count in fumed silica slurries and its correlation with scratch defects generated by CMP. *J. Electrochem. Soc.*, 153:G453–G461, 2006.

[Roy95] S. R. Roy. Post chemical-mechanical planarization cleanup process for interlayer dielectric films. *J. Electrochem. Soc.*, 142:216, 1995.

[Ruz06] J. Ruzyllo. Wet cleaning technology-implementation. *Semiconductor Note*, 17, 2006.

[Sch85]   S. Schwartzman. Megasonic particle removal from solid state wafers. *RCA Rev.*, 46, 1985.

[Shu04]   M. S. Shur. *GaN-based materials and devices: growth, fabricatio, characterization and performance*. World Scientific Publishing Company, River Edge, 2004.

[Sim04]   G. Simin. Insulated gate III-N heterostructure field effect transistors. *Int. J. High Speed Electron.*, 14(1):197, 2004.

[Sim17]   E. Simoncelli. Lecture notes in geometric review of linear algebra, October 2017.

[SM97]   C. Srinivasa-Murthy. Stress distribution in chemical mechanical polishing. *Thin Solid Films*, pages 533–537, 1997.

[Sol94]   M. Soltani. On particle adhesion and removal mechanisms in turbulent flows. *J. Adhes. Sci. Technol.*, 8:763–785, 1994.

[Ste04]   J. M. Steigerwald. *Chemical Mechanical Planarization of Microelectronic Materials*. Wiley, Weinheim, 2004.

[Tal90]   L. Talbot. Thermophoresis of particles in a heated boundary layer. *J. Fluid Mech.*, 101:737, 1990.

[Tam04]   D. Tamboli. Novel interpretations of cmp removal rate dependencies on slurry particle size and concentration. *Electrochem. Solid State Lett.*, 7:F62–F65, 2004.

[Tav02]   P. R. Tavernier. Chemical mechanical polishing of gallium nitride. *Electrochem. Solid-State Lett.*, 5(8):G61, 2002.

[To98]   S. To. Substrate-polarity dependence of metal-organic vapor-phase epitaxy-grown gan on sic. *Journal of Applied Physics*, 64(9):4531, 1998.

[Tse03]   W. Tseng. Post copper cmp hybrid clean process for advanced beol technology. *IEEE Trans. Semicond. Manuf.*, 26:493, 2003.

[Ume15]   R. Umesh. Synthesis and characterization of gallium nitride (GaN) thin films deposited by low pressure chemical vapor deposition (LPCVD) technique. *Proceedings of Manipal Research Colloquium*, 2015.

[Vis95]   J. Vissar. Particle adhesion and removal: A review. *Part. Sci. Technol.*, 13:169–196, 1995.

[Wal13]   T. W. Walker. Enhanced particle removal using viscoelatic fluids. *Journal of Rheology*, 58(1):63–68, 2013.

[Wan11]   C. H. Wang. Efficiency and droop improvement in GaN-based high-voltage light-emitting diodes. *IEEE Electron Device Letters*, 32(8):1098, 2011.

[Wei13]   X. Wei. Fabrication and properties of ZnO/GaN heterostructure nanocolumnar thin film on si (111) substrate. *Nanoscale Research Letters*, 8(1):112, 2013.

[Wey97]   J.L. Weyher. Chemical polishing of bulk and epitaxial gan. *J. Cryst. Growth*, 182:17–22, 1997.

[Xu03]   X. Xu. Chemical mechanical polishing for decoration and measurement of dislocations on freestanding gan wafers. *Phys. Status Solid.*, pages 2460–2463, 2003.

[Xu04]   K. Xu. Particle adhesion and removal mechanisms during brush scrubber cleaning. *J. Vac. Sci. Technol.*, 22:2844, 2004.

[Yan09]   H. Yan. Chemical mechanical polishing of freestanding gan substrates. *J. Semicond.*, 30, 2009.

[Yia95]   S. G. Yiantsios. Detachment of spherical microparticles adhering on flat surfaces by hydrodynamic forces. *J. Colloid Interface Sci.*, 176:74–85, 1995.

[Yor69]   D. York. Least squares fitting of a straight line with correlated errors. *Earth and planetary science letters*, 5:320–324, 1969.

[Zha98]   G. Zhang. Assessment of post-cmp cleaning mechanisms using statistically designed experiments. *Thin Solid Films*, 332:379, 1998.

[Zha99]   L. Zhang. Minimization of chemical mechanical planarization (cmp) defects and post-cmp cleaning. *J. Vac. Sci. Technol.*, 17:2248, 1999.

[Zha00]   F. Zhang. The removal of deformed submicron particles from silicon wafers by spin rinse and megasonics. *J. Electron. Mater.*, 29:199–204, 2000.

[Zha01]   X. G. Zhang. *Electrochemistry of Silicon and Its Oxide*. Kluwer Academic/Plenum Publishers, New York, 2001.

[Zha12]   H. Zhang. Processing pathway dependence of amorphous silica nanoparticle toxicity: colloidal vs pyrolytic. *J. Am. Chem. Soc.*, 134:15790–15804, 2012.

[Zhu05]   D. Zhuang. Wet etching of gan, aln, and sic: a review. *Materials Science and Engineering*, 48:1–46, 2005.

[Zou15]   C. Zou. A study of surface defects of gan during cmp process. *In Planarization/CMP Technology (ICPT) 2015 International Conference IEEE*, page 1, 2015.

VITA

Sebnem Ozbek was born in Istanbul. She completed primary and secondary education in V.K.V. Koc Elementary and High School and received her BSc degree from Ozyegin University Mechanical Engineering Department in 2016. In the same year, she began to study on CMP of GaN project for her MSc degree in Ozyegin University in Mechanical Engineeing Department.